UNIVERSIDAD NACIONAL AUTÓNOMA DE MÉXICO
POSGRADO EN CIENCIAS FÍSICAS
INSTITUTO DE CIENCIAS NUCLEARES

THE STRUCTURE OF COSMIC STRINGS FOR A U(1) GAUGE FIELD RELATED TO THE CONSERVATION OF THE BARYON-NUMBER MINUS LEPTON-NUMBER

TESIS

QUE PARA OPTAR POR EL GRADO DE:
MAESTRO EN CIENCIAS (FÍSICA)

PRESENTA:
VICTOR DENNIS MUÑOZ VITELLY

TUTOR
DR. WOLFGANG PETER BIETENHOLZ
INSTITUTO DE CIENCIAS NUCLEARES

MIEMBROS DEL COMITÉ TUTOR
DR. DANIEL EDUARDO SUDARSKY SAIONZ
INSTITUTO DE CIENCIAS NUCLEARES
DR. ISAAC PÉREZ CASTILLO
INSTITUTO DE FÍSICA

CIUDAD UNIVERSITARIA, CD. MX., ABRIL DE 2022

Agradecimientos

Este trabajo fue realizado gracias al Programa de Apoyo a Proyectos de Investigación e Innovación Tecnológica (DGAPA-PAPIIT) de la UNAM, IG100219 “Exploración teórica y experimental del diagrama de fase de la cromodinámica cuántica” e IG100322 “Materia fuertemente acoplada en condiciones extremas con el MPD-NICA”. Así mismo al CONACYT por la beca otorgada durante mis estudios de posgrado.

Resumen

En esta tesis investigamos los defectos topológicos conocidos como cuerdas cósmicas en una extensión del Modelo Estándar (ME). Estas cuerdas cósmicas son vórtices con una estructura de tipo filamento que surgen a partir del campo de norma usado en esta extensión y relacionado al grupo unitario $U(1)_{Y'}$ con la carga $Y' = \alpha Y + \beta(B - L)$. Este es un grupo de simetría formado por una combinación lineal de la hipercarga Y y el número bariónico menos el número leptónico, $B - L$. Incluímos este campo de norma con el objetivo de convertir a $B - L$ en una simetría local, de forma que sea naturalmente exacta. También añadimos un neutrino derecho por cada generación de fermiones para curar la anomalía de norma triangular que prohibía este campo de norma en la versión tradicional del ME. Asimismo podemos escribir términos de masa para los neutrinos izquierdos y derechos usando el mecanismo de Higgs. Para que estos términos de masa sean invariantes de norma, requerimos de un campo escalar adicional. Este nuevo campo tiene un valor de expectación en el vacío (VEV) mayor que el del campo de Higgs estándar. Encontramos que el modelo es consistente y usamos el formalismo Lagrangiano de teoría de campos para obtener las ecuaciones de movimiento de los campos involucrados. La parte relevante de la Lagrangiana consiste de dos campos de Higgs con su respectivo potencial cuártico y un campo de norma acoplado a los otros campos con diferentes cargas. Para obtener soluciones de cuerdas cósmicas usamos un ansatz con simetría cilíndrica. Este procedimiento nos lleva a un sistema de ecuaciones diferenciales no-lineales, de segundo orden. Condiciones de frontera adecuadas se imponen para asegurar la continuidad en el origen y para que los campos tomen sus VEVs apropiados lejos de la cuerda. Resolvemos este sistema utilizando métodos numéricos. Las soluciones corresponden a los perfiles de las cuerdas cósmicas en la parte radial de los campos. Nuestra extensión tiene parámetros libres adicionales al ME y encontramos que las soluciones dependen fuertemente del número de veces que las configuraciones de los campos dan vuelta al rededor de la cuerda cósmica. Los resultados se reportan como gráficas con distintos valores de los parámetros libres. Concluimos que este tipo de cuerdas cósmicas es concebible. Su existencia puede tener consecuencias en la masa de los rayos cósmicos, cuando pasan a través o cerca de ellas. Los campos de Higgs cambian su valor con la distancia al núcleo y los términos de masa de las partículas dependen de ellos.

Abstract

In this thesis we investigate topological defects known as cosmic strings in an extension of the Standard Model (SM). These cosmic strings are vortices with a filament structure arising from the gauge field used in this extension and related to the unitary group $U(1)_{Y'}$, with the charge $Y' = \alpha Y + \beta(B - L)$. This is a symmetry group formed by a linear combination of the weak hypercharge Y and the baryon number minus lepton number, $B - L$. The reason we include this gauge field is to turn $B - L$ into a local symmetry, such that it becomes naturally exact. We also include a right-handed neutrino to each fermion generation so that we can cure the triangular gauge anomaly that prohibited this gauge field in the traditional version of the SM. Furthermore we can write mass terms for the left- and right-handed neutrinos using the Higgs mechanism. For these mass terms to be gauge invariant we require an additional scalar field. This new field has a larger vacuum expectation value (VEV) than the standard Higgs field. We find that the model is consistent, we use the Lagrangian formalism of field theory to obtain the equations of motion for the involved fields. The relevant part of the Lagrangian consists of two Higgs fields with their respective quartic potential and the gauge field coupled to the other fields with different charges. To obtain cosmic string solutions we use a cylindrically symmetric ansatz. This procedure leads to a system of non-linear differential equations. Suitable boundary conditions are imposed to guarantee continuity in the origin and for the fields to attain the appropriate VEVs far away from the string. This system is solved using numerical methods. The solutions correspond to the profiles of the cosmic strings in the radial part of the fields. Our extension has free parameters additional to the SM and we find that the field solutions are strongly dependent on the winding numbers. The results are reported as plots with different values of the free parameters. We conclude this type of cosmic strings is conceivable. Their existence would have consequences in cosmic ray masses when passing through or nearby the string. The Higgs fields change their values with the distance from the core and particles mass terms depend on them.

Contents

Chapter 1

Introduction

Cosmic strings are hypothetical large-scale objects in the universe which can be obtained from a Lagrangian description of quantum fields. To this day there is no evidence of their existence, but they are still an open and fruitful possibility, being studied theoretically and observationally. It is an open possibility because constraints on the proposed models are compatible with the present observational data. They are fruitful because their cosmological consequences can be used advantageously, for example in structure formation. There are many types of theorized cosmic strings associated with different fields, they can have distinct physical properties like superconductivity when they are associated with electromagnetic fields. They can have mass and dynamical properties which could result in the production of gravitational waves. Their origin can be speculated in the early universe at phase transitions and traces of them can be searched for in the Cosmic Microwave Background (CMB).

While we have no evidence for the existence of cosmic strings, there are analogous phenomena in systems of condensed matter which are known as quantized vortices. Such structures have been described and observed experimentally in superconductors, superfluids and liquid crystals. So we have a better comprehension of them and it is easier to study them since they can be generated in laboratories. Even if the physical description of these structures is different from 4-dimensional field theory, they are a motivation for cosmic strings research since they are solutions of similar equations of motion which arise from symmetries and topological arguments like the homotopy groups. Many authors have proposed to study these systems and recognize analogies between the properties of the universe and the behaviour in phase transitions.

1.1 Overview

The Standard Model (SM) of particle physics describes with great precision the observed content of matter and its interactions in the universe, at the fundamental level available with the current technology. Many authors have contributed to the study of experimental particle physics, from the discovery of electrons and atoms to the big contemporary collaborations in experiments of particle accelerators. The SM contains a set of elementary particles, including three generations

of quarks and leptons. Imposing local symmetry to the theory, leads to gauge invariance and this introduces the elementary particles known as force carrier bosons, which mediate three interactions (strong, weak and electromagnetic). At last the Higgs mechanism is used to give mass to the particles and also the Higgs field has its associated boson.

However, the SM still contains some short-comings, and extensions of it are proposed to account them. For example neutrinos in the SM are assumed as massless, although we now know they are not, due to the neutrino oscillations experiments. There are many attempts to introduce the mass adding a right-handed neutrino. Another example in cosmology is dark matter, necessary to explain certain astronomical observations. The content of matter we see with light can't account for all the observed gravitational effects. This could be explained by unknown particles which might be added to the SM in some extension.

In this thesis we will focus on the baryon number minus lepton number, $B-L$, conservation. In the SM this is a global and exact symmetry. In theory, there are certain processes where the conservation of baryon or lepton number is violated, but the difference is not. The basic idea is to turn the unitary group $U(1)_{B-L}$ into a local symmetry as it is more natural for an exact symmetry to be a gauged. This is the first step in our extension of the SM proposal and this gauge field would be coupled to all particles with $B-L \neq 0$. We can even gauge a unitary group which considers a linear combination of the hypercharge and the $B-L$ number $U(1)_{Y'}$, $Y' = \alpha Y + \beta(B-L)$. The introduction of this gauge field is accompanied by a triangular gauge anomaly with fermionic internal lines. Our proposal to this point can't cure this anomaly, but adding a right-handed neutrino to each fermion generation, cancels it. With right-handed neutrinos at our disposal we can give mass to the neutrinos, both to the left- and right-handed. We write a Dirac term which gives mass to the neutrinos by means of the usual Higgs mechanism. Furthermore we write a Majorana mass term for the right-handed neutrino. This mass term can be added without breaking the new Y' gauge symmetry if we include a new scalar field with $B-L=2$ and apply the Higgs mechanism.

Therefore our extension of the SM is a minimal extension to explain why $B-L$ is exact. It contains additional fields, namely the Y' gauge field, a right-handed neutrino to each fermion generation and a new scalar Higgs field. Even though these particles have never been observed, this can be justified as follows. For the case of the new Higgs particle, we can assume that it has a vacuum expectation value (VEV) v' much larger than the standard Higgs VEV, $v' \gg 246$ GeV, accelerator physics experiments do not allow for systematic search at these energies.

We conclude that the model is well posed and constructed in a self-consistent way with the traditional constituents. We will start from this extension and just consider a sector of it, the one which is related to the relevant fields under some assumptions like a constant fermion background. This sector will consist of three fields, the standard and new Higgs fields and the $U(1)_{Y'}$ gauge field. Using the Lagrangian formulation we can derive the equations of motion of this system. They turn out to be a system of second order, non-linear differential equations with specific boundary values. They do not have any analytic solution but they can be solved through numerical methods, for instance with Python. Just as the SM contains free parameters, our extension contains a set which needs to be fixed to specify solutions using the numerical methods. There are five additional free parameters in the relevant sector that we consider, seven additional free parameters considering a first generation of neutrinos and eleven considering

three generations. Our results will consist of cosmic string solutions for these equations, they are obtained by using a cylindrically symmetric ansatz. The profiles of the solutions will be reported as plots for the radial part of the fields using distinct values of the free parameters. We will also investigate the presence of a possible behaviour which differs from typical cosmic strings in the literature, which we call co-axial cosmic strings.

1.2 Outline

This thesis consists of five chapters and two appendices. Chapter 2 is a review of the basic and relevant features of the SM. Here we will present the theoretical basis of our model and we will be led to the search of admissible cosmic string solutions. Chapter 3 is a review of topological defects, particularly of vortices appearing in condensed matter systems as superconductors and superfluids. This chapter will provide a picture of what we are looking for in 4-dimensional field theory. We close this chapter with remarks about cosmic strings and their important general features. Chapter 4 describes our work and results for cosmic strings in this extension of the SM. At last, Chapter 5 contains the conclusions and prospects for future work. Throughout the thesis two appendices are needed to substantiate this work. Appendix A is a note on how to define the derivatives of real and complex scalar fields, including a complex doublet. Appendix B explains the algorithms we used for the numerical solutions of the cosmic strings; this also involves tests of reliability and self-consistency.

Chapter 2

The Standard Model

The Standard Model (SM) of elementary particle physics describes three of the four known gauge interactions in the universe. It consists of fermionic fields whose excitations give rise to three generations of quarks and leptons. It also includes gauge fields which are associated with the force carriers bosons and the Higgs field associated with the Higgs boson. The anti-particles of the corresponding particles with opposite charges are also included. Figure 2.1 shows the content of particles of the SM along with their properties; the already mentioned three generations of matter, the 8 gluons as the gauge bosons for the strong interaction, the photon as the gauge boson of electromagnetism, the $W^{\pm}$ and Z^0 bosons for the weak interaction and the Higgs boson.

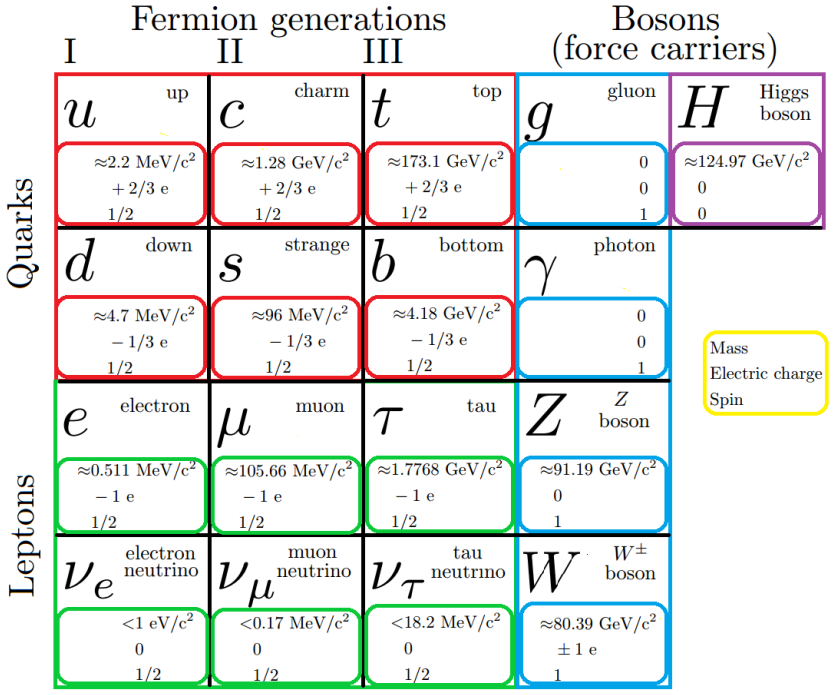

Figure 2.1: Particles of the Standard Model.

In this chapter we will discuss the SM as a field theory in a Lagrangian formulation, using natural units $\hbar = 1$, $c = 1$. The fields presented here are not operator valued, so they can define a classical or quantum system. The quantization procedure does not modify the Lagrangian structure or equations of motion; but it indeed requires a reinterpretation of the field variables. When fields are quantized, particles emerge as quantized excitations of their respective fields. With respect to gauge invariance we mean taking a global symmetry group and requiring the Lagrangian to be invariant locally as a principle of the theory. Imposing this condition leads to additional fields (gauge fields) which represent another set of particles that are the force carriers, they mediate the interactions. This idea goes back to Weyl [3] in 1918, he used the symmetry group $U(1)$ (complex phases) and Yang and Mills [4] in 1954 using the symmetry group $SU(2)$, complex 2×2 unitary matrices with determinant 1, where the Pauli matrices are the generators.

Let us look at Weyl's proposal [3]. We start from the Dirac Lagrangian in eq. (2.1) for the fermionic fields ψ, $\overline{\psi}$ which represents a free spin-1/2 particle with mass m,

$$\mathcal{L} = \overline{\psi}\left(i\gamma^\mu \partial_\mu - m\right)\psi. \tag{2.1}$$

By inspection we see that it is invariant under a global phase transformation $\psi \to e^{i\theta}\psi$, $\overline{\psi} \to e^{-i\theta}\overline{\psi}$, $\theta \in \mathbb{R}$. But if this phase depends on spacetime, $\theta(x)$, then it is not invariant. This is a local phase transformation $\psi \to e^{-iq\theta(x)}\psi$, $\overline{\psi} \to e^{iq\theta(x)}\overline{\psi}$, where q is the electric charge. If we perform this transformation, the system picks up an extra term. In order to implement gauge invariance we add a massless vector field A_μ. The gauge invariant Lagrangian we obtain is

$$\mathcal{L} = \overline{\psi}\left(i\gamma^\mu D_\mu - m\right)\psi - \frac{1}{4}F^{\mu\nu}F_{\mu\nu}. \tag{2.2}$$

The last term in eq. (2.2) is the gauge term $F_{\mu\nu} = \partial_\mu A_\nu - \partial_\nu A_\mu$. Moreover we have substituted the partial derivative by a covariant derivative $D_\mu = \partial_\mu + ieqA_\mu$, this is called the minimal coupling rule and e is the electron charge. The gauge field should transform as $A_\mu \to A_\mu + \frac{1}{e}\partial_\mu\theta$. The difference between eqs. (2.1) and (2.2) is that the second one is gauge invariant. This Lagrangian describes electrodynamics, A_μ is the electromagnetic potential and its quantization leads to the photon.

We can generalize this to a Yang-Mills theory, for instance using the symmetry group $SU(2)$ [4]. We start with two fermionic fields ψ_1, ψ_2 with the same mass m. Writing them as a two-component column vector

$$\psi = \begin{pmatrix}\psi_1 \\ \psi_2\end{pmatrix}, \tag{2.3}$$

we obtain the free Dirac Lagrangian

$$\mathcal{L} = \overline{\psi}\left(i\gamma^\mu \partial_\mu - m\right)\psi. \tag{2.4}$$

In complete analogy we observe that this Lagrangian is invariant under global $SU(2)$ transformations $\psi \to e^{i\sigma_a\theta^a}\psi$, $\overline{\psi} \to e^{-i\sigma_a\theta^a}\overline{\psi}$, where $a = \{1, 2, 3\}$, σ_a are the 3 Pauli matrices and θ^a real constants. If we turn this into a local symmetry, that is $\theta_a(x)$, we have to add three vector fields $W_a^\mu = (W_1^\mu, W_2^\mu, W_3^\mu)$. The gauge invariant Lagrangian reads

$$\mathcal{L} = \overline{\psi}\left(i\gamma^\mu D_\mu - m\right)\psi - \frac{1}{4}W_a^{\mu\nu}W^a_{\mu\nu}. \tag{2.5}$$

The difference between eqs. (2.4) and (2.5) is again that the second one is gauge invariant. We also have used a covariant derivative $D_\mu = \partial_\mu + igW_\mu$, with $W_\mu = igW_\mu^a\sigma_a/2$. Now we have 3 gauge field components that include a self-interaction in $W_{\mu\nu} = \partial_\mu W_\nu - \partial_\nu W_\mu + g[W_\mu, W_\nu]$, because of the commutator. This theory describes two fermion fields with equal masses interacting with three massless vector gauge fields.

The SM is a QFT, starting from the Lagrangian formalism, one can obtain the Feynman rules. The free part of the Lagrangian defines the free propagator and the interaction terms lead to the vertex factor, so the Feynman diagrams can be computed. With these diagrams one can obtain for instance the cross sections and decay rates in the perturbative approximation, that are of great interest in particle phenomenology.

In the quantization through the path integral formulation, we use the action (or Lagrangian) of some field ϕ to define the generating functional in Minkowski spacetime

$$\mathcal{Z}[J] = \int \mathcal{D}\phi e^{i\int d^4x\mathcal{L}(\phi,\partial_\mu\phi)+i\int d^4xJ\phi}. \tag{2.6}$$

All the n-point functions or Green functions, can be obtained through functional derivatives with respect to the source field $J(x)$ as

$$\langle\phi(x_1)\dots\phi(x_n)\rangle = \frac{1}{i^n\mathcal{Z}[0]}\frac{\delta^n\mathcal{Z}[J]}{\delta J(x_1)\dots\delta J(x_n)}\bigg|_{J=0}. \tag{2.7}$$

Therefore the quantum theory is complete, the physical observables can be obtained using these functions.

2.1 The strong interaction

After the discovery of the electron and the already known atoms, Thomson suggested atoms were composed of electrons enclosed in a positively charged volume [5]. Accepting this idea and as atoms are electrically neutral, Rutherford's scattering experiments showed that the positive charge and most of the mass were contained in the center of the atom, the nucleus. In 1932 Chadwick discovered the neutron [6], a neutral particle with a mass similar to the proton. With these three elements, an atom mass and its nucleus charge could be explained consistently. The nucleus is then formed of protons and neutrons, while electrons surrounding it compose together the atom. However there was a piece still missing. The existence of a strong force was proposed, produced by a field that held together protons and neutrons in the nucleus, overcoming the electromagnetic repulsion of the positive charged protons.

Upon quantization of this new field, as Yukawa proposed, there should be exchange particles that mediate the interaction. As a short range force, Yukawa's proposition led to an exchange particle named meson. Later the (charged) pion π was discovered, along with the muon μ in 1947 using cosmic rays [7]. This π particle had the characteristics that Yukawa predicted. Now we know these are not the exchange particles of the strong interaction at the fundamental level, but the name meson was kept to classify them as we will see later in this section. The neutral kaon K^0 was discovered by Rochester and Butler using a cloud chamber and cosmic rays; they

observed the reaction $K^0 \to \pi^+ + \pi^-$ [8]. In 1949 the K^+ was discovered by Brown et al. through the reaction $K^+ \to \pi^+ + \pi^+ + \pi^-$ seen in photographs of cosmic rays [9]. In some aspects, the kaons behave like the pions, so they are also classified in the meson family. In the following years, many more mesons were discovered like η, η', ϕ, ω, ρ, etc.

The law of baryon number conservation was proposed in 1938 by Stückelberg to account for the proton stability, even though the expression "baryon" was introduced by Pais only in 1953 [10]. A number $B = +1$ was assigned to baryons and $B = -1$ to anti-baryons. In an elementary particle reaction, the difference of the number of baryons and the number of anti-baryons should be conserved following this law. According to Stückelberg, the stability of the proton as the lightest baryon is assured by the conservation of the baryon number.

In 1932 Heisenberg noticed that despite the different electric charge, the proton and neutron were similar particles. In particular their masses are really close. So he proposed that they are different states of the same particle, the nucleon [11]. By direct analogy to the spin, he introduced the isospin $\vec{I}$ from the symmetry group $SU(2)$. Then the nucleon has isospin $I = 1/2$ and its projections give rise to the proton $I_3 = +1/2$ and the neutron $I_3 = -1/2$, they belong to the 2-dimensional representation of $SU(2)$. Heisenberg's proposal tells us that the strong interactions are invariant under rotations in isospin space, thus by Noether's theorem, isospin is conserved in strong interactions.

However, in that epoch the proton and neutron were the only known baryons. It was not until 1950 that the Λ particle was discovered by Hopper and Biswas [12] through the reaction $\Lambda \to p + \pi$. Using the baryon number conservation law, we see that it must be classified as a baryon. In the following years, many more baryons were discovered like Σ's, Ξ's, Δ's, etc.

In 1961 Gell-Mann noticed that he could arrange the known particles in group theoretic patterns which he called the eightfold way [13]. We can see the case of the lightest hadrons in Fig. 2.2 forming an hexagonal structure, where Q is the electric charge and S is the strangeness[1]. All these particles carry similar masses.

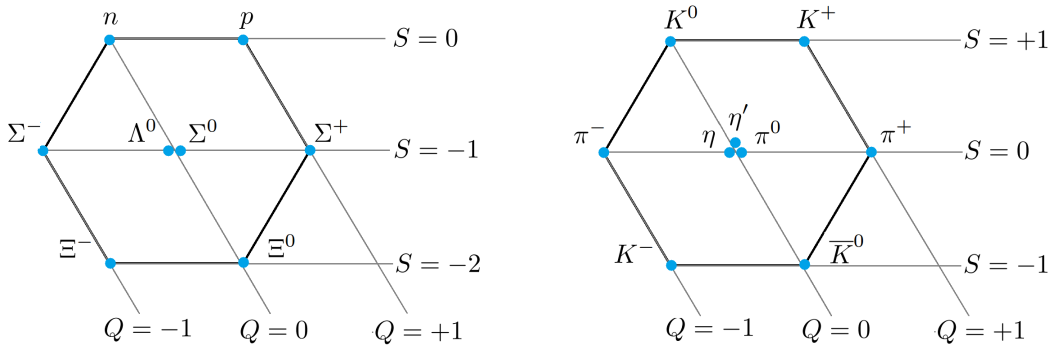

Figure 2.2: The light baryon octet (a) and the meson nonet (b).

[1] Another quantum number associated to the strange quark: it is a conserved quantity in the strong interaction, given by the number of strange anti-quarks minus quarks.

The baryon decuplet in Fig. 2.3 led to the prediction of the Ω^- particle and its mass. This particle was discovered afterwards in 1964 [14], so Gell-Mann's scheme was affirmed.

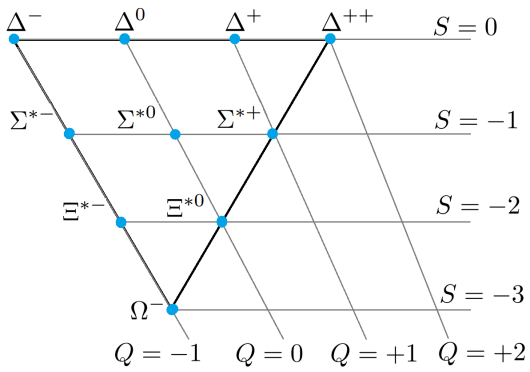

Figure 2.3: Baryon decuplet.

Gell-Mann and Zweig proposed that hadrons (baryons and mesons) are composed of elementary constituents called quarks, whose combinations lead to the quark model and the understanding of these group theoretic patterns as multiplets of $SU(2)$ group representations, a generalization of Heisenberg's idea. For example, all particles in the baryon octet in Fig. 2.2 carry spin 1/2, regarding all these particles as a supermultiplet meant they belonged to a representation of some enlarged group where isospin is a subgroup. $SU(N_f)$ is the group, where N_f is the number of flavors, six according the already mentioned three generations of quarks (matter) in Fig. 2.1 and they are labelled by a flavor index $f = \{u, d, s, c, t, b\}$, up, down, strange, charm, top and bottom. It is an approximate symmetry because the masses in the supermultiplets are not the same, indeed their difference become larger as we add more flavors. This breaking of flavor symmetry is due to the fact that quarks have different masses. Thus in the quark model, hadrons are bound-states of these quarks. Baryons are composed of three valence quarks. Mesons are composed of a valence quark and anti-quark pair.

Quarks have never been directly observed as free particles. We call this phenomena quark confinement. It can be understood as a long distance confining property of the strong interaction. The up, down, strange, charm and bottom quarks hadronize but the top quark has no time to do so [15]. On the other hand, one of the reasons to include a color index $N_c = \{r, g, b\}$ (red, green, blue) is that, in order for quarks to constitute an hadron (and as quarks have spin-1/2) they must satisfy the Pauli exclusion principle. Then a quark can have 3 different charges and hadrons are colorless particles. A baryon is composed of 3 valence quarks of different color and a meson is composed of 2 valence quarks with a color and anti-color. All we have seen so far is the constituent quark model where hadrons are composed of valence quarks.

As a more fundamental description, the strong interaction can be treated as a field theory known as Quantum Chromodynamics (QCD). It is formulated as an $SU(3)$ gauge field theory. Then a quark is represented as a triplet consisting of spinor fields

$$= \begin{pmatrix} r \\ g \\ b \end{pmatrix}. \tag{2.8}$$

The QCD Lagrangian takes the form

$$\mathcal{L}_{QCD} = \sum_{f=1}^{N_f} \overline{\psi}_f \left(i\gamma^\mu D_\mu - m_f\right) \psi_f - \frac{1}{4} G^a_{\mu\nu} G^{\mu\nu}_a, \tag{2.9}$$

where ψ_f is the quark field of flavor f, m_f is its mass and the last term is the gauge term. Upon quantization the gauge fields give rise to the gluons, which are understood as massless particles that are the force carriers of the strong interaction. We can write the gluon field with a set of generators of $SU(3)$ (Gell-Mann matrices λ_a) as

$$G_\mu(x) = \frac{i}{2} G^a_\mu(x) \lambda_a, \quad a \in \{1, \ldots, 8\}, \tag{2.10}$$

there are 8 gluons. The covariant derivative takes the form

$$D_\mu = \partial_\mu + g_s G_\mu, \tag{2.11}$$

where g_s is the strong coupling constant and the field strength tensor is

$$G^a_{\mu\nu} = \partial_\mu G^a_\nu - \partial_\nu G^a_\mu - g_s f^a_{bc} G^b_\mu G^c_\nu, \tag{2.12}$$

where f^a_{bc} are the $SU(3)$ structure constants. Applying perturbation theory leads to a running coupling strength g^R_s which satisfies the β-function (a differential equation of the coupling constant with respect to a renormalization scale μ) given by

$$\mu \frac{\partial g^R_s}{\partial \mu} = -\frac{(g^R_s)^3}{16\pi^2} \left(11 - \frac{2}{3} N_f\right), \tag{2.13}$$

to 1-loop. The solution is given by

$$\alpha^R_s = \frac{(g^R_s)^2}{4\pi}, \quad \alpha^R_s(\mu) = \frac{6\pi}{33 - 2N_f} \frac{1}{\ln(\mu/\Lambda_{QCD})}, \tag{2.14}$$

where Λ_{QCD} is the natural energy scale for QCD. Taking into account that there are 6 flavors, eq. (2.13) is negative, which implies a decreasing coupling strength for increasing μ and the so-called asymptotic freedom of QCD at high energies. Equation (2.14) describes a logarithmically decreasing coupling strength.

2.2 The Higgs mechanism

Let us now take a look at the Higgs sector and the Higgs mechanism proposed in 1964 [16] to explain why particles can have mass. Higgs was inspired by the phenomenon in which plasmon modes from a superconducting Fermi gas acquire mass when the gas becomes charged [17]. The idea is basically to have a new quantum field permeating space-time and spontaneous symmetry breaking (SSB) of a local symmetry causes the particles to acquire mass, as we will see in this section. This mechanism was also proposed independently by Brout and Englert [18] and by Kibble, Guralnik and Hagen [19].

Before gauging we can address a global symmetry group $SU(2)_L \otimes SU(2)_R$ where the subscript L and R refers to left and right chirality. The Higgs field is a complex scalar doublet $\Phi \in \mathbb{C}^2$ given by

$$\Phi = \frac{1}{\sqrt{2}} \begin{pmatrix} \phi_+(x) \\ \phi_0(x) \end{pmatrix}, \tag{2.15}$$

where the upper component carries electric charge. The Lagrangian reads

$$\mathcal{L} = \partial^\mu \Phi^\dagger \partial_\mu \Phi - V = \partial^\mu \Phi^\dagger \partial_\mu \Phi - m^2 \Phi^\dagger \Phi - \lambda (\Phi^\dagger \Phi)^2, \tag{2.16}$$

where the mass term and self-coupling term are the Higgs potential. Under the condition $\lambda > 0$ for the potential to be bounded from below, we can distinguish two cases: if $m^2 \geqslant 0$, there is a single minimum $\Phi = 0$. If $m^2 < 0$ then we have a Mexican hat potential, $\Phi = 0$ is an unstable local maximum, but we can also find a set of minima which represent a degenerate vacuum with

$$|\Phi| = \frac{v}{\sqrt{2}} = \sqrt{-\frac{m^2}{2\lambda}}. \tag{2.17}$$

It is invariant under $SU(2)_L \otimes SU(2)_R$ transformations. In order to describe the vacuum and break the local symmetry, we can select a state

$$\Phi = \frac{v}{\sqrt{2}} \begin{pmatrix} 0 \\ 1 \end{pmatrix}, \tag{2.18}$$

with fluctuations

$$\Phi = \frac{1}{\sqrt{2}} \begin{pmatrix} \pi_1(x) + i\pi_2(x) \\ v + \sigma(x) + i\pi_3(x) \end{pmatrix}. \tag{2.19}$$

The fields π_1, π_2, π_3 and σ describe the fluctuations around the Higgs field vacuum expectation value (VEV) $v = 246$ GeV. This is the perturbation procedure where we start from a ground state and fields are fluctuations around that state. In this way we can expand the Lagrangian in eq. (2.16) using the state in eq. (2.19) and find that there is a σ particle with mass $m_\sigma^2 = 2\lambda v^2$ and three massless particles π_i. They correspond to Nambu-Goldstone bosons because of the symmetry breaking, according to the Goldstone theorem. The Goldstone Theorem states that under the SSB of the global symmetry groups $G \to H$, there will be $n_G - n_H$ massless particles or Nambu-Goldstone bosons, where n is the dimension of the symmetry group.

The next step is to promote the global symmetry to a local one. To do so we introduce the gauge fields $W_\mu(x)$ and $B_\mu(x)$ for the $SU(2)_L$ and $U(1)_Y$ groups, respectively, so that the kinetic term becomes invariant. $U(1)_Y$ is a subgroup of $SU(2)_R$. In this way, the Higgs sector Lagrangian takes the form

$$\mathcal{L}_H = D^\mu \Phi^\dagger D_\mu \Phi - V - \frac{1}{4} W_a^{\mu\nu} W^a_{\mu\nu} - \frac{1}{4} B^{\mu\nu} B_{\mu\nu} \tag{2.20}$$

with the potential

$$V = m^2 \Phi^\dagger \Phi + \lambda (\Phi^\dagger \Phi)^2 \tag{2.21}$$

and the covariant derivative

$$D_\mu \Phi = \left[\partial_\mu + i \frac{g}{2} W_\mu^a \sigma_a + i \frac{g'}{2} B_\mu \right] \Phi, \tag{2.22}$$

where g and g' are coupling constants. Notice that this follows from the Yang-Mills proposal [4] we referred at the beginning of this chapter.

The $SU(2)_L$ non-Abelian gauge field $W_\mu(x)$ has 2×2 complex matrices as field variables. It can be written in terms of the Pauli matrices σ_a as

$$W_\mu(x) = \frac{i}{2}\sum_{a=1}^{3} W_\mu^a(x)\sigma_a, \tag{2.23}$$

and a gauge transformation

$$W_\mu(x)' = G(x)\left(W_\mu + \frac{1}{g}\partial_\mu\right)G^\dagger(x), \quad G(x) \in SU(2)_L. \tag{2.24}$$

The field strength tensor includes a commutator which makes the gauge field self-interacting, it takes the form

$$W_{\mu\nu} = \partial_\mu W_\nu - \partial_\nu W_\mu + g[W_\mu, W_\nu]. \tag{2.25}$$

The $U(1)_Y$ gauge field B_μ transforms with a scalar function $\phi(x)$, as usual

$$B_\mu(x)' = B_\mu(x) + \frac{1}{g'}\partial_\mu\varphi(x) \tag{2.26}$$

and its field strength tensor is

$$B_{\mu\nu} = \partial_\mu B_\nu - \partial_\nu B_\mu. \tag{2.27}$$

These symmetry groups and gauge fields describe the electroweak interaction. The unification of the weak and electromagnetic interactions, that is the electroweak sector, was pursued since Fermi [20] and found first by Glashow [21] requiring the existence of neutral weak processes. The motivation was that leptons just seemed to interact with photons and the intermediate bosons of weak interactions, so there was a suspicion that we could construct a unique theory for both interactions. The weak neutral processes were already proposed by Bludman who added the neutral gauge boson Z^0, a partner of $W^\pm$ [22]. But the complete formulation was proposed by Weinberg and Salam [23], employing the Glashow model but as an SSB of gauge theory using the Higgs mechanism. The main difference between these two models is that Glashow introduced symmetry breaking terms in the Lagrangian instead of using the Higgs mechanism, this led to less definite predictions [23]; for example Glashow could not justify the weak gauge bosons masses in his approach. In 1973 first evidence of neutral weak interactions was found, through the scatterings $\overline{\nu}_\mu + e \to \overline{\nu}_\mu + e$ and the neutrino-quark (nucleon) processes $\overline{\nu}_\mu + N \to \overline{\nu}_\mu + N$, $\nu_\mu + N \to \nu_\mu + N$ using bubble chamber photos at CERN [24].

In the case of symmetry breaking with $m^2 < 0$, we can select the vacuum solution in eq. (2.18). This vacuum state does not break completely the $SU(2)_L \otimes U(1)_Y$ symmetry, instead this solution is invariant under certain gauge transformations which we identify as $U(1)_{\text{em}}$, the gauge group of electromagnetism. These transformations take the form

$$\Phi(x)' = \begin{pmatrix} e^{ie\varphi/2} & 0 \\ 0 & 1 \end{pmatrix}\Phi(x). \tag{2.28}$$

By selecting a vacuum solution with real fluctuations due to gauge invariance and a transformation of a combination of isospin and hypercharge, given by

$$\Phi = \frac{1}{\sqrt{2}} \begin{pmatrix} 0 \\ v + H(x) \end{pmatrix}, \tag{2.29}$$

and expanding the Lagrangian in eq. (2.20) around this vacuum solution eq. (2.29), we find a massive Higgs particle with mass $m_H^2 = -2m^2$, two W-bosons with mass $m_W = gv/2$, along with a linear combination we define the Z_μ field and the photon field A_μ

$$\begin{pmatrix} A_\mu \\ Z_\mu^0 \end{pmatrix} = \begin{pmatrix} \cos\theta_W & \sin\theta_W \\ -\sin\theta_W & \cos\theta_W \end{pmatrix} \begin{pmatrix} B_\mu \\ W_\mu^3 \end{pmatrix}, \tag{2.30}$$

which correspond to a massive Z^0 boson with mass $m_Z = v\sqrt{g^2 + g'^2}/2$ and a massless photon. Now we have an explanation for the bosons mass. We call θ_W the weak mixing angle and it is given by $\cos\theta_W = g/\sqrt{g^2 + g'^2}$ and $\sin\theta_W = g'/\sqrt{g^2 + g'^2}$. Due to the Higgs mechanism, the W and Z bosons become massive. The coupling constant for the photon is the electric charge e and by re-arranging of the fields in the kinetic term, we can identify it with

$$e = \frac{gg'}{\sqrt{g^2 + g'^2}}. \tag{2.31}$$

This is the weak and electromagnetic interaction described as an unified gauge theory, the Glashow-Weinberg-Salam theory.

Quantization of the photon field leads to Quantum Electrodynamics, where the photon is the gauge boson which mediates the electromagnetic interactions. Regarding the discovery of the photon γ we have to go back to the history of light. In 1900 Planck postulated electromagnetic radiation to be quantized with energy quanta $E = \hbar\omega$ and avoided the ultraviolet catastrophe. In that epoch this was understood as a mathematical artifact instead of a change in the understanding of nature. But in 1905 Einstein employed this postulate for the photoelectric effect using a momentum of semi-corpuscular nature for the light, even though this was not a direct proof for the existence of the photon. Finally in 1932 Compton found the scattering of a particle at rest and the shift in the wavelength of light, which indeed proves that the photon is a quantum particle.

The $W^\pm$ and Z^0 bosons were found experimentally in 1983 using a proton-antiproton collider constructed at CERN [25]. The Higgs boson was found in 2012 by the experiments ATLAS [26] and CMS [27], also at CERN.

2.3 Leptons and quarks

Leptons and quarks, which are fermions, should now be included. First let us take a fermion field ψ and distinguish between left-handed (L) and right-handed (R)

$$\psi_{L,R} = \frac{1}{2}(1 \mp \gamma^5)\psi, \tag{2.32}$$

where γ^5 is the product of the Dirac gamma matrices $\gamma^5 = i\gamma^0\gamma^1\gamma^2\gamma^3$, ψ_L and ψ_R are its eigenvectors. The distinction between L and R is called chirality. In the case of massless fermions, chirality and helicity are the same and it is defined as the projection of the spin onto the direction of motion. We say a massless particle is left-handed if the spin is opposite to its direction of motion and right-handed if they have the same direction.

If we work just with the first generation of leptons and quarks, we should include electrons, electron neutrinos and the up and down quarks. First let us consider the leptons. The electron was discovered in 1897 by Thomson using the deflection by an electromagnetic field of cathode rays from a hot filament. The neutrino was a hypothetical particle proposed by Pauli, to justify the energy spectrum of the electron in β-decay, which did not seem to conserve energy. The neutrino was observed in 1956 in the Savannah River nuclear reactor using the inverse β-decay $\overline{\nu} + p \to n + e^+$ [28].

In the SM there are only left-handed neutrinos and they are massless, so this will be our approach in the continuation of this chapter. The other leptons and quarks acquire mass through the Higgs mechanism via Yukawa interaction terms in the Lagrangian. The left-handed neutrino $\nu_L(x)$ and the left-handed electron $e_L(x)$ can be written as a $SU(2)_L$ doublet, while the right-handed electron $e_R(x)$ is written as a singlet, so the Lagrangian reads

$$\mathcal{L} = (\overline{\nu}_L, \overline{e}_L) i\gamma^\mu \left[\partial_\mu + i\frac{g}{2}W^a_\mu \sigma_a - i\frac{g'}{2}B_\mu\right]\begin{pmatrix}\nu_L \\ e_L\end{pmatrix} + \overline{e}_R i\gamma^\mu(\partial_\mu - ig'B_\mu)e_R. \tag{2.33}$$

Defining the charged fields $W^\pm_\mu = (W^1_\mu \mp iW^2_\mu)/\sqrt{2}$ and using the Z^0_μ field and photon field A_μ which are natural after the SSB, we can write the Lagrangian as

$$\begin{aligned}\mathcal{L} =& (\overline{\nu}_L, \overline{e}_L) i\gamma^\mu \begin{pmatrix} \partial_\mu + \frac{i\sqrt{g^2+g'^2}}{2}Z^0_\mu & \frac{ig}{\sqrt{2}}W^+_\mu \\ \frac{ig}{\sqrt{2}}W^-_\mu & \partial_\mu + \frac{i(g'^2-g^2)}{2\sqrt{g^2+g'^2}}Z^0_\mu - \frac{igg'}{\sqrt{g^2+g'^2}}A_\mu \end{pmatrix}\begin{pmatrix}\nu_L \\ e_L\end{pmatrix} \\ &+ \overline{e}_R i\gamma^\mu \left(\partial_\mu - \frac{ig'}{\sqrt{g^2+g'^2}}(g'Z^0_\mu + gA_\mu)\right) e_R.\end{aligned} \tag{2.34}$$

Here we can appreciate how the photon field couples to the electron but not to the neutrino, making it an electrically neutral particle. Indeed we will find that neutrinos interact just through the weak force and the Yukawa couplings.

A first generation of quarks must be added to this first generation of leptons. This is because of the $U(1)_Y$ gauge anomaly which comes from the fermionic triangle diagrams, and Witten's global anomaly in the $SU(2)$ interaction. Adding quarks cancels these gauge anomalies. As they participate in the strong interaction, they carry an $SU(3)$ color charge with the color index $c = \{r, g, b\}$, anomaly cancellation requires an odd number of colors. We can write the left-handed quarks up $u_L(x)$ and down $d_L(x)$ as $SU(2)_L$ doublets, and the right-handed quarks $u_R(x)$, $d_R(x)$ as flavor singlets.

As we mentioned before, we should include a Yukawa term for the electrons to have mass. This term reads

$$\mathcal{L} = f_e\left[\overline{e}_R\Phi^\dagger\begin{pmatrix}\nu_L \\ e_L\end{pmatrix} + (\overline{\nu}_L, \overline{e}_L)\Phi e_R\right] = \frac{f_e}{\sqrt{2}}\left[\overline{e}_R(\phi^*_+, \phi^*_0)\begin{pmatrix}\nu_L \\ e_L\end{pmatrix} + (\overline{\nu}_L, \overline{e}_L)\begin{pmatrix}\phi_+ \\ \phi_0\end{pmatrix} e_R\right]. \tag{2.35}$$

Under the SSB we suppose the Higgs field to choose the VEV

$$\Phi = \frac{1}{\sqrt{2}} \begin{pmatrix} 0 \\ v \end{pmatrix}. \tag{2.36}$$

This will give us an electron mass $m_e = f_e v$ while the neutrino remains massless. For the down quark $d(x)$ we include another Yukawa term

$$\mathcal{L} = f_d \left[\overline{d}_R \Phi^\dagger \begin{pmatrix} u_L \\ d_L \end{pmatrix} + (\overline{u}_L, \overline{d}_L) \Phi d_R \right] = \frac{f_d}{\sqrt{2}} \left[\overline{d}_R (\phi_+^*, \phi_0^*) \begin{pmatrix} u_L \\ d_L \end{pmatrix} + (\overline{u}_L, \overline{d}_L) \begin{pmatrix} \phi_+ \\ \phi_0 \end{pmatrix} d_R \right], \tag{2.37}$$

where we obtain a down quark mass $m_d = f_d v$ and a massless up quark. For the up quark to acquire a mass we should write a slightly different Yukawa term using the Higgs field

$$\widetilde{\Phi} = \frac{1}{\sqrt{2}} \begin{pmatrix} \phi_0^* \\ -\phi_+^* \end{pmatrix}. \tag{2.38}$$

This Yukawa term reads

$$\mathcal{L} = f_u \left[\overline{u}_R \widetilde{\Phi}^\dagger \begin{pmatrix} u_L \\ d_L \end{pmatrix} + (\overline{u}_L, \overline{d}_L) \widetilde{\Phi} u_R \right] = \frac{f_u}{\sqrt{2}} \left[\overline{u}_R (\phi_0, -\phi_+) \begin{pmatrix} u_L \\ d_L \end{pmatrix} + (\overline{u}_L, \overline{d}_L) \begin{pmatrix} \phi_0^* \\ -\phi_+^* \end{pmatrix} u_R \right], \tag{2.39}$$

which provides an up quark mass $m_u = f_u v$.

The next step is to introduce the remaining generations of fermions, following the pattern of the first generation of leptons. The second generation consists of an $SU(2)_L$ doublet with the left-handed muon neutrino $\nu_L^\mu(x)$ and the left-handed muon $\mu_L(x)$, and a singlet with the right-handed muon $\mu_R(x)$. The same reasoning applies to the third generation of leptons, with an $SU(2)_L$ doublet consisting of the left-handed tauon neutrino $\nu_L^\tau(x)$ and the left-handed tauon $\tau_L(x)$, and a singlet for the right-handed tauon $\tau_R(x)$. The muon was discovered in 1947 by Powell et al., in experiments with cosmic rays [7]. The tauon was discovered in 1975 by Perl et al. [29], when observing the reaction $e^- + e^+ \to e^\pm + \mu^\mp + ...$ Then it was proposed and discovered in the reaction $e^- + e^+ \to \tau^- + \tau^+ \to e^\pm + \mu^\mp + 2\nu + 2\overline{\nu}$, where the tau particles are an intermediate state.

The law of lepton number conservation was proposed in 1953 by Konopinsky and Mahmoud [30] in order to discriminate whether certain reactions are possible. They assigned a number $L = +1$ to leptonic particles and $L = -1$ to their anti-particles. Thus in an elementary particle reaction, the lepton number before and after the reaction should be the same according to this law. This explained why the analogous reaction of the β-decay $\overline{\nu} + n \to p + e^-$ has never been observed. The fact that the neutrino is an electrically neutral particle, raised the question if it was its own anti-particle. In addition, lepton number families were defined L_e, L_μ, L_τ to account for the absence of reactions like $\mu^- \to e^- + \gamma$, using also the fact that neutrinos fall in these families.

In the case of the remaining generation of quarks, as we did with the u and d, we write the left-handed quarks as $SU(2)_L$ doublets and the right-handed as singlets. The second generation is composed of the charm (c) and strange (s) quarks and the third generation with the top (t) and bottom (b) quarks.

So in the end we have the three generations of fermionic fields

$$\begin{aligned}
&\begin{pmatrix}\nu_L^e\\ e_L\end{pmatrix}, \quad e_R; \quad \begin{pmatrix}u_L^c\\ d_L^c\end{pmatrix}, \quad u_R^c, \quad d_R^c;\\
&\begin{pmatrix}\nu_L^\mu\\ \mu_L\end{pmatrix}, \quad \mu_R; \quad \begin{pmatrix}s_L^c\\ c_L^c\end{pmatrix}, \quad s_R^c, \quad c_R^c;\\
&\begin{pmatrix}\nu_L^\tau\\ \tau_L\end{pmatrix}, \quad \tau_R; \quad \begin{pmatrix}t_L^c\\ b_L^c\end{pmatrix}, \quad t_R^c, \quad b_R^c.
\end{aligned} \tag{2.40}$$

With these generations we can write a Lagrangian as we did for the first one, including the free terms, the couplings with the gauge fields W_μ, B_μ and the Yukawa interactions, which provide mass through the Higgs mechanism to all fermions except to the neutrinos.

In this version of the SM, neutrinos are massless left-handed particles, while the anti-neutrinos are massless and right-handed. The chirality can be observed experimentally by considering some special decays as follows. First, the β-decay $n \to p + e^- + \overline{\nu}_e$, consisting of a neutron decaying into a proton, an electron and an electron anti-neutrino; or written as a weak interaction $d \to u + W^- \to u + e^- + \overline{\nu}_e$. Parity (P) or mirror symmetry is broken in this process as first observed by Wu and her collaborators in the reaction ${}^{50}_{27}\mathrm{Co} \to {}^{60}_{28}\mathrm{Ni} + e^- + \overline{\nu}_e + 2\gamma$. In the Wu experiment, γ-rays[2] were emitted in two directions, while the observed electrons were preferentially emitted in the direction opposed to the nuclear spin [31]. This was a proof of P-violation and it also implies charge conjugation C-violation [32, 33]. Now let us consider the decay $\pi^- \to \mu^- + \overline{\nu}_\mu$, which was used as an indirect method to measure the anti-neutrino helicity and identify it as right-handed [34]. While even the detection of neutrinos is hard to achieve, these kind of indirect methods accounts for the measurement of the neutrino helicity. When the pion is at rest, the muon and neutrino will come in opposite directions and as the pion has spin 0, the muon and the neutrino spins must be oppositely aligned. This led to identify the neutrino as left-handed and the anti-neutrino as right-handed, with no evidence of a right-handed neutrino or left-handed antineutrino. Indeed this characteristic of the neutrino is the perfect example for P-violation and C-violation.

Now let us focus on the quarks and consider the SSB. We obtain a general quark mass term

$$(\overline{u}_L, \overline{c}_L, \overline{t}_L) M^U \begin{pmatrix} u_R \\ c_R \\ t_R \end{pmatrix} + (\overline{d}_L, \overline{s}_L, \overline{b}_L) M^D \begin{pmatrix} d_R \\ s_R \\ b_R \end{pmatrix}, \tag{2.41}$$

using bi-unitary transformations to the 3×3 mass matrices M^U and M^D defined above. We can diagonalize them by

$$U_L^{U\dagger} M^U U_R = \mathrm{diag}(m_u, m_c, m_t), \quad U_L^{D\dagger} M^D U_R = \mathrm{diag}(m_d, m_s, m_b), \tag{2.42}$$

where the terms in the diagonals are the physical quark masses. Subsequently, we relate the gauge eigenstates f to the mass eigenstates f' as

$$\begin{pmatrix} u_L \\ c_L \\ t_L \end{pmatrix} = U_L^U \begin{pmatrix} u'_L \\ c'_L \\ t'_L \end{pmatrix}, \quad \begin{pmatrix} u_R \\ c_R \\ t_R \end{pmatrix} = U_R^U \begin{pmatrix} u'_R \\ c'_R \\ t'_R \end{pmatrix}, \tag{2.43}$$

[2]The resulting ^{60}Ni nuclei is in an excited state and decays to its ground state through the emission of two photons. These photons are measured and used to determine the nuclei polarization and its associated anisotropy.

$$\begin{pmatrix} d_L \\ s_L \\ b_L \end{pmatrix} = U_L^D \begin{pmatrix} d'_L \\ s'_L \\ b'_L \end{pmatrix}, \quad \begin{pmatrix} d_R \\ s_R \\ b_R \end{pmatrix} = U_R^D \begin{pmatrix} d'_R \\ s'_R \\ b'_R \end{pmatrix}. \tag{2.44}$$

The Cabbibo-Kobayashi-Maskawa (CKM) quark mixing matrix is given by

$$V = U_L^{U\dagger} U_L^D \in U(3), \tag{2.45}$$

which accounts for the strength of the flavour-changing weak interactions coming from the charged currents. Examples of flavor changing transitions are the β-decay mentioned before, and the decay $\Lambda \to p + e + \overline{\nu}_e$, where respectively the involved processes are $u \to d + W^-$ and $s \to u + W^-$.

In order to explain the decay rates of these two processes, in 1963 Cabibbo suggested an extra factor of $\cos\theta_C$ and $\sin\theta_C$ in the vertex of the Feynman diagrams of these processes respectively [35], where θ_C is known as the Cabibbo angle. Explicitly, as we can foresee from the eq. (2.44), they are related as

$$\begin{pmatrix} d' \\ s' \end{pmatrix} = \begin{pmatrix} \cos\theta_C & \sin\theta_C \\ -\sin\theta_C & \cos\theta_C \end{pmatrix} \begin{pmatrix} d \\ s \end{pmatrix}. \tag{2.46}$$

However, the Cabibbo angle caused another problem, it predicted the decays $\overline{K}^0 \to \mu^- + \mu^+$, $K^+ \to \pi^+ + l + \bar{l}$, etc., which do not happen in nature. This problem was solved by Glashow, Iliopoulos and Maiani (GIM) in 1970 by introducing a forth quark, the charm [36]. We can see two Feynman diagrams for the leptonic decay of the neutral kaon in Fig. 2.4. These diagrams cancel each other due to the large W mass, suppressing this neutral current.

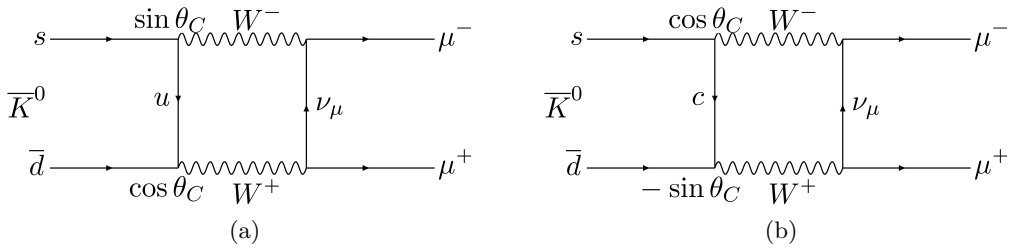

Figure 2.4: Leptonic decay of the neutral kaon.

By that time just three quark flavors were known, according to the content of discovered particles. Four years later, the charm quark was found by experimental evidence through the discovery of the ψ/J meson. The interpretation of the GIM scheme was that instead of using the quarks d, s, in weak interactions one should use the mass eigenstates d', s'.

Subsequently the other quark flavors were found. The fifth quark flavor b was discovered through the meson Υ and the sixth quark flavor t was discovered through the processes $u + \overline{u} \to t + \overline{t}$ and $d + \overline{d} \to t + \overline{t}$ in 1995 with the Tevatron.

For three generations of matter, that is with the six quark flavors, Kobayashi and Maskawa in 1973 [37] generalized the Cabibbo-GIM scheme in a 3×3 matrix V given in eq. (2.45). This matrix has 9 parameters but some of them are redundant. In fact there are just four free parameters, three mixing angles θ_C^i (or Cabibbo angles) and a complex phase δ.

P, C and CP (the combination of charge and parity symmetries) are violated in weak interactions. We have seen how processes involving neutrinos violate P and C, but CP is not violated by neutrinos. Nevertheless, CP is violated in other weak interactions, for example in processes involving neutral kaons decays. This is accommodated in the SM as above, by the introduction of the complex phase δ in the CKM matrix.

At last we repeat that neutrinos in the SM are considered to be massless. However this is not true. A consequence of neutrinos being massive particles[3] is neutrino oscillations. The first observation of neutrino oscillations was found in the Super-Kamiokande experiment in 1998 with atmospheric neutrino fluxes [38] and in the SNO experiment in 2001 [39]. This phenomenon can be understood as a lepton mixing process, where neutrinos in a certain lepton family changes into a different one. In analogy to the CKM matrix, this can be explained in what is known as the Pontecorvo-Maki-Nakagawa-Sakata (PMNS) matrix [40, 41].

Extensions of the SM can be made to include neutrino masses in several ways, adding for example Dirac or Majorana terms to the Lagrangian. For the Dirac neutrinos, the mass term uses the Higgs mechanism as we have already seen

$$\mathcal{L} = f_\nu \left[\overline{\nu}_R \widetilde{\Phi}^\dagger \begin{pmatrix} \nu_L \\ e_L \end{pmatrix} + (\overline{\nu}_L, \overline{e}_L) \widetilde{\Phi} \nu_R \right] = \frac{f_\nu}{\sqrt{2}} \left[\overline{\nu}_R (\phi_0, -\phi_+) \begin{pmatrix} \nu_L \\ e_L \end{pmatrix} + (\overline{\nu}_L, \overline{e}_L) \begin{pmatrix} \phi_0^* \\ -\phi_+^* \end{pmatrix} \nu_R \right]. \quad (2.47)$$

This is a Yukawa interaction and the right-handed neutrino is sterile because it is not coupled to any gauge field.

On the other hand, for Majorana neutrinos, the neutrino is its own anti-particle. The mass term can be written as

$$\mathcal{L} = \frac{1}{2} (\overline{\nu}_R M_R C \overline{\nu}_R^T + \nu_R^T C M_R^\dagger \nu_R), \quad (2.48)$$

where C is the charge conjugation matrix. This mass term violates the lepton number by $\Delta L = \pm 2$. One of the major consequences of Majorana neutrinos is the still undetected neutrinoless double β-decay.

[3] This holds for at least two of the three generations.

Chapter 3

Topological defects

Topological defects can be found in a great variety of systems in condensed matter. Some examples are the quantized magnetic flux lines in type-II superconductors, vortices in superfluids as ^{3}He or ^{4}He, dislocations and other defects in crystals. Furthermore some proposals in and beyond the SM exist with cosmological effects. Some examples of topological defects include dislocations, domain walls, monopoles, textures, instantons, time dependent solitons and vortices. Topological defects are associated with phase transitions since they arise from SSB and they are characterized by the topological properties of the order parameter space or vacuum manifold. Thus, topology can help us to establish a classification and prediction of this type of phenomena in a physical system.

Within his contributions to the standard theory of phase transitions, particularly in his studies about critical phenomena, Lev Landau, around the year 1932, was motivated to define the order parameter η to characterize thermodynamic systems near their critical point [42]. This was done by expressing the molar Gibbs free energy (or another thermodynamic potential) as a power series of η, as an assumption. The order parameter is defined as a property of the system that takes the value $\eta = 0$ in a symmetric or disordered phase, and $\eta \neq 0$ at an ordered phase. While Landau's theory was successful in predicting critical exponents, sometimes with a numerical value near the experimental one, the analytic solution of the 2-dimensional Ising model by Lars Onsager [43] was in contradiction. The order parameter led to conceptual clarity and now we understand Landau's proposal as an effective description.

The order parameter contains information about the topological defects. Phase transitions are frequently associated with SSB. The SSB is a process in which an ordered state emerges from a state of higher symmetry phase. This can lead to the formation of certain kinds of defects defined as high symmetry regions covered by an ordered phase. The existence of topological defects is related to the topology in which the order parameter of the system is defined, which corresponds to a degenerate vacuum.

In order to clarify some concepts let us consider the molecular structure of water as an example. In its liquid phase, water has a continuous translational symmetry and a continuous rotational symmetry. But in the solid phase, the ice, water acquires a crystal structure that

breaks these symmetries. Now it is invariant only under discrete translations and rotations. We can see this in Fig. 3.1, ice (left) is just invariant under 120° rotations and not under arbitrary rotations as in the liquid phase (right). In this way we identify the symmetric phase with the disordered phase while the ordered phase corresponds to symmetry breaking.

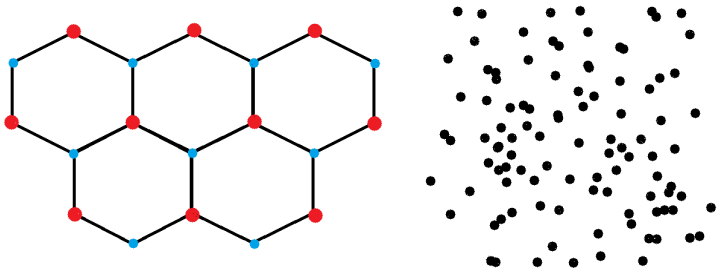

Figure 3.1: Molecular structure of water in its solid phase (left) and liquid phase (right).

Another example is the 2-dimensional Ising model. It is formulated on a lattice where each point carries a classical spin σ_i that can only take two values ± 1. The spins could represent atomic dipolar moments. This is one of the simplest models of statistical physics that exhibits a phase transition. There is a paramagnetic and a ferromagnetic phase. In the high temperature regime, spins are randomly distributed and the magnetization is $M = \sum_i \sigma_i/N = 0$. In this phase, the Hamiltonian has a $\mathbb{Z}^2$ symmetry, it is spin flip invariant $\sigma_i \to -\sigma_i \ \forall \ i$. But when the system cools down, the spins align. In this phase, the spin rotation symmetry is broken and magnetization is non-zero. Thus, the order parameter is the magnetization $M = \sum_i \sigma_i/N$.

Now let us consider a ferromagnetic model, where spins are defined in space on a 3-dimensional lattice. Spins are now 3-dimensional unit vectors and their direction is randomly distributed in the symmetric phase where the order parameter is zero. But in the ferromagnetic phase, spins align in an arbitrary direction. This gives rise to a parameter space equivalent to a 2-sphere, as we can see in Fig. 3.2, and it corresponds to the direction of the magnetization.

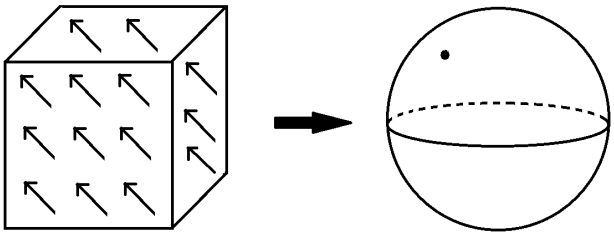

Figure 3.2: The parameter space for a 3-dimensional ferromagnet is equivalent to a 2-sphere.

Homotopy groups are used to classify topological spaces and they contain information about the basic shape or holes on a manifold. The definition of the n-th homotopy group π_n is given as follows. Let us consider two maps that preserve the base point $f, g : S^n \to \mathcal{M}$ defined from the n-sphere to a topological space or manifold $\mathcal{M}$. These maps are homotopic if they can be smoothly deformed into each other. Such homotopic maps form an equivalence class and each

map can be considered as an element of a group called π_n, the n-th homotopy group. Figure 3.3 shows an application of the homotopy group π_1 which consist of closed curves in space. In this way we show how two topological spaces X and Y are distinct. In this figure the curves α and β are homotopic, but α' and β' are not, because α' contains a hole and it can't be continuously deformed into β'.

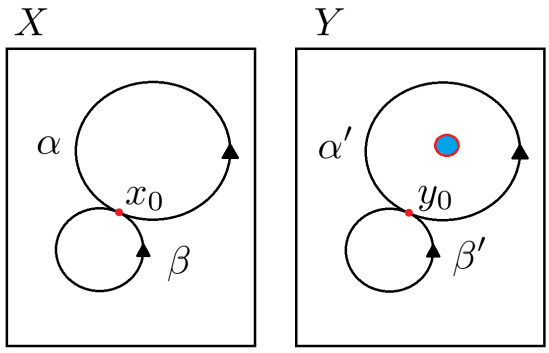

Figure 3.3: Two distinct topological spaces X and Y.

Now let us consider an example of an application of the homotopy groups in topological defects. For a crystal, the important degrees of freedom are associated to translational symmetry breaking. The order parameter for a 2-dimensional lattice is the displacement $\vec{d}'(\vec{r})$ which is given by

$$\vec{d}'(\vec{r}) = \vec{d}(\vec{r}) + na\hat{x} + ma\hat{y}, \tag{3.1}$$

where $\hat{x}$ and $\hat{y}$ are the unit vectors in the plane. This displacement takes an ion from the real lattice to the ideal regular lattice and this implies discrete translational symmetry. (n, m) are integers and a is the lattice spacing. However in the presence of a dislocation, this symmetry is lost. The set of equal order parameters form a lattice with periodic boundary conditions, which is equivalent to a 2-torus. In Fig. 3.4 we see a dislocation in a lattice as a hole; a curve surrounding it is represented as a curve which contains the center of the torus. We have an infinite number of curves but we can classify them in two types, those which contain the hole and those that do not. This can be described by two integers and it is important to highlight that the homotopy of the torus is $\pi_1(T^2) = \mathbb{Z} \otimes \mathbb{Z}$.

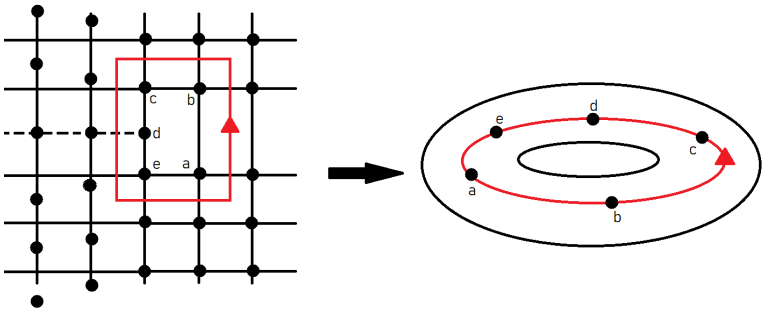

Figure 3.4: Dislocation on a lattice represented with a closed curve that contains the center of the torus.

In this way a pair of integers (n, m), which are the winding numbers, determines the number of extra rows and columns of atoms, respectively. The winding number of a curve is the number of times a curve turns around the image of the map, as depicted in Fig. 3.5.

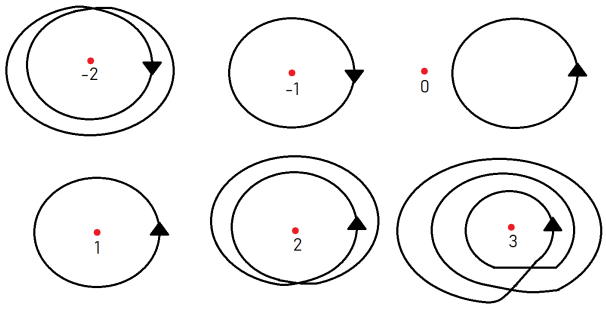

Figure 3.5: Winding number.

Up to now, we have taken just classical physics examples. In Quantum Mechanics and in QFT, instead of an order parameter, we use the wavefunction and the vacuum manifold, respectively. In this terminology we will take the vacuum state. If this state space is topologically non-trivial, particularly if there are non-trivial homotopy groups, then it can have topological defects. In this case, a QFT is described by a symmetry group $\mathcal{G}$, and under a SSB to a symmetry group $\mathcal{H}$, topological defects arise if the homotopy group of the quotient space $\mathcal{M} = \mathcal{G}/\mathcal{H}$ (the space of all accessible vacua) is topologically non-trivial, i.e. $\pi_n(\mathcal{M}) \neq 1$. This translates to a system that has different ground states: in certain regions the system will choose different states and the differences will be the topological defects.

3.1 Vortices

3.1.1 Type-II superconductors

A superconductor is a type of material whose electric resistance falls abruptly to zero below a critical temperature. This phenomenon was discovered in 1911 by Kamerlingh Onnes [44]. Additionally the magnetic fields are repelled by this material, this is known as the Meissner effect [45].

Superconductivity is a quantum phenomenon that, although it may seem like a classical idealization of conductivity, is conventionally explained by the microscopic theory of BCS (Bardeen-Cooper-Schrieffer) [46]. This theory states that two electrons can be correlated to form a Cooper pair. The mechanism consists of an electron moving through the material that attracts positive charge around it, this in turn will attract a second electron overcoming the Coulomb repulsion, with the opposite spin moving in the region of greater positive charge than the first electron. Superconductivity is explained as a macroscopic effect of the condensation of Cooper pairs.

Superconductors have a classification as type-I and type-II. For the first type there is only one critical magnetic field H_c, the maximum magnetic field in which the material keeps being

superconducting and the magnetic field is expelled from the material. It is exponentially suppressed in the penetration depth. On the other hand, type-II superconductors have two critical fields H_{c1} and H_{c2}, in the region between them, the magnetic field is able to penetrate in certain points called vortices.

Figure 3.6 shows vortices in the magnetic field of a 200 nm thin film of Yttrium Barium Copper Oxide (YBCO), which is a ceramic superconducting material composed of oxides of yttrium, barium and copper. This figure was taken from Ref. [47], which used the SQUID technique for microscopy by superconducting quantum interference scanning, in order to measure the local magnetic field on the surface of the thin film.

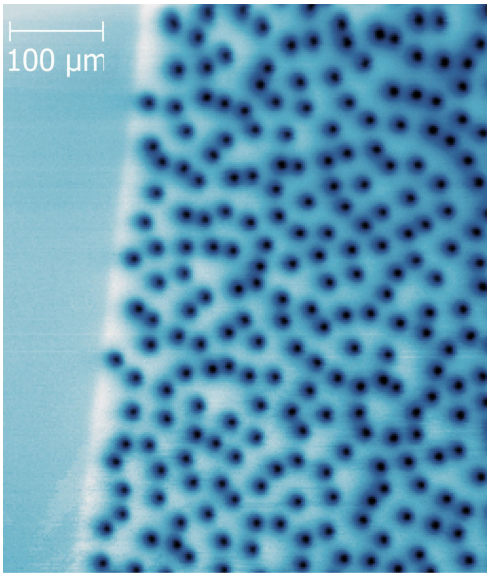

Figure 3.6: Vortices in the local magnetic field of a 200 nm thin film of YBCO superconductor, image taken from Ref. [47].

Let us start from the Ginzburg-Landau theory to obtain an equation of motion for the vortices in a superconductor. The wavefunction ψ represents the superconducting electrons and the modulus $|\psi|$ is the analogue of the order parameter in this quantum phenomenon. The ordered phase is the superconducting phase, and for higher temperatures above a critical temperature T_c, one obtains $|\psi| = 0$. For lower temperatures one obtains $|\psi| \neq 0$. The free energy F can be expressed as a series in $|\psi|$ around T_c as we have seen in Landau's proposal

$$F = F_0 + \alpha|\psi|^2 + \frac{\beta}{2}|\psi|^4, \tag{3.2}$$

subject to the equilibrium conditions

$$\frac{\partial F}{\partial|\psi|^2} = 0, \quad \frac{\partial^2 F}{\partial^2|\psi|^2} > 0. \tag{3.3}$$

In this way we can determine the coefficients in the critical point as $\alpha_c = 0$ and $\beta_c > 0$, while for $T < T_c$, we obtain $\alpha < 0$. In the equilibrium superconducting phase we arrive at

$$0 = \frac{\partial F}{\partial|\psi|^2} = \alpha + \beta|\psi|^2, \tag{3.4}$$

which determines

$$|\psi|^2 = |\psi_\infty|^2 = -\frac{\alpha}{\beta} = -\frac{T_c - T}{\beta_c}\left(\frac{d\alpha}{dT}\right)_c, \tag{3.5}$$

where we assume $\alpha(T) = (T_c - T)(d\alpha/dT)_c$ and $\beta(T) = \beta_c$ as valid in the expansion. Substituting in eq. (3.2) we also obtain

$$\begin{aligned} F &= F_0 + \alpha|\psi|^2 + \frac{\beta}{2}|\psi|^4 = F_0 - \alpha\frac{\alpha}{\beta} + \beta\frac{\alpha^2}{2\beta^2} \\ &= F_0 - \frac{\alpha^2}{2\beta} = F_0 - \frac{(T_c - T)^2}{2\beta_c}\left(\frac{d\alpha}{dT}\right)_c^2. \end{aligned} \tag{3.6}$$

Now let us assume the superconductor to be immersed in a time-independent magnetic field. The above equation has to be modified to include the energy density of the magnetic field $H^2/8\pi$, where $\vec{H}$ is the magnetic field strength, and the kinetic energy density in quantum mechanics

$$\frac{\hbar^2}{2m}|\nabla\psi|^2 \to \frac{1}{2m}\left|-i\hbar\nabla\psi - \frac{2e}{c}\vec{A}\psi\right|^2, \tag{3.7}$$

where $\vec{A}$ is the vector potential. This substitution is due to the fact that in the presence of a magnetic field, the canonical moment is used for a Cooper pair of charge $2e$ [48], which gives rise to the above expression. In this way, the free energy takes the form

$$F = F_0 + \alpha|\psi|^2 + \frac{\beta}{2}|\psi|^4 + \frac{H^2}{8\pi} + \frac{1}{2m}\left|i\hbar\nabla\psi + \frac{2e}{c}\vec{A}\psi\right|^2. \tag{3.8}$$

Now, in order to obtain the equations of motion outside the superconductor $z > 0$, we vary the free energy $\mathcal{F} = \int F dV$ with respect to ψ^* (or ψ for the conjugated equation) requiring it to be minimal

$$\delta_{\psi^*}\mathcal{F} = \int dV \left(\alpha\psi + \beta\psi|\psi|^2 + \frac{1}{2m}\left(i\hbar\nabla\psi + \frac{2e}{c}\vec{A}\psi\right)^2\right)\delta\psi^* = 0. \tag{3.9}$$

If we write

$$\left(i\hbar\nabla\psi + \frac{2e}{c}\vec{A}\psi\right)^2\delta\psi^* = \left(i\hbar\nabla + \frac{2e}{c}\vec{A}\right)^2\psi\delta\psi^* + \hbar\nabla\cdot\left(\hbar\nabla - \frac{2ie}{c}\vec{A}\right)\psi\delta\psi^*, \tag{3.10}$$

we obtain a term as a total derivative (the term with the divergence) that will give zero when being integrated due to the boundary conditions, so the minimum free energy condition results in an equation of motion that takes the form

$$\alpha\psi + \beta\psi|\psi|^2 + \frac{1}{2m}\left(i\hbar\nabla + \frac{2e}{c}\vec{A}\right)^2\psi = 0. \tag{3.11}$$

Under an appropriate re-scaling of the variables $\vec{r}$, ψ and $\vec{A}$ [49], this equation can be written in a dimensionless form as

$$\left(\frac{i}{\chi}\nabla + \vec{A}\right)^2\psi = \psi - \psi|\psi|^2. \tag{3.12}$$

The parameter

$$\chi^2 = \frac{1}{2\pi}\left(\frac{mc}{2e\hbar}\right)^2, \tag{3.13}$$

is used to classify superconductors. Ginzburg and Landau only considered cases with small χ ($\chi \ll 1/\sqrt{2}$). But Zavaritskii and Abrikosov [50, 51] showed that for $\chi > 1/\sqrt{2}$ they could describe thin films of pure condensed metals and suggested the division of superconductors in two groups: type-I superconductors with $\chi < 1/\sqrt{2}$ and type-II with $\chi > 1/\sqrt{2}$. This parameter is used to determine the surface tension between the superconducting and normal phases of a material.

Analogously we obtain an equation of motion for the field $\vec{A}$, for which we also impose the minimum condition on the free energy

$$\delta_{\vec{A}}\mathcal{F} = \int dV \left(\frac{2H\delta\vec{H}}{8\pi} + \frac{2e\delta\vec{A}}{2mc} \; * \left(i\hbar\nabla\psi + \frac{2e}{c}\vec{A} \right) + \text{c.c.} \right), \tag{3.14}$$

where the second and third term (its complex conjugate) come from expressing the modulus $|w|^2$ of a complex function as $\overline{w}w$. The first term is

$$\frac{H\delta\vec{H}}{4\pi} = \frac{1}{4\pi}\nabla\times\vec{A}\cdot\delta\nabla\times\vec{A} = \frac{1}{4\pi}\nabla\times\vec{A}\cdot\nabla\times\delta\vec{A}. \tag{3.15}$$

Using the vector identity

$$\nabla\cdot\left(\vec{a}\times\vec{b}\right) = \vec{a}\cdot(\nabla\times\vec{b}) - \vec{b}\cdot(\nabla\times\vec{b}), \tag{3.16}$$

we can write

$$\nabla\times\vec{A}\cdot\nabla\times\delta\vec{A} = \nabla\cdot\left(\delta\vec{A}\times\nabla\times\vec{A}\right) + \nabla\times\nabla\times\vec{A}, \tag{3.17}$$

and in this way, omitting the total derivative, we obtain the equation

$$\nabla\times\nabla\times\vec{A} = -\frac{e}{mc} \; * \left(i\hbar\nabla\psi + \frac{2e}{c}\vec{A} \right) + \text{c.c.} \tag{3.18}$$

With the same change of variables used before, this can be written in a dimensionless form

$$\nabla\times\nabla\times\vec{A} = -|\psi|^2\vec{A} + \frac{1}{2\chi}\left(\psi^*\nabla\psi - \psi\nabla\psi^*\right). \tag{3.19}$$

Equations (3.12) and (3.19) are the Ginzburg-Landau equations for the superconductors [49]. Let us suppose the superconductor to occupy all the volume and the field $\vec{A}$ to be oriented in the y direction [51],

$$\vec{A} = H_0 x\hat{y}, \quad \vec{H} = H_0\hat{z}. \tag{3.20}$$

As a first approximation we can neglect the effects of ψ in the vector field, so we can use just the linearized version of eq. (3.12). Solving by variable separation and assuming z-independence

$$\psi(x, y; k) = e^{iky}\phi(x), \tag{3.21}$$

where k is the wavenumber, eq. (3.12) takes the form

$$\frac{d^2\phi}{dx^2} = -\chi^2\phi\left[1 - H_0^2\left(x - \frac{k}{\chi H_0}\right)^2\right]. \tag{3.22}$$

This is the harmonic oscillator equation, and a physical solution is given by the condition

$$\chi = H_0(2n+1), \tag{3.23}$$

where n is an integer. Thus, the general solution is a linear combination [51]

$$\psi(x,y) = \sum_{n=-\infty}^{\infty} C_n e^{ikny} \exp\left(-\frac{\chi^2}{2}\left(x - \frac{k}{\chi^2}\right)^2\right). \tag{3.24}$$

To illustrate the behaviour of this solution let us do some simplifications. First let us note that this solution is periodic in y with period $y_0 = 2\pi/k$. Let us take a simple example that will reproduce a rectangular lattice, this is given when we take the same value for the coefficients C_n. In this way, the periodicity range in x is $x_0 = k/\chi^2$ and we obtain a square lattice geometry with area $x_0 y_0 = 2\pi/\chi^2 = \xi^2$ corresponding to a quantum of flux per cell and ξ is the correlation length. The solution is then

$$\psi(x,y) = C\sum_{n=-\infty}^{\infty} \exp\left(2\pi i\frac{ny}{y_0}\right)\exp\left(-\frac{\chi^2}{2}(x - x_0 n)^2\right) \tag{3.25}$$

and we show the modulus $|\psi|$ of the solution in Fig. 3.7.

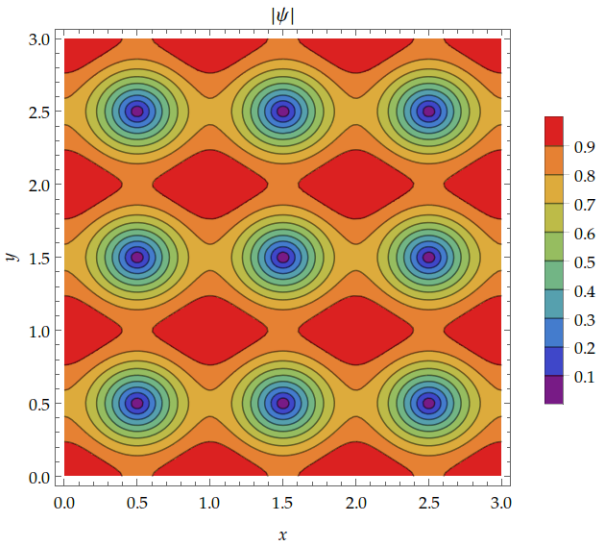

Figure 3.7: Contour lines of the solution $|\psi|$ with square lattice symmetry.

To give an interpretation to this result, let us note that from eq. (3.19) we can define the current

$$\vec{J} = -|\psi|^2\vec{A} + \frac{1}{2\chi}\left(\psi^*\nabla\psi - \psi\nabla\psi^*\right). \tag{3.26}$$

The solution given in eq. (3.25) allows us to relate the derivatives as

$$\frac{\partial\psi}{\partial x} = -i\frac{\partial}{\partial y} - H_0 x\psi. \tag{3.27}$$

For the component J_x, remembering $\vec{A}$ is oriented in the y-axis, it is clear that

$$\begin{aligned} i\psi^*\frac{\partial}{\partial x} - i\psi\frac{\partial\psi^*}{\partial x} &= i\psi^*\left(-i\frac{\partial}{\partial y} - H_0 x\psi\right) - i\psi\left(i\frac{\partial}{\partial y}^* - H_0 x\psi^*\right) \\ &= \psi^*\frac{\partial\psi}{\partial y} + \frac{\partial\psi^*}{\partial y} \\ &= \frac{\partial|\psi|^2}{\partial y}. \end{aligned} \tag{3.28}$$

The component J_y behaves analogously. In this way we can write the components of the current as

$$J_x = -\frac{1}{2\chi}\frac{\partial|\psi|^2}{\partial y}, \quad J_y = \frac{1}{2\chi}\frac{\partial|\psi|^2}{\partial x}. \tag{3.29}$$

Thus we can conclude that $|\psi|^2$ is the current function since the flux runs through lines with constant $|\psi|$. We define a *quantized vortex* as a linear object (in 3 dimensions) that is characterized by a quantized circulation of the phase of the order parameter around this line. This theoretical prediction in superconductors was made by Abrikosov in 1957 [51]. In the case of type II superconductors, a second order phase transition to a superconducting phase occurs with the formation of quantized vortices. More precisely, because of z-independence, the vortices are in fact filaments or strings, that when intersected with a plane we see the vortices as in Fig. 3.7, together with the direction of the flux given by the current in Fig. 3.8.

Up to now, the analysis presented here treats multiple vortices near each other at a distance of the coherence length order. The coherence length is the characteristic distance in which the order parameter goes from zero in the center of the vortex to its asymptotic value outside the core. Nevertheless we also study the case of a single vortex in 3 dimensions, considering cylindrical coordinates and independence of the z-axis. So we start from the ansatz

$$= f(\rho)e^{i\phi}, \tag{3.30}$$

where ρ is the radial distance and ϕ is the azimuthal angle. With this ansatz and a vector field given in the angular direction $\vec{A} = A_\varphi\hat{\varphi}$, using the non-linear eq. (3.12), the equation of motion becomes

$$\frac{\partial^2 f}{\partial\rho^2} + \frac{1}{\rho}\frac{\partial f}{\partial\rho} = \left(\frac{4e^2Q^2}{\hbar^2c^2} + \chi^2 - \chi^2 f^2\right) f, \tag{3.31}$$

where we have used a gauge transformation in the vector potential

$$\vec{Q} = \vec{A} - \frac{\hbar c}{2e}\nabla\lambda = \left(A_\varphi - \frac{\hbar c}{2e\rho}\right)\hat{\varphi} = Q\hat{\varphi}. \tag{3.32}$$

On the other hand, for the equation of motion of the vector potential we obtain

$$\nabla\times\nabla\times\vec{Q} + f^2\vec{Q} = \vec{0}, \tag{3.33}$$

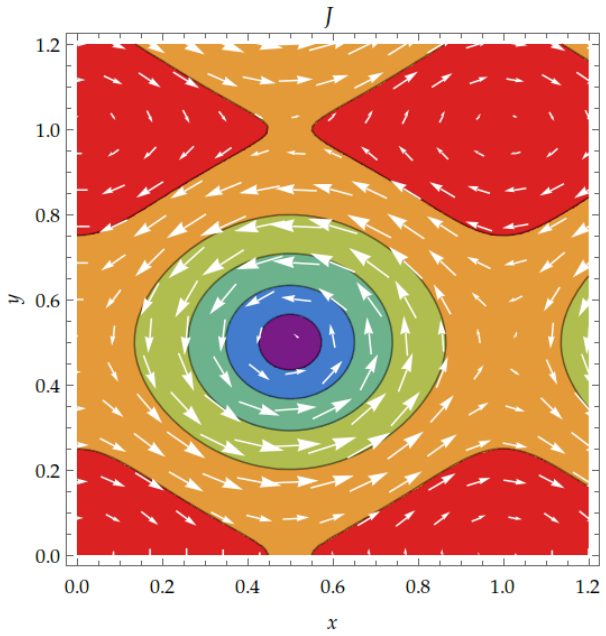

Figure 3.8: Current as a vector field in the vortex.

and simplifying

$$\frac{\partial^2 Q}{\partial \rho^2} + \frac{1}{\rho}\frac{\partial Q}{\partial \rho} = \frac{Q}{\rho^2} + f^2 Q. \tag{3.34}$$

Equations (3.31) and (3.34) are a system of non-linear second order differential equations which describe superconductivity, they relate and determine the wavefunction and vector potential, which can be solved numerically. Equivalently, they relate the current and electromagnetic field.

3.1.2 Superfluids

Superfluidity is a fluid state of matter with no viscosity. Some superfluids also exhibit vortices in complete analogy with superconductors. But a difference is that in this case, circulation is quantized. And instead of an electromagnetic field, we talk about a velocity field.

Beyond an analogy, we can argue as follows: a universality class is a set of physical systems that have the same critical behavior. It turns out that the behavior of a superconductor near its critical region is classified within the class of universality of λ-transitions. Within this class there are also some superfluids such as ^{3}He, ^{4}He and liquid crystals [52]. This class regroups systems with a phase diagram which has the shape of the Greek letter λ.

In a low temperature regime, the helium isotopes ^{3}He, which is a fermion, and ^{4}He, which is a boson, reach the superfluid phase. Because of its bosonic nature, ^{4}He is easier to describe. Figure 3.9, taken from Ref. [53], shows the structure of these vortices shaped as filaments or strings (as we mentioned before when using cylindrical symmetry). The visualization of these filaments is done by injecting cold hydrogen atoms, which are then trapped by the vortices.

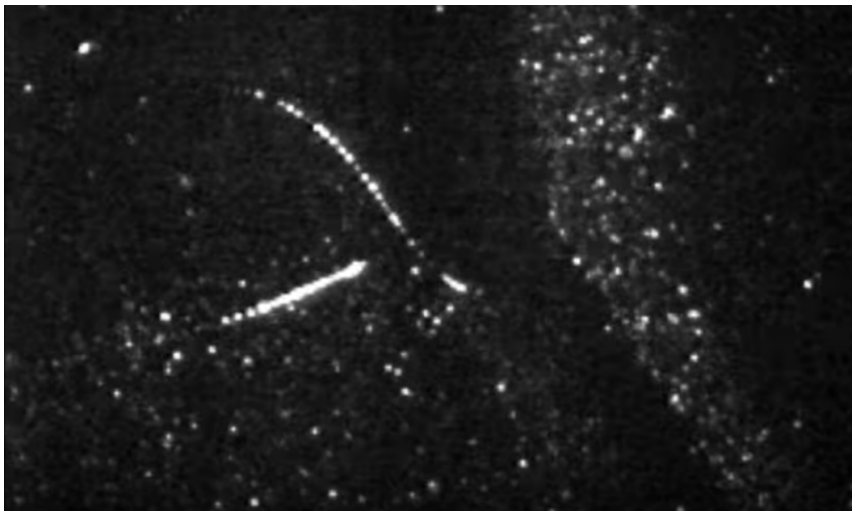

Figure 3.9: Visualization of filaments in ^{4}He superfluid, image from Ref. [53].

When a substance such as ^{4}He cools down sufficiently, it achieves Bose-Einstein condensation and a fraction of it is in its ground state described by a macroscopic wavefunction ψ which represents the superfluid state as a coherent one. The wavefunction can be written as

$$\psi(\vec{r}) = Ae^{i\phi} = A\exp\left(i\frac{m_4}{\hbar}\vec{v}_S\cdot\vec{r}\right), \tag{3.35}$$

where m_4 is the mass of a ^{4}He atom, A is the amplitude and $\vec{v}_S$ is the superfluid velocity. The phase can be written in this way, as in the case of a free particle. Because of the topology of space which, might contain holes, we see that the circulation is quantized

$$\oint \vec{v}_S\cdot d\ell = \frac{nh}{m_4}. \tag{3.36}$$

Therefore, around a singularity we expect circulation to be quantized in units of h/m_4 and the formation of a vortex around it. Because of the macroscopic wavefunction, this imply that the vortex is indeed a vortex line, as in the case of superconductors. Typically, for ^{4}He the core radius of those vortices amounts to 0.1 nanometers and therefore the coherence length is very short.

The fermion nature of ^{3}He changes the behaviour of the phase diagram and indeed we find two superfluid phases A and B with distinct magnetic properties. Figure 3.10 shows the phase diagram of ^{3}He. We have a second order phase transition from the fluid to the superfluid A phase and a first order from A to B, both occur by reducing the temperature. The superfluid A phase is reached at a lower temperature of the order of miliKelvin [54, 55], where nuclei correlate to form pairs by an attractive interaction and we can use the BCS theory to describe this new state of matter. This attractive interaction takes place because of the magnetic properties, namely the nuclear magnetic moment. So as it happens in superconductors, an atom of ^{3}He leaves the medium polarized and attracts another ^{3}He atom.

For superfluids like ^{3}He, the order parameter turns out to be a 3×3 matrix, which is the vector representation of the symmetry group $SO(3)$ of the Cooper pair amplitude $\langle a_\sigma(\vec{p})a_{\sigma'}(-\vec{p})\rangle$.

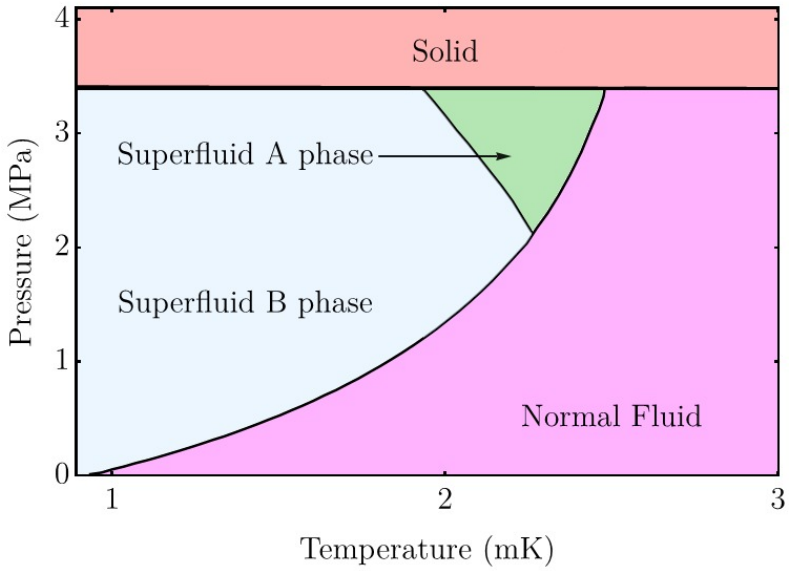

Figure 3.10: Phase diagram of ^{3}He.

This is a correlator where a is the annihilation operator and σ is the spin index. The pairs of ^{3}He contain extra degrees of freedom because of their properties, they involve spin and angular momentum. In the superfluid phase, the spin-orbit symmetry is spontaneously broken [55] which gives rise to net (collective) spin and spatial ordering. Other symmetries are also broken in this system but they are not relevant for this discussion. The A phase contains states of equally paired spins $|\uparrow\uparrow\rangle$, $|\downarrow\downarrow\rangle$ while the B phase involves also the unpaired state $(|\uparrow\downarrow\rangle + |\downarrow\uparrow\rangle)/\sqrt{2}$.

The same arguments apply to the case of superfluid ^{3}He in the formation of vortices, even though due to a more complicated nature, there are several types of vortices. As we saw above for a superfluid velocity $\vec{v}_S$, we will find the circulation to be quantized

$$\oint \vec{v}_S \cdot d\ell = \frac{nh}{2m_3}, \tag{3.37}$$

where m_3 is the mass of a ^{3}He atom and the factor of 2 comes from the pairing. One of the main differences with ^{4}He is that in ^{3}He, the coherence length is much larger, which requires more energy for regular quantized vortex lines to form. However this is not an impediment in both phases and also implies the existence of meta-stable vortices. These additional types of vortices [52, 56] are for the A phase the half-integer quantized vortex lines and the vortex sheets which occur by a planar soliton singularity[1]. In the case of the B phase there are vortex lines with double core and hybrid spin-mass vortices consisting of a linear mass vortex, a linear spin vortex and a planar soliton singularity.

[1] A domain wall which separates two regions with perpendicular spin and angular momenta in opposite direction.

3.2 Topology in field theory

As we mentioned before, baryon number B and lepton number L conservation laws were proposed. However now we know that at very high energy, the SM allows B and L violations, even though this has not been observed experimentally. These violations correspond to the Adler-Bell-Jackiw anomaly

$$\partial^\mu J^B_\mu = \partial^\mu J^L_\mu = N_g \mathcal{P} = -\frac{N_g}{32\pi^2}\epsilon^{\mu\nu\rho\sigma}\mathrm{Tr}[W_{\mu\nu}W_{\rho\sigma}], \tag{3.38}$$

in the divergence of the B current J^B_μ which equals the divergence of the L current J^L_μ. N_g is the number of fermion generations and $\mathcal{P}$ is known as the Chern-Pontryagin density. $W_{\mu\nu}$ is the field strength tensor of the $SU(2)_L$ gauge field W_μ. This anomaly is caused by the winding of the weak gauge fields. At the classical level, the divergence of a current must be zero to obtain a conservation law. But upon quantization, these divergences pick up quantum corrections known as instanton and sphaleron processes that represent the violations. From this equation we can also see that the baryon and lepton currents have the same anomaly, so $B - L$ is still preserved.

For simplicity, we first consider the vacuum structure of the $SU(2)$ gauge theory. It contains a set of classical vacua. These states can't be transformed continuously into one another without passing through non-vacuum states, since they are separated by energy barriers. On the other hand, $SU(2)$ is topologically equivalent to the 3-sphere S^3. This means that the vacuum states can be characterized as elements in $\pi_3(S^3) = \mathbb{Z}$. Vacuum states can be divided into different topological sectors classified by the Chern-Simons or winding number given by

$$N_{CS} = \frac{1}{24\pi^2}\int_{S^3} d^3x\epsilon_{ijk}\mathrm{Tr}\left[G_i(x)G_j(x)G_k(x)\right], \tag{3.39}$$

where $G_i(x)$ is a pure gauge potential, defined as the set of field configurations of the null-field

$$G_\mu \underset{|x|^2\to\infty}{=} U^{-1}\partial_\mu U, \tag{3.40}$$

for some $U \in SU(2)$. Equation (3.39) comes from a four-dimensional integral which is reduced to an integral over S^3. This is due to the boundary condition established in the pure gauge potential.

Another important quantity is the topological charge

$$Q = \int d^4x\epsilon_{\mu\nu\rho\sigma}\mathrm{Tr}\left[G_{\mu\nu}(x)G_{\rho\sigma}(x)\right]. \tag{3.41}$$

The absolute value of the topological charge is the minimum number of discontinuous steps to arrive from a given field configuration to a trivial one. For an evolution of a gauge field configuration, we can define the topological charge as a function of time and in a gauge where boundary terms vanish, we find

$$\Delta Q(t) = N_{CS}(t) - N_{CS}(0). \tag{3.42}$$

The $SU(2)$ instanton is a gauge field configuration which minimizes the Euclidean action in the topological sector with $Q = 1$, its action takes the value

$$S_E = \frac{8\pi^2}{g^2}. \tag{3.43}$$

The transition amplitude T between two vacuum states can be obtained in QFT at finite temperature and is given by

$$T = \langle n|\, e^{-H/T}\, |n+1\rangle = \int \mathcal{D}G_\mu e^{-S_E}, \tag{3.44}$$

integrated over closed paths of length $1/T$. At zero temperature ($g \approx 0.64$) the transition rate of quantum tunneling is exponentially suppressed by a factor

$$T \propto e^{-16\pi^2/g^2} \propto 10^{-164} \tag{3.45}$$

[57], which explains the lack of experimental evidence.

On the other hand, a sphaleron is an unstable solution of the equations of motion of the electroweak theory [58, 59]. In contrast to the instanton, it sits on the top of the barrier and it has sufficient energy E_0 to pass between topological sectors, as depicted in Fig. 3.11. In this figure we symbolically illustrate the field configuration space which is given by the blue curve, each point represents a configuration and the minima are the vacuum states labelled by the winding number N_{CS} in eq. (3.39). The sphaleron is a saddle point in between neighboring vacua, and its decay to one of them changes N_B (N_L).

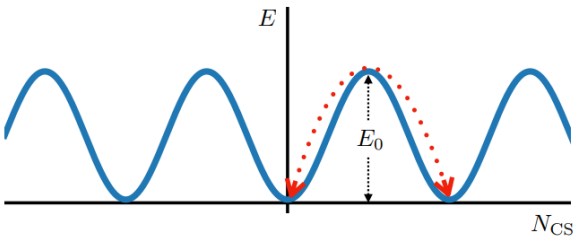

Figure 3.11: Sphaleron transition between sectors of the electroweak vacua. The sphaleron is on the top of the barrier and it might fall into the vacuum states next to it, labelled by the winding number N_{CS}. Image taken from Ref. [60].

The transition rate of the sphalerons can be obtained with numerical methods as the Ref. [61] shows with a lattice formulation. There are cases at finite temperature where thermal fluctuations enable crossing the barrier classically.

For vacuum transitions, ΔQ is an integer given by the difference of the winding numbers

$$\Delta N_B = \Delta N_L = N_g \Delta Q, \tag{3.46}$$

associated with a process where the bosonic fields jump between different vacuum sectors. This implies a change in the baryon number. If the gauge fields evolve from one vacuum, say with $N_{CS} = 0$, to a neighbouring one with $N_{CS} = \pm 1$, then the baryon or lepton number will change with ± 1. This means that the quark number will change with ± 3. For example, a process in terms of quarks could look like $2q \to 7\overline{q} + 3\overline{\ell}$.

As we can see, the difference $B - L$ is conserved. $B - L$ is an exact symmetry and it is more natural if we gauge it. This will be our first step in an extension of the SM and will be discussed in the next chapter.

3.2.1 Cosmic strings

Cosmic strings or vortices are the main subject of this thesis. They are one-dimensional topological defects with a filament structure, analogous to type-II superconductors or superfluids in condensed matter. In the context of QFT, cosmic strings are field configurations of symmetric theories where vorticity is concentrated in the core while it dissipates according to their equations of motion until they acquire their respective VEV. They can be considered as lines of trapped energy density [62].

In the context of cosmology, the Kibble mechanism [63] states that topological defects might have been formed in phase transitions in the early universe, in a high temperature regime after inflation took place, in the radiation dominated era. Inflation is an epoch of the universe at an age of 10^{-36} seconds, which solves three fundamental problems. The horizon problem associated to the isotropy in the Cosmic Microwave Background although there is no causal contact, the flatness problem given by the fact that initial conditions in the universe would have major effects in curvature today and the magnetic-monopole problem as stable zero-dimensional topological defects in magnetic field configurations. Inflation also has the effect of sweeping away topological defects, that is why we investigate them after this epoch. As traces of those phase transitions, the case of stable topological defects might still exist in the present. Additionally, these defects are of great importance since they can be used for explaining the origin of structure at very early stages because of its interaction with matter [64, 65]. The particular case of cosmic strings is believed to help in galaxy formation by the inhomogeneities they produce. However, at present times, if they do exist, there might be just one within the observable universe [63].

Now the analogies with condensed matter we saw in the previous section can be put into place for superconductors and superfluids. Because of the characteristics of ^{4}He, it was proposed to be used in experiments which mimic the universe [66, 67, 68]. Near the second order phase transition, the free energy density can be written as eq. (3.2) which looks like the Higgs potential, as we have seen already. This will lead to vortex solutions in the equations of motion as we already seen. It is possible to test key elements of vortex formation during rapid phase transitions [66]. For ^{3}He the tests are also available, while being of a more complicated nature, measurements are easier due to its magnetic properties and the nuclear magnetic resonance (NMR) technique [52]. Another analogy can be made with the reaction

$$^3\mathrm{He} + \mathrm{n} \rightarrow {}^1\mathrm{H} + {}^3\mathrm{H} + 764\ \mathrm{keV} \tag{3.47}$$

which converts ^{3}He into hydrogen, tritium and thermal energy. This process creates inhomogeneities in the superfluid which can build vorticities in the emerging phases [56]. This is a process of rapid phase transition which can be used as a cosmological experiment as we have mentioned above.

The simplest theory exhibiting string solutions [69] is described by a complex scalar field ϕ and a globally symmetric $U(1)$ invariant Lagrangian

$$\mathcal{L} = \partial_\mu \phi^* \partial^\mu \phi - V = \partial_\mu \phi^* \partial^\mu \phi - \mu^2 \phi^* \phi - \lambda (\phi^* \phi)^2, \tag{3.48}$$

for $\lambda > 0$ and $\mu^2 < 0$, it has the ground state or vacuum solution

$$\phi = v e^{i\alpha_0}. \tag{3.49}$$

This solution is not invariant under $U(1)$ phase rotations, the symmetry is said to be broken. Besides the vacuum, there are static solutions with non-zero energy density, in a cylindrically symmetric ansatz

$$\phi(r, \varphi; n) = f(r)e^{in\varphi}, \tag{3.50}$$

where n is an integer. The field equations reduce to the non-linear differential equation

$$\frac{d^2 f}{dr^2} + \frac{1}{r}\frac{df}{dr} = \left(\frac{n^2}{r^2} + \mu^2 + 2\lambda f^2\right) f, \tag{3.51}$$

which corresponds to the Euler-Lagrange equations, as we will see explicitly in the next chapter for an extension of the SM. Dynamic cosmic strings can be studied with the Nambu-Goto action, see Ref. [69] for a review. Notice that as $r \to 0$, continuity of ϕ requires $f \to 0$ and at infinity $f \to v$, so the field has finite energy. This is the equation of motion of a (global) cosmic string [70]. Here we observe another analogy. This equation is quite similar to the one we found for a quantized vortex in type-II superconductors, namely eq. (3.31) but without gauge field. In this globally symmetric model, the energy per unit length of the string is infinite. But if we consider $U(1)$ to be a local symmetry, this will be the Abelian Higgs model still presenting stable vortex solutions and the energy per unit length will be finite [71]. The Lagrangian is

$$\mathcal{L} = D_\mu \phi^* D^\mu \phi - \mu^2 \phi^* \phi - \lambda(\phi^* \phi)^2 - \frac{1}{4} F^{\mu\nu} F_{\mu\nu}, \tag{3.52}$$

with the covariant derivative

$$D_\mu \phi = (\partial_\mu + ieA_\mu)\phi \tag{3.53}$$

and the electromagnetic field strength tensor

$$F_{\mu\nu} = \partial_\mu A_\nu - \partial_\nu A_\mu. \tag{3.54}$$

The stable vortex solutions in a cylindrically symmetric ansatz takes the form

$$\phi(r) = f(r)e^{in\varphi}, \quad A_\mu = \frac{a(r)}{r}\hat{\varphi}. \tag{3.55}$$

Following the same arguments as before, applying the Euler-Lagrange equations lead to equations of motion which describe vortices. Now the important feature is that these vortices have a quantized magnetic flux

$$\int F_{\mu\nu} d\sigma^{\mu\nu} = \frac{2\pi n}{e}. \tag{3.56}$$

Using this model we find a distance away from the vortex core, called the penetration depth given by $L = 1/ev$, where the current decays.

A typical profile of a static cosmic string is depicted in Fig. 3.12. Generally for the radial part $f(r)$ of a field satisfying equations of motion like eq. (3.51), a cosmic string profile starts at $r = 0$ taking a value $f = 0$ and it grows rapidly to its asymptotic value $f(r \to \infty) \to v$, with $v > 0$.

There is another behaviour for $f(r)$ that can also be classified as a cosmic string, with a profile satisfying the initial and asymptotic conditions but changing its sign in between. We call this solution a co-axial cosmic string and it is depicted in Fig. 3.13. To the best of our

knowledge, they are not reported in the literature but at first sight there is no reason to exclude them. The co-axial cosmic string is a proposal in which the field starts at $f = 0$, then it takes negative values and at last it grows towards positive values achieving asymptotically the condition $f(r \to \infty) \to v$.

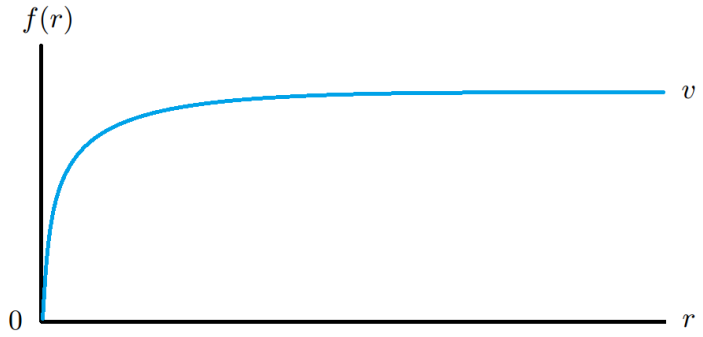

Figure 3.12: Typical profile of a cosmic string.

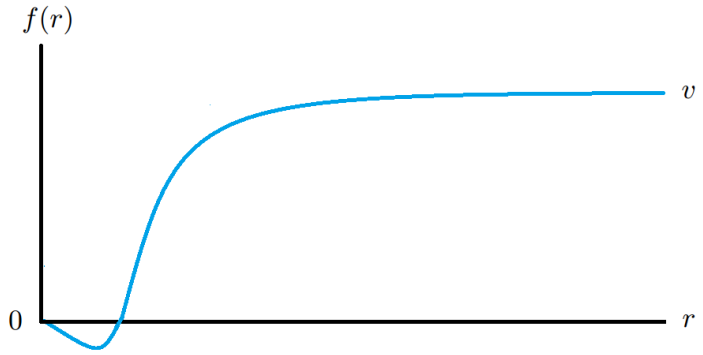

Figure 3.13: Typical profile of a (hypothetical) co-axial cosmic string.

Finally, conditions of dynamical stability of the vortices can be studied by numerical methods, as Ref. [72, 73] shows by comparing the minima in the energy of a vortex with a winding number n and n vortices. In this model the condition states that vortices are stable to perturbations when $\lambda < 2e^2$ for any n and unstable for $\lambda > 2e^2$ and $|n| > 1$ [72, 74]. The instability can be explained physically by considering a vortex with a winding number n, splitting apart — because of the repulsive interaction of the magnetic flux lines — into n separate vortices. In contrast, for a stable vortex we will have an attractive force keeping together the vortex because of the potential.

Let us consider a multicomponent scalar field ϕ which transforms under the representation of a compact Lie Group $\mathcal{G}$. Let $\mathcal{M}$ be the vacuum manifold and let $v \in \mathcal{M}$ a point in the manifold. For any element of the group $g \in \mathcal{G}$ we also have $gv \in \mathcal{M}$. But many different elements g yield to the same point, so we introduce the isotropy group $\mathcal{H}$ with all elements $h \in \mathcal{G}$ such that $hv = v$. Then the points on $\mathcal{M}$ are in one-to-one correspondence with $\mathcal{M} = \mathcal{G}/\mathcal{H}$. In this way

we can relate the vacuum manifold and the symmetry group of the theory. A solution for the field configuration could be given by

$$\phi(\varphi) = g(\varphi)v, \tag{3.57}$$

where g might be regarded as defining a loop in $\mathcal{M}$, a map $S^1 \to \mathcal{M}$. Whether or not there is a vortex solution depends on the topological characterization of this loop. In the extension of the SM of this work, we use the symmetry group $U(1)_{B-L}$ and we have a non-trivial first homotopy group

$$\pi_1(U(1)) = \mathbb{Z}. \tag{3.58}$$

There is a condition that assures the existence of stable cosmic strings, an unbroken discrete symmetry group at low energies.

The concepts we treated before in the SM come into place with cosmology and cosmic strings when treating the electroweak sector which — as we mentioned before — undergoes a symmetry breaking $SU(2)_L \otimes U(1)_Y \to U(1)_{\text{em}}$. This corresponds to a phase transition in the early universe when it had an energy above 100 GeV or an age below 10^{-11} seconds. Unfortunately there are no topologically stable or dynamically meta-stable vortex solutions for this phase transition according to the free parameters of the SM measured experimentally [75, 76], unless extensions of the SM are taken into account. Topological stability of a quantized vortex solution means that it can't be deformed continuously into the vacuum solution. It should be emphasized that this is different from the dynamical stability defined above, where the decay of the cosmic is not energetically favored.

Similarly cosmic strings are expected in Grand Unified Theories (GUTs) where a larger symmetry group with non-trivial topology can allow them [69, 77, 78]. This larger symmetry group is thought to unify at high energies the three known gauge interactions into one and its breaking would lead to the SM. The GUT phase transitions are expected in the history of the universe at an age of 10^{-35} seconds. As an important and relevant fact, $B - L$ is expected to be conserved in any GUT by invariance of $SU(3)_c \otimes SU(2)_L \otimes U(1)_Y$ [79, 80].

An example of a GUT is the symmetry group $SO(10)$ which also has $B - L$ as a local symmetry, it contains the SM as $SU(3)_c \otimes SU(2)_L \otimes U(1)_Y \subset SU(5) \subset SO(10)$ [81]. $SO(10)$ contains cosmic strings, we can find an example in Ref. [82] where they are formed in the phase transition $\text{Spin}(10) \to SU(5) \otimes \mathbb{Z}_2$. Two types of cosmic strings are found in this reference, an effectively Abelian one which enables baryon number violation and a non-Abelian which can turn leptons into quarks as they travel around the string. Baryon number violation in GUTs due to cosmic strings has been investigated and they can be used to explain the baryon asymmetry in the universe. This requires leptons and quarks to have CP-violating couplings to the strings [83, 84, 85].

Another example of an extension of the SM, with topological defects, is the Peccei-Quinn theory. The axion is a non-standard particle in the theory proposed by Peccei-Quinn [86, 87]. This proposal tries to solve the strong CP problem by introducing an additional field and a new anomalous symmetry $U(1)_A$ in the QCD Lagrangian. This symmetry is spontaneously broken at low energies and gives rise to the axion, making it a pseudo Nambu-Goldstone particle. Axionic strings are a particular case associated with a spontaneously broken axial $U(1)_A$ symmetry. The breaking of this symmetry leads to cosmic strings [88], as the ones already reviewed. But

there are more effects upon quantization because of the axial anomaly, the theory couples to instantons and leads to temperature dependent non-trivial configurations of the gluon field.

Last but not least, cosmic strings have dynamics and tension which makes space-time deform, thus certain characteristics such as mass and gravitational consequences arise. We have already talked about the equations of motion for static cosmic strings but they can also have temporal dependence with moving string solutions and present oscillations which could induce gravitational radiation [89]. For example, in electroweak generalizations, the cosmic strings can have a mass of the order of 10^6 g for a length equal to the solar radius ($\approx 7 \times 10^8$ m), while for some GUTs they may have a mass of the solar mass order which would produce gravitational lensing [90, 91]. Measurements on the Cosmic Microwave Background can test their existence, even though all observations have just established constraints on the possible string tension [92, 93]. With respect to the Cosmic Microwave Background what should be looked for is step-like discontinuities in the temperature spectrum [94]. Furthermore, models of oscillating loops in cosmic strings are able to produce powerful bursts of gravitational radiation [95]. Recent achievements in the observation of gravitational waves also provide constraints for the parameters of cosmic strings [96].

As we have seen in the case of the electroweak scale, the gravitational effects of cosmic strings are small and therefore they might not be observable. But they are not the only kind of interactions a cosmic string can have. They can have a superconducting core which enables them to interact with magnetic fields in the universe with significant astrophysical effects. This happens in the general case of a theory with symmetry $G \otimes U(1)$ where $U(1)$ is related to electromagnetism or to a linear combination (for example between electric, electroweak charges and baryon number minus lepton number [97]) and G is spontaneously broken. Superconductivity can be achieved — while stability and particularities depend on the model — by Goldstone bosons if a charged Higgs field has a VEV inside the core, or if there are charged fermions trapped inside the string [98, 99].

Chapter 4

Cosmic strings for Y'

Before starting the section about cosmic strings and the solutions, we describe the extension of the SM we propose. In the SM there exist processes involving baryon and lepton number violations, while the difference is kept invariant. This turns $B - L$ into a global and exact symmetry of the SM. So the first step we take is to gauge this symmetry such that it becomes more natural for it to be exact.

We start by considering an extension of the SM with $U(1)_{B-L}$ as a local symmetry, instead of a global one. We call $\mathcal{A}_\mu(x)$ the gauge field of the $U(1)_{B-L}$ symmetry group. As a global symmetry, $B-L$ is a conserved quantum number. Gauging it leads to an anomaly given by the divergence of the current

$$\partial^\mu J_\mu^{B-L} = -\frac{1}{16\pi^2}\mathcal{F}^{\mu\nu}\mathcal{F}_{\mu\nu}. \tag{4.1}$$

where $\mathcal{F}_{\mu\nu} = \partial_\mu\mathcal{A}_\nu - \partial_\nu\mathcal{A}_\mu$ is the field strength tensor of $\mathcal{A}_\mu$. This anomaly originates from the fermion triangle diagram depicted in Fig. 4.1.

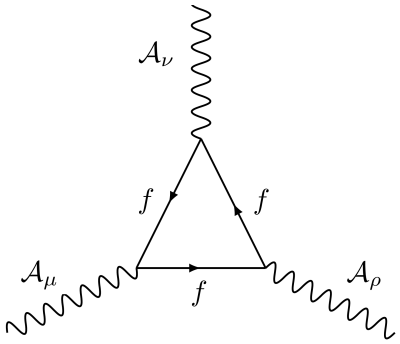

Figure 4.1: Fermion triangle diagram with gauge fields $\mathcal{A}$ and fermions f.

Explicitly, we will take a linear combination of the hypercharge Y and the quantum number $B - L$, namely

$$Y' = \alpha Y + \beta(B - L) \tag{4.2}$$

as it is more general (α not to be confused with the fine structure constant) and the symmetry group is $U(1)_{Y'}$, with $\mathcal{A}_\mu$ the gauge field.

We have gone a step forward by gauging Y' but as a result we have found an anomaly. The absence of right-handed neutrinos prevents the $B-L$ charges from summing zero. Our approach consists of adding a right-handed neutrino $\nu_R(x)$ with $B-L=-1$ to each fermion generation, this procedure cancels this anomaly. Now we have solved the problem in a consistent form and furthermore with this right-handed neutrinos, we can construct mass terms for neutrinos. For the neutrinos we can add a Dirac mass term using the Higgs mechanism, as the ones we saw in Chapter 2. Defining

$$\widetilde{\Phi} = \frac{1}{\sqrt{2}} \begin{pmatrix} \phi_0^* \\ -\phi_+^* \end{pmatrix}, \tag{4.3}$$

this mass term will take the form

$$\mathcal{L} = f_\nu \left[(\overline{\nu}_L, \overline{e}_L) \widetilde{\Phi} \nu_R + \overline{\nu}_R \widetilde{\Phi}^\dagger \begin{pmatrix} \nu_L \\ e_L \end{pmatrix} \right] = \frac{f_\nu}{\sqrt{2}} \left[(\overline{\nu}_L, \overline{e}_L) \begin{pmatrix} \phi_0^* \\ -\phi_+^* \end{pmatrix} \nu_R + \overline{\nu}_R (\phi_0, -\phi_+) \begin{pmatrix} \nu_L \\ e_L \end{pmatrix} \right], \tag{4.4}$$

Under SSB, the neutrino will acquire a mass $m_\nu = f_\nu v$ where f_ν is the Yukawa coupling, v is the standard Higgs VEV.

As we expect right-handed neutrinos to have a larger mass than the left-handed, an additional mass term is proposed. We can't use a Majorana mass term because it would violate $B-L$ conservation. This is not a problem in the SM, because a global symmetry like this can be broken. But in this extension we consider it as a gauge symmetry. So we write a Majorana mass term and use the Higgs mechanism. This type of term requires an additional complex scalar Higgs field $\chi(x)$. This is the third field we add to our model and the last one. The mass term for the right-handed neutrino takes the form

$$\mathcal{L} = f_M \left(\chi \overline{\nu^C}_R \nu_R + \chi^* \overline{\nu}_R \nu_R^C \right). \tag{4.5}$$

Since the Lagrangian must be invariant under $U(1)_{Y'}$ transformations, the new Higgs field requires a quantum number of $B-L=2$. This will be constructed in a similar way as the singlet majoron model [100]. Furthermore, the new gauge field and the SSB will lead to a new massive and neutral Z'-boson in addition to the $W^\pm$, Z^0 bosons and photon A of the SM.

We can now take a look at our extension of the SM, at least in the Higgs and electroweak sectors which are involved. In this extension we have the bosonic part of the Lagrangian with $SU(2)_L \otimes U(1)_{Y'} \otimes U(1)_Y$ local symmetry. It is an extension of the eq. (2.20) with the same prescriptions and is given by

$$\mathcal{L}_b = D_\mu \Phi^\dagger D^\mu \Phi + D_\mu \chi^* D^\mu \chi - V - \frac{1}{4} W_a^{\mu\nu} W^a_{\mu\nu} - \frac{1}{4} B^{\mu\nu} B_{\mu\nu} - \frac{1}{4} \mathcal{F}_{\mu\nu} \mathcal{F}^{\mu\nu}, \tag{4.6}$$

with the Mexican hat potential for both Higgs fields plus an interaction term between them with coupling κ

$$V = \mu^2 \Phi^\dagger \Phi + \lambda (\Phi^\dagger \Phi)^2 + \mu'^2 \chi^* \chi + \lambda' (\chi^* \chi)^2 - \kappa \Phi^\dagger \Phi \chi^* \chi, \tag{4.7}$$

with $\lambda, \lambda' > 0$ and $\kappa < 2\sqrt{\lambda \lambda'}$ for the potential to be bounded from below.

The covariant derivative D_μ is given by

$$D_\mu = \partial_\mu + i \frac{g}{2} W_\mu^a \sigma_a + i g' Y B_\mu + i h Y' \mathcal{A}_\mu, \tag{4.8}$$

where g, g' and h are $SU(2)_L$, $U(1)_Y$ and $U(1)_{Y'}$ coupling constants. This covariant derivative couples the standard Higgs field to W_μ, B_μ and to the hypercharge contribution from the $\mathcal{A}_\mu$, while it just couples the new Higgs field to the $B-L$ contribution from $\mathcal{A}_\mu$ as

$$D_\mu\Phi = \left(\partial_\mu + i\frac{g}{2}W_\mu^a\sigma_a + i\frac{g'}{2}B_\mu + i\frac{h\alpha}{2}\mathcal{A}_\mu\right)\Phi, \quad D_\mu\chi = \left(\partial_\mu + 2ih\beta\mathcal{A}_\mu\right)\chi, \tag{4.9}$$

where σ_a are the Pauli matrices and we have used the values of Y, $B-L$ and Y' in Table 4.1. Notice that the covariant derivative acts differently in each Higgs field.

	Y	$B-L$	Y'
Φ	$1/2$	0	$\alpha/2$
χ	0	2	2β

Table 4.1: Weak hypercharge, baryon number minus lepton number and Y' values for the Higgs fields.

At last the field strength tensors are given by these expressions

$$W_{\mu\nu} = \partial_\mu W_\nu - \partial_\nu W_\mu + g[W_\mu, W_\nu], \quad B_{\mu\nu} = \partial_\mu B_\nu - \partial_\nu B_\mu, \quad \mathcal{F}_{\mu\nu} = \partial_\mu\mathcal{A}_\nu - \partial_\nu\mathcal{A}_\mu. \tag{4.10}$$

So this Lagrangian is gauge invariant, Lorentz invariant and power counting renormalizable. The $U(1)_{Y'}$ gauge transformation takes the form

$$\Phi \to \Phi' = e^{-ih\alpha\theta/2}\Phi, \quad \chi \to \chi' = e^{-2ih\beta\theta}\chi, \quad \mathcal{A}_\mu \to \mathcal{A}'_\mu = \mathcal{A}_\mu + \frac{1}{h}\partial_\mu\theta. \tag{4.11}$$

To explain the consistency of these modifications we add some remarks. The field $\mathcal{A}_\mu$ should acquire a mass dynamically, in order not to create long range interactions between macroscopic objects that are charged under $B-L$. The new Higgs field should have a larger VEV than the standard Higgs. And also we need a heavy right-handed neutrino.

In the case of a first generation of lepton and quarks, we will have electrons, neutrinos, up and down quarks, all of them with left- and right-handed chirality. The Lagrangian reads

$$\begin{aligned}\mathcal{L}_{\rm f} = {} & (\overline{\nu}_L, \overline{e}_L)i\gamma^\mu D_\mu \begin{pmatrix}\nu_L \\ e_L\end{pmatrix} + \overline{e}_R i\gamma^\mu D_\mu e_R + (\overline{u}_L, \overline{d}_L)i\gamma^\mu D_\mu \begin{pmatrix}u_L \\ d_L\end{pmatrix} + \overline{u}_R i\gamma^\mu D_\mu u_R + \overline{d}_R i\gamma^\mu D_\mu d_R \\ & + \overline{\nu}_R i\gamma^\mu D_\mu \nu_R + \Big\{ f_e(\overline{\nu}_L, \overline{e}_L)\Phi e_R + f_d(\overline{u}_L, \overline{d}_L)\Phi d_R + f_u(\overline{u}_L, \overline{d}_L)\widetilde{\Phi} u_R + f_\nu(\overline{\nu}_L, \overline{e}_L)\widetilde{\Phi}\nu_R \\ & + f_M \overline{\nu}_R \chi C\overline{\nu}_R^T + \text{h.c.}\Big\}\end{aligned} \tag{4.12}$$

Now let us inspect the Lagrangian structure. The first line of eq. (4.12) contains the kinetic terms for the left-handed lepton doublet, the right-handed electron, the left-handed quark doublet and the right-handed up and down quarks, respectively. Explicitly, the covariant derivatives of eq. (4.8) read

$$D_\mu \begin{pmatrix}\nu_L \\ e_L\end{pmatrix} = \left(\partial_\mu + i\frac{g}{2}W_\mu^a\sigma_a - i\frac{g'}{2}B_\mu - ih\left(\frac{\alpha}{2} + \beta\right)\mathcal{A}_\mu\right)\begin{pmatrix}\nu_L \\ e_L\end{pmatrix}, \tag{4.13}$$

$$D_\mu e_R = (\partial_\mu - ig'B_\mu - ih(\alpha+\beta)\mathcal{A}_\mu)e_R, \tag{4.14}$$

$$D_\mu \begin{pmatrix} u_L \\ d_L \end{pmatrix} = \left(\partial_\mu + i\frac{g}{2}W_\mu^a\sigma_a + i\frac{g'}{6}B_\mu + ih\frac{\alpha+2\beta}{6}\mathcal{A}_\mu\right)\begin{pmatrix} u_L \\ d_L \end{pmatrix}, \tag{4.15}$$

$$D_\mu u_R = \left(\partial_\mu + i\frac{2g'}{3}B_\mu + ih\frac{2\alpha+\beta}{3}\mathcal{A}_\mu\right)u_R, \tag{4.16}$$

$$D_\mu d_R = \left(\partial_\mu - i\frac{g'}{3}B_\mu - ih\frac{2\alpha-\beta}{3}\mathcal{A}_\mu\right)d_R. \tag{4.17}$$

The second line of eq. (4.8) consists of the kinetic term for the right-handed neutrino which only couples to $B-L$, as we can see in

$$D_\mu \nu_R = (\partial_\mu - ih\beta\mathcal{A}_\mu)\nu_R. \tag{4.18}$$

In this second line of the Lagrangian, we also have all the Yukawa interaction terms, which upon SSB give mass to the first generation of fermions, now including the neutrino as we can see in the last term. Furthermore we have the additional Majorana mass term in the third line, which gives mass only to the right-handed neutrino.

	Y	$B-L$	Y'
e_L	$-1/2$	-1	$-\alpha/2-\beta$
ν_L	$-1/2$	-1	$-\alpha/2-\beta$
e_R	-1	-1	$-\alpha-\beta$
ν_R	0	-1	$-\beta$
u_L	$1/6$	$1/3$	$(\alpha+2\beta)/6$
d_L	$1/6$	$1/3$	$(\alpha+2\beta)/6$
u_R	$2/3$	$1/3$	$(2\alpha+\beta)/3$
d_L	$-1/3$	$1/3$	$(-\alpha+\beta)/3$

Table 4.2: Weak hypercharge, baryon number minus lepton number and Y' values for the first generation of fermions.

This hypothetical model can be placed into a more physically realistic scenario by embedding it into the $SO(10)$ GUT subgroup $SU(3)_c \otimes SU(2)_L \otimes U(1)_{Y'} \otimes U(1)_Y$ [101], where the Y'-charge is given by

$$Y' = Y - \frac{5}{4}(B-L), \tag{4.19}$$

and the $U(1)_{Y'}$ coupling constant is proportional to the electroweak coupling constant. This embedding is obtained in our model by fixing the parameters as

$$\alpha = 1, \quad \beta = -\frac{5}{4}, \quad h = \sqrt{\frac{2}{3}}g'. \tag{4.20}$$

This GUT is constructed exactly as our model[1], the Y'-charge is a linear combination which is fixed by the orthonormality conditions $\mathrm{Tr}(YY') = 0$, $\mathrm{Tr}(Y^2) = \frac{2}{3}\mathrm{Tr}(Y'^2)$. The right-handed neutrino acquires a Majorana mass using a new scalar Higgs field through the sequential SSB

$$SU(3)_c \otimes SU(2)_L \otimes U(1)_{Y'} \otimes U(1)_Y \underset{v'}{\to} SU(3)_c \otimes SU(2)_L \otimes U(1)_Y \underset{v}{\to} SU(3)_c \otimes U(1)_{\mathrm{em}}. \tag{4.21}$$

[1]The inclusion of the gauge group $SU(3)_c$ and the gluon field is straightforward.

In this scenario, the right-handed (heavy) neutrino masses are bounded from above by the energy scale v' which is of the order of 1 TeV and the small masses of the left-handed neutrinos are explained by the see-saw mechanism [101, 102]. The massless photon and the neutral Z^0 fields are expressed as usual

$$\begin{aligned} A_\mu &= \cos\theta_W B_\mu + \sin\theta_W W^3_\mu, \\ Z^0_\mu &= -\sin\theta_W B_\mu + \cos\theta_W W^3_\mu, \end{aligned} \tag{4.22}$$

but now we have two massive neutral Z and Z' bosons given by

$$\begin{aligned} Z_\mu &= \cos\Theta Z^0_\mu - \sin\Theta \mathcal{A}_\mu, \\ Z'_\mu &= \sin\Theta Z^0_\mu + \cos\Theta \mathcal{A}_\mu. \end{aligned} \tag{4.23}$$

Experimental data might constrain the new free parameters, for example the Higgs masses are modified. We can identify them by diagonalizing the mass matrix $M^{(2)}$ defined by the second variational derivatives of the potential V in eq. (4.7),

$$\begin{aligned} M^{(2)} &= \begin{pmatrix} \frac{\delta^2 V}{\delta\phi\delta\phi^*} & \frac{\delta^2 V}{\delta\phi\delta\xi^*} \\ \frac{\delta^2 V}{\delta\phi^*\delta\xi} & \frac{\delta^2 V}{\delta\xi\delta\xi^*} \end{pmatrix}\Bigg|_{\text{VEV}} = \begin{pmatrix} \mu^2 + 4\lambda v^2 - \kappa v'^2 & -\kappa v v' \\ -\kappa v v' & \mu'^2 + 4\lambda' v'^2 - \kappa v^2 \end{pmatrix} \\ &= \begin{pmatrix} 2\lambda v^2 & -\kappa v v' \\ -\kappa v v' & 2\lambda' v'^2 \end{pmatrix}. \end{aligned} \tag{4.24}$$

the eigenvalues of the diagonalized mass matrix are

$$m^2_\pm = \lambda v^2 + \lambda' v^2 \pm \sqrt{(\lambda' v'^2 - \lambda v^2)^2 + \kappa^2 v^2 v'^2}. \tag{4.25}$$

We associate the masses to the fields as

$$m^2_\Phi = \lambda v^2 + \lambda' v^2 - \sqrt{(\lambda' v'^2 - \lambda v^2)^2 + \kappa^2 v^2 v'^2}, \quad m^2_\chi = \lambda v^2 + \lambda' v^2 + \sqrt{(\lambda' v'^2 - \lambda v^2)^2 + \kappa^2 v^2 v'^2}.$$

These expressions relate the particles masses associated to our two Higgs fields with the free parameters of our proposal, namely the VEVs v, v' and the coupling constants λ, λ' and κ. In the limit $v' \gg v$, factorizing the term $\lambda' v'^2$ we arrive at

$$m^2_\pm = \lambda v^2 + \lambda' v'^2 \pm \lambda' v'^2 \sqrt{\left(1 - \frac{\lambda v^2}{\lambda' v'^2}\right)^2 + \frac{\kappa^2 v^2 v'^2}{\lambda'^2 v'^4}}. \tag{4.26}$$

Expanding the square root we obtain simpler expressions for the masses given by

$$m^2_\Phi \approx 2\lambda v^2 - \frac{\kappa^2 v^2}{2\lambda'}, \quad m^2_\chi \approx 2\lambda' v'^2. \tag{4.27}$$

In order to describe the cosmic strings associated to the Y' gauge field, we will derive — in a semi-classical approach — the equations of motion or Euler-Lagrange equation of a Lagrangian involving the standard Higgs field Φ, the new Higgs field χ and the gauge field $\mathcal{A}_\mu$ to simplify the problem. This simplification can be justified as a decoupling with the heavy $W^\pm$ and Z fields by considering a low energy effective theory and constant fermion background. We will comment more on this simplification in Chapter 5. Because of the structure of cosmic strings we apply a cylindrically symmetric ansatz and radial boundary conditions.

4.1 Equations of motion

First let us consider a Lagrangian with a global $U(1)$ symmetry

$$\mathcal{L} = \partial_\mu \Phi^\dagger \partial^\mu \Phi + \partial_\mu \chi^* \partial^\mu \chi - V, \tag{4.28}$$

with the potential

$$V = \mu^2 \Phi^\dagger \Phi + \lambda (\Phi^\dagger \Phi)^2 + \mu'^2 \chi^* \chi + \lambda' (\chi^* \chi)^2 - \kappa \Phi^\dagger \Phi \chi^* \chi, \tag{4.29}$$

where $\Phi \in \mathbb{C}^2$ is the standard Higgs field and $\chi \in \mathbb{C}$ is an additional Higgs field. The Lagrangian is in natural units, $\hbar = 1$, $c = 1$, it must have the dimensions of length $\left[l^{-4}\right]$, so $[\Phi] = \left[l^{-1}\right] = [\chi]$. The equations of motion can be obtained with the Euler-Lagrange equations

$$\partial_\mu \frac{\delta \mathcal{L}}{\delta \partial_\mu \Phi^\dagger} = \frac{\delta \mathcal{L}}{\delta \Phi^\dagger}, \quad \partial_\mu \frac{\delta \mathcal{L}}{\delta \partial_\mu \chi^*} = \frac{\delta \mathcal{L}}{\delta \chi^*}. \tag{4.30}$$

We refer to Appendix A for a discussion of the derivatives respect to the complex fields. Then

$$\begin{aligned}
\frac{\delta \mathcal{L}}{\delta \Phi^\dagger} &= -\frac{\delta V}{\delta \Phi^\dagger} = -\mu^2 \Phi - 2\lambda \Phi (\Phi^\dagger \Phi) + \kappa \Phi \chi^* \chi, \\
\frac{\delta \mathcal{L}}{\delta \chi^*} &= -\frac{\delta V}{\delta \chi^*} = -\mu'^2 \chi - 2\lambda' \chi (\chi^* \chi) + \kappa \Phi \Phi^\dagger \chi, \\
\frac{\delta \mathcal{L}}{\delta \partial_\mu \Phi^\dagger} &= \frac{\delta}{\delta \partial_\mu \Phi^\dagger} \partial_\nu \Phi^\dagger \partial^\nu \Phi = \eta^\mu_\nu \partial^\nu \Phi = \partial_\mu \Phi \quad \Rightarrow \quad \partial_\mu \frac{\delta \mathcal{L}}{\delta \partial_\mu \Phi^\dagger} = \partial_\mu \partial^\mu \Phi = \Box \Phi, \\
\frac{\delta \mathcal{L}}{\delta \partial_\mu \chi^*} &= \frac{\delta}{\delta \partial_\mu \chi^*} \partial_\nu \chi^* \partial^\nu \chi = \eta^\mu_\nu \partial^\nu \chi = \partial_\mu \chi \quad \Rightarrow \quad \partial_\mu \frac{\delta \mathcal{L}}{\delta \partial_\mu \chi^*} = \partial_\mu \partial^\mu \chi = \Box \chi.
\end{aligned} \tag{4.31}$$

Thus, the equations of motion for the global cosmic strings are

$$\begin{aligned}
\Box \Phi + \mu^2 \Phi + 2\lambda \Phi (\Phi^\dagger \Phi) - \kappa \Phi \chi^* \chi = 0, \\
\Box \chi + \mu'^2 \chi + 2\lambda \chi (\chi^* \chi) - \kappa \Phi^\dagger \Phi \chi = 0.
\end{aligned} \tag{4.32}$$

We look for static solutions which we express in cylindrical coordinates, so we use the Laplacian in cylindrical coordinates and take the ansatz

$$\Phi(t, r, \varphi, z) = \begin{pmatrix} 0 \\ \phi(r) \end{pmatrix} e^{in\varphi}, \quad \chi(t, r, \varphi, z) = \xi(r) e^{in'\varphi}, \tag{4.33}$$

with dimensions $[\phi] = \left[l^{-1}\right] = [\xi]$. Substituting ansatz (4.33) into eq. (4.32) we obtain the explicit form for the equations of motion as a system of non-linear differential equations

$$\begin{aligned}
\frac{d^2\phi}{dr^2} + \frac{1}{r}\frac{d\phi}{dr} &= \left(\frac{n^2}{r^2} + \mu^2 + 2\lambda \phi^2 - \kappa \xi^2 \right) \phi, \\
\frac{d^2\xi}{dr^2} + \frac{1}{r}\frac{d\xi}{dr} &= \left(\frac{n'^2}{r^2} + \mu'^2 + 2\lambda' \xi^2 - \kappa \phi^2 \right) \xi.
\end{aligned} \tag{4.34}$$

Notice that the exponential in ansatz (4.33) can be factorized in these equations. We take the vacuum expectation value of the fields as

$$\lim_{r \to \infty} \phi(r) = v, \quad \lim_{r \to \infty} \chi(r) = v'. \tag{4.35}$$

We can fix the parameters μ and μ' in terms of λ, λ' and κ, by referring to the equations (4.34) and neglecting the field derivatives. In the large-r limit we obtain

$$\begin{aligned} \mu^2 v + 2\lambda v^3 - \kappa v v'^2 = 0 \quad &\Rightarrow \quad \mu^2 = -2\lambda v^2 + \kappa v'^2, \\ \mu'^2 v' + 2\lambda' v'^3 - \kappa v^2 v' = 0 \quad &\Rightarrow \quad \mu'^2 = -2\lambda' v'^2 + \kappa v^2. \end{aligned} \tag{4.36}$$

The next step is to promote the $U(1)$ global symmetry to a gauge symmetry associated to a gauge field $\mathcal{A}_\mu$, since we are mostly interested in this gauged model and local cosmic string solutions. Here we start from the Lagrangian

$$\mathcal{L} = D_\mu \Phi^\dagger D^\mu \Phi + D_\mu \chi^* D^\mu \chi - \frac{1}{4}\mathcal{F}_{\mu\nu}\mathcal{F}^{\mu\nu} - V, \tag{4.37}$$

with the unchanged potential

$$V = \mu^2 \Phi^\dagger \Phi + \lambda(\Phi^\dagger \Phi)^2 + \mu'^2 \chi^* \chi + \lambda'(\chi^* \chi)^2 - \kappa \Phi^\dagger \Phi \chi^* \chi, \tag{4.38}$$

with the covariant derivatives similar to eq. (4.8) given by

$$D_\mu \Phi = \partial_\mu \Phi + i\frac{h\alpha}{2}\mathcal{A}_\mu \Phi, \quad D_\mu \chi = \partial_\mu \chi + 2ih\beta \mathcal{A}_\mu \chi, \tag{4.39}$$

or under a redefinition of $h\alpha/2 \to h$ and $2h\beta \to h'$ for simplicity

$$D_\mu \Phi = \partial_\mu \Phi + ih\mathcal{A}_\mu \Phi, \quad D_\mu \chi = \partial_\mu \chi + ih'\mathcal{A}_\mu \chi, \tag{4.40}$$

and the field strength tensor

$$\mathcal{F}_{\mu\nu} = \partial_\mu \mathcal{A}_\nu - \partial_\nu \mathcal{A}_\mu. \tag{4.41}$$

Again we have $\Phi \in \mathbb{C}^2$ as the standard Higgs field, an additional Higgs field $\chi \in \mathbb{C}$ and the $U(1)_{Y'}$ gauge field $\mathcal{A}_\mu$ with dimensionless couplings h and h', respectively, for the Higgs fields. Notice the case $\alpha = 0$ where only the $B - L$ symmetry is gauged, the gauge field $\mathcal{A}_\mu$ has no Y'-charge and the standard Higgs field does not directly couple to it. We can again verify $[\Phi] = [\chi] = [\mathcal{A}_\mu] = \left[l^{-1}\right]$. The equations of motion are obtained from the Euler-Lagrange equations. Let us compute first the case for the Higgs field,

$$\frac{\delta \mathcal{L}}{\delta \Phi^\dagger} = \frac{\delta}{\delta \Phi^\dagger} D_\mu \Phi^\dagger D^\mu \Phi - \frac{\delta V}{\delta \Phi^\dagger} = -ih\mathcal{A}_\mu D^\mu \Phi - \mu^2 \Phi - 2\lambda \Phi(\Phi^\dagger \Phi) + \kappa \Phi \chi^* \chi, \tag{4.42}$$

$$\frac{\delta \mathcal{L}}{\delta \partial_\mu \Phi^\dagger} = \frac{\delta}{\delta \partial_\mu \Phi^\dagger} D_\nu \Phi^\dagger D^\nu \Phi = \eta^\mu_\nu D^\nu \Phi = D^\mu \Phi \quad \Rightarrow \quad \partial_\mu \frac{\delta \mathcal{L}}{\delta \partial_\mu \Phi^\dagger} = \partial_\mu D^\mu \Phi. \tag{4.43}$$

So by equating these two terms

$$\partial_\mu D^\mu \Phi = -ih\mathcal{A}_\mu D^\mu \Phi - \mu^2 \Phi - 2\lambda \Phi(\Phi^\dagger \Phi) + \kappa \Phi \chi^* \chi, \tag{4.44}$$

we arrive at

$$D^\mu D_\mu \Phi = -\mu^2 \Phi - 2\lambda \Phi(\Phi^\dagger \Phi) + \kappa \Phi \chi^* \chi. \tag{4.45}$$

At last, the left-hand side of eq. (4.45) can be written as

$$\begin{aligned} D^\mu D_\mu \Phi &= (\partial^\mu + ih\mathcal{A}^\mu)(\partial_\mu + ih\mathcal{A}_\mu)\Phi \\ &= \partial^\mu \partial_\mu \Phi + ih\partial^\mu(\mathcal{A}_\mu \Phi) + ih\mathcal{A}^\mu \partial_\mu \Phi - h^2 \mathcal{A}^\mu \mathcal{A}_\mu \Phi \\ &= \Box \Phi + 2ih\mathcal{A}^\mu \partial_\mu \Phi + ih\partial^\mu \mathcal{A}_\mu \Phi - h^2 \mathcal{A}^\mu \mathcal{A}_\mu \Phi. \end{aligned} \tag{4.46}$$

Finally we obtain the equation of motion for the standard Higgs field as

$$\Box\Phi + 2ih\mathcal{A}^\mu\partial_\mu\Phi + ih(\partial^\mu\mathcal{A}_\mu)\Phi - h^2\mathcal{A}^\mu\mathcal{A}_\mu\Phi = -\mu^2\Phi - 2\lambda\Phi(\Phi^\dagger\Phi) + \kappa\Phi\chi^*\chi. \tag{4.47}$$

Analogously, we use the Euler-Lagrange equations for the extra Higgs field χ

$$\frac{\delta\mathcal{L}}{\delta\chi^*} = \frac{\delta}{\delta\chi^*}D_\mu\chi^*D^\mu\chi - \frac{\delta V}{\delta\chi^*} = -ih'\mathcal{A}_\mu D^\mu\chi - \mu'^2\chi - 2\lambda'\chi(\chi^*\chi) + \kappa\Phi^\dagger\Phi\chi, \tag{4.48}$$

$$\frac{\delta\mathcal{L}}{\delta\partial_\mu\chi^*} = \frac{\delta}{\delta\partial_\mu\chi^*}D_\nu\chi^*D^\nu\chi = \eta^\mu_\nu D^\nu\chi = D^\mu\chi \quad \Rightarrow \quad \partial_\mu\frac{\delta\mathcal{L}}{\delta\partial_\mu\chi^*} = \partial_\mu D^\mu\chi, \tag{4.49}$$

which has the same structure treated before, so the equation of motion becomes

$$\Box\chi + 2ih'\mathcal{A}^\mu\partial_\mu\chi + ih'(\partial^\mu\mathcal{A}_\mu)\chi - h'^2\mathcal{A}^\mu\mathcal{A}_\mu\chi = -\mu'^2\chi - 2\lambda'\chi(\chi^*\chi) + \kappa\Phi^\dagger\Phi\chi. \tag{4.50}$$

The equation of motion of the gauge field is obtained by writing

$$\begin{aligned}
\frac{\delta\mathcal{L}}{\delta\mathcal{A}_\mu} &= -ih\Phi^\dagger\eta^\mu_\nu D^\nu\Phi + D_\nu\Phi^\dagger(ih\Phi\eta^\nu_\mu) - ih'\eta^\mu_\nu\chi^*D^\nu\chi + D_\nu\chi^*(ih'\eta^\nu_\mu\chi)\\
&= ih((D^\mu\Phi^\dagger)\Phi - \Phi^\dagger(D^\mu\Phi)) + ih'(\chi(D^\mu\chi^*) - \chi^*(D^\mu\chi))\\
&= ih((\partial^\mu\Phi^\dagger)\Phi - \Phi^\dagger(\partial^\mu\Phi)) + ih(-ih\mathcal{A}^\mu\Phi^\dagger\Phi - \Phi^\dagger(ih\mathcal{A}^\mu\Phi)) + ih'(\chi(\partial^\mu\chi^*) - \chi^*(\partial^\mu\chi))\\
&+ ih'(-ih'\mathcal{A}^\mu\chi^*\chi - \chi^*(ih'\mathcal{A}^\mu\chi))\\
&= ih((\partial^\mu\Phi^\dagger)\Phi - \Phi^\dagger(\partial^\mu\Phi)) + ih'(\chi(\partial^\mu\chi^*) - \chi^*(\partial^\mu\chi)) + 2h^2\mathcal{A}^\mu\Phi^\dagger\Phi + 2h'^2\mathcal{A}^\mu\chi\chi^*,
\end{aligned}$$

$$\begin{aligned}
\frac{\delta\mathcal{L}}{\delta\partial_\nu A_\mu} &= -\frac{1}{4}\frac{\delta}{\delta\partial_\nu A_\mu}\mathcal{F}_{\rho\sigma}\mathcal{F}^{\rho\sigma}\\
&= -\frac{1}{4}\frac{\delta}{\delta\partial_\nu A_\mu}(\partial_\rho\mathcal{A}_\sigma - \partial_\sigma\mathcal{A}_\rho)(\partial^\rho\mathcal{A}^\sigma - \partial^\sigma\mathcal{A}^\rho)\\
&= -\frac{1}{4}((\eta^\nu_\rho\eta^\mu_\sigma - \eta^\nu_\sigma\eta^\mu_\rho)\mathcal{F}^{\rho\sigma} + \mathcal{F}_{\rho\sigma}(\eta^\rho_\nu\eta^\sigma_\mu - \eta^\sigma_\nu\eta^\rho_\mu))\\
&= \mathcal{F}^{\mu\nu},
\end{aligned}$$

where in the last step we have used the antisymmetry of the tensor $\mathcal{F}$. So by equating these two terms, we obtain the equation of motion for the gauge field

$$\partial^\nu\mathcal{F}_{\mu\nu} = ih((\partial_\mu\Phi^\dagger)\Phi - \Phi^\dagger(\partial_\mu\Phi)) + ih'(\chi(\partial_\mu\chi^*) - \chi^*(\partial_\mu\chi)) + 2h^2\mathcal{A}_\mu\Phi^\dagger\Phi + 2h'^2\mathcal{A}_\mu\chi\chi^*. \tag{4.51}$$

Now, let us insert the ansatz

$$\Phi = \begin{pmatrix}0\\1\end{pmatrix}\phi(r)e^{in\varphi}, \quad \chi = \xi(r)e^{in'\varphi}, \quad \mathcal{A}_\mu = \mathcal{A}_\varphi\hat{\varphi} = \frac{a(r)}{r}\hat{\varphi}, \tag{4.52}$$

where n and n' are winding numbers and the gauge field gives a "magnetic" field in $\hat{z}$ direction. The dimensions of these fields now reads $[\phi] = [\xi] = \left[l^{-1}\right]$. On the other hand as $[\mathcal{A}_\mu] = \left[l^{-1}\right]$, then we get a dimensionless function $[a] = \left[l^0\right]$.

Equation (4.51) is a vectorial differential equation in Minkowski space and the μ-components can be written in cylindrical coordinates as

$$\partial^\nu \mathcal{F}_{\mu\nu} = \partial^\nu(\partial_\mu \mathcal{A}_\nu - \partial_\nu \mathcal{A}_\mu) = \partial^\nu \partial_\mu \mathcal{A}_\nu - \partial^\nu \partial_\nu \mathcal{A}_\mu = -\partial^\nu \partial_\nu \mathcal{A}_\mu. \tag{4.53}$$

The first term is eliminated because the only non-zero component is $\mathcal{A}_\varphi$ which does not depend on the coordinate φ. As an observation, using Cartesian coordinates and a Cartesian basis for the vector field $\mathcal{A}$, both terms in eq. (4.53) are non-zero. It is just in this cylindrical case where the eq. (4.53) reduces to a Laplacian. Then the Laplacian operator of a vector field reduces to $-\partial^\nu \partial_\nu \mathcal{A}_\mu(r) = -\Box \mathcal{A}_\mu(r) = \nabla^2 \mathcal{A}_\mu(r)$. The φ-component of this equation turns out to be the only non-zero component as we see by using the Laplacian of a vector in cylindrical coordinates. Thus, we arrive at

$$\begin{aligned}
\partial^\nu \mathcal{F}_{\mu\nu} = \nabla^2 \mathcal{A}_\mu &= \left[\frac{1}{r}\frac{\partial}{\partial r}\left(r\frac{\partial \mathcal{A}_\varphi}{\partial r}\right) - \frac{\mathcal{A}_\varphi}{r^2}\right]\hat{\varphi} = \left[\frac{1}{r}\frac{\partial}{\partial r}\left(r\frac{\partial}{\partial r}\frac{a(r)}{r}\right) - \frac{a(r)}{r^3}\right]\hat{\varphi} \\
&= \left[\frac{1}{r}\frac{\partial}{\partial r}\left(\frac{da}{dr} - \frac{a}{r}\right) - \frac{a}{r^3}\right]\hat{\varphi} = \left[\frac{1}{r}\left(\frac{d^2a}{dr^2} - \frac{1}{r}\frac{da}{dr} + \frac{a}{r^2}\right) - \frac{a}{r^3}\right]\hat{\varphi} \\
&= \left[\frac{1}{r}\frac{d^2a}{dr^2} - \frac{1}{r^2}\frac{da}{dr}\right]\hat{\varphi}.
\end{aligned} \tag{4.54}$$

On the other hand, using the ansatz (4.52) we see that the φ-component of the right-hand side of eq. (4.51) (also the non-zero component) is, written explicitly term by term

$$\begin{aligned}
ih((\partial_\mu \Phi^\dagger)\Phi - \Phi^\dagger(\partial_\mu \Phi)) &= ih\frac{1}{r}(-in\phi^2 - in\phi^2)\hat{\varphi} = 2h\frac{1}{r}\phi^2 n\hat{\varphi}, \\
ih'((\partial_\mu \chi^*)\chi - \chi^*(\partial_\mu \chi)) &= ih'\frac{1}{r}(-in'\xi^2 - in'\xi^2)\hat{\varphi} = 2h'\frac{1}{r}\xi^2 n'\hat{\varphi},
\end{aligned} \tag{4.55}$$

where we have used the gradient in cylindrical coordinates

$$\partial_\mu f(r,\varphi) = \nabla f(r,\varphi) = \frac{\partial f}{\partial r}\hat{r} + \frac{1}{r}\frac{\partial f}{\partial \varphi}\hat{\varphi}. \tag{4.56}$$

The φ-component of the last terms of the right-hand side are

$$\begin{aligned}
2h^2 \mathcal{A}_\mu \Phi^\dagger \Phi &= 2h^2 \frac{a(r)}{r}\phi^2\hat{\varphi}, \\
2h'^2 A_\mu \chi^2 &= 2h'^2 \frac{a(r)}{r}\xi^2\hat{\varphi}.
\end{aligned} \tag{4.57}$$

Inserting into eq. (4.51) the terms (4.55)-(4.57), we obtain the equation of motion for the gauge field. Analogously, adding the gauge term into eqs. (4.47) and (4.50), we obtain the equations of motion for the fields ϕ and ξ, respectively. Thus for the local cosmic strings, we obtain a system of second order differential equations given by

$$\begin{aligned}
\frac{d^2\phi}{dr^2} + \frac{1}{r}\frac{d\phi}{dr} &= \left(\frac{(n+ha)^2}{r^2} + \mu^2 + 2\lambda\phi^2 - \kappa\xi^2\right)\phi, \\
\frac{d^2\xi}{dr^2} + \frac{1}{r}\frac{d\xi}{dr} &= \left(\frac{(n'+h'a')^2}{r^2} + \mu'^2 + 2\lambda'\xi^2 - \kappa\phi^2\right)\xi, \\
\frac{d^2a}{dr^2} - \frac{1}{r}\frac{da}{dr} &= 2h\phi^2(n+ha) + 2h'\xi^2(n'+h'a).
\end{aligned} \tag{4.58}$$

Taking the large-r limit, we find — using eq. (4.58) — the quantization conditions

$$\lim_{r\to\infty} a(r) = -\frac{n}{h} = -\frac{n'}{h'}. \tag{4.59}$$

There is also a particular solution which we will not use because it is not consistent with the other two equations (if one requires the factors of order $1/r^2$ to cancel). It and is given by

$$\lim_{r\to\infty} a(r) = -\frac{hnv^2 + h'n'v'^2}{h^2v^2 + h'^2v'^2}. \tag{4.60}$$

4.2 Solutions

As we stated before, eqs. (4.34) and (4.58) are non-linear second order differential equations corresponding to the global and local cosmic string equations of motion. We explore solutions for both of them in order to analyze if there are significant differences. They can be treated as an initial value problem and as such, four and six initial values are needed, respectively. These initial values should be given by the fields and their first derivatives evaluated at $r = 0$.

Up to now we just have the values of the fields at the origin $r = 0$ which are zero (if the winding numbers are non-zero). We also have asymptotic conditions at $r \to \infty$ which do not fulfill the job of the remaining initial values to solve the problem. The missing initial values are the first derivatives of the fields at the origin. We can say there is a set of solutions that satisfy these initial values and asymptotic conditions; we will call them cosmic string solutions. There is another set of solutions that does not satisfy the conditions we need, so we are not interested in them. On the other hand the asymptotic conditions are imposed on the potential, but as an initial value problem we have no way to restrict the values of the derivatives in order to find only the cosmic strings. We can translate this problem into a boundary value problem (BVP), where we can impose the asymptotic conditions as boundary values at some final point r_f. This does not completely solve the problem, the set of cosmic string solutions can surely be found, however there might be other sets of solutions satisfying the conditions. This can be justified by the large number of free parameters we have and we will review them later in this chapter when we discuss the phase space of a particular case.

Nevertheless, the equations of motion can be solved using Python and the function `solve_bvp` which implements numerical methods to solve a system of non-linear differential equations with boundary conditions. The solutions are graphically presented in this section. For details about the algorithm that the function `solve_bvp` use, see Appendix B. The reliability of the solutions presented here can be tested using the Cauchy criterion `tol` inside the function `solve_bvp` and the additional Python function `status`. Furthermore we can perform a self-consistency test using the solutions computed in Python. These details can also be found also in Appendix B.

In all the plots given by Figs. 4.2-4.4 we use $v = 0.5$, $v' = 1$, $\lambda = 1 = \lambda'$. Implicitly we have $\mu^2 = -0.5 + \kappa$, $\mu'^2 = -2 + 0.25\kappa$. Converting to dimensional quantities, we have the Higgs VEV $v = 246$ GeV and therefore $v' = 492$ GeV as it is double. The variation of these parameters does not change the qualitative behaviour of the solutions. We also take $h = n$ and $h' = n'$. It turns out that the winding numbers establish the behaviour of the solutions. We vary $\kappa \in [-1, 1]$ to identify a set of κ-dependent solutions.

Figure 4.2 shows a case with winding numbers $n = 0$ and $n' = 1$. When $n = 0$, the gauge field decouples from the standard Higgs field. Nevertheless we have an indirect coupling because the two Higgs fields are coupled by the κ-term. For this reason the profile of the standard Higgs fields still gets modified. We also note that it does not vanish at the origin because the winding number is zero and we don't have problems with continuity.

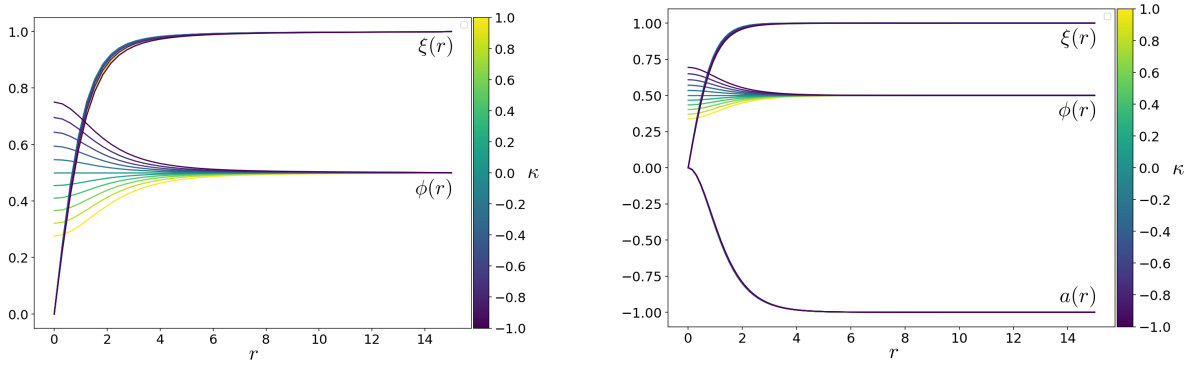

(a) (b)

Figure 4.2: Cosmic string solutions with (a) global symmetry (eq. (4.34)) and (b) local symmetry (eq. (4.58)) with a gauge field, with parameters $v = 0.5$, $v' = 1$, $\lambda = 1 = \lambda'$, $n = h = 0$, $n' = h' = 1$.

Figure 4.3 shows a case where the winding numbers are the same, $n = n' = 1$ and so both of the fields take a loop around the cosmic string. The profiles also have asymptotically stable solutions with respect to κ. At last, Fig. 4.4 represents a case where both winding numbers are non-zero but they are different, $n = 1$ and $n' = 2$. The standard Higgs field performs one loop around the cosmic string but the new Higgs field performs two loops. In contrast to the previous plots, we notice that near the origin there are solutions of the standard Higgs field which are larger than the new Higgs field, we call this an "overshooting" behaviour.

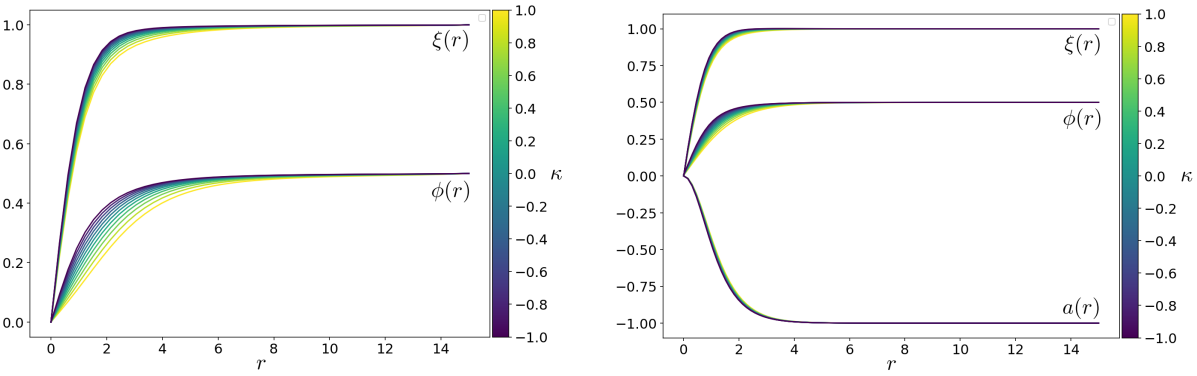

(a) (b)

Figure 4.3: Cosmic string solutions with (a) global symmetry (eq. (4.34)) and (b) local symmetry (eq. (4.58)) with a gauge field, with parameters $v = 0.5$, $v' = 1$, $\lambda = 1 = \lambda'$, $n = h = 1$, $n' = h' = 1$.

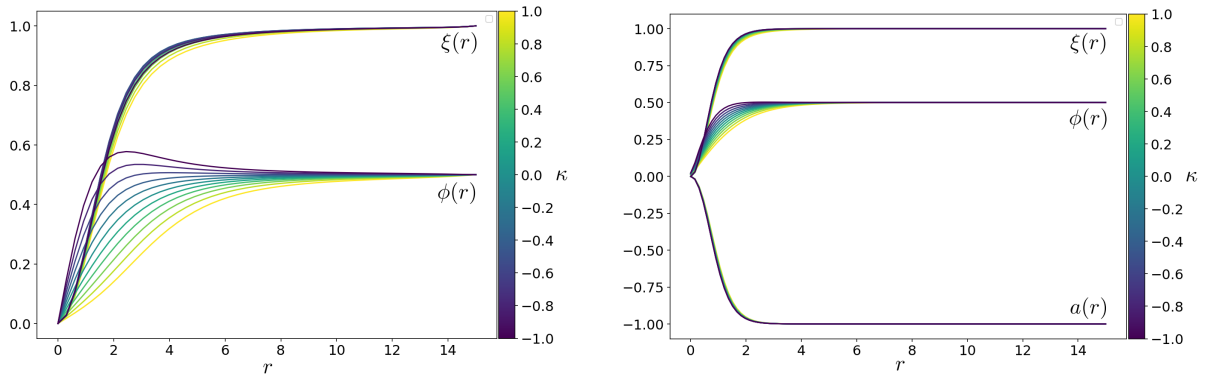

(a) (b)

Figure 4.4: Cosmic string solutions with (a) global symmetry (eq. (4.34)) and (b) local symmetry (eq. (4.58)) with a gauge field, with parameters $v = 0.5$, $v' = 1$, $\lambda = 1 = \lambda'$, $n = h = 1$, $n' = h' = 2$.

As we mentioned before, varying the parameters not involved with the winding numbers, does not change the qualitative behaviour of the solutions. We can select another set to check this, for example $v = 0.5$, $v' = 1.5$ and introducing back the units $v = 246$ GeV, $v' = 738$ GeV. Implicitly we have $\mu^2 = -0.25 + 2.25\kappa$ and $\mu'^2 = -4.5 + 0.25\kappa$. Additionally we can take distinct and smaller values for the self-couplings like $\lambda = 0.5$ and $\lambda' = 1$. These parameters are chosen in the set of Figs. 4.5-4.7.
Figure 4.5 refers to the case with the winding numbers $n = 0$ and $n' = 1$. We have the same qualitative behaviour as above, the standard Higgs field can take non-zero values at the origin because of the non-zero winding number while the cosmic string profile is only visible on the non-standard Higgs field. At last for the asymptotic value of the gauge field is determined by $h' = n' = 1$ while $h = n = 0$.

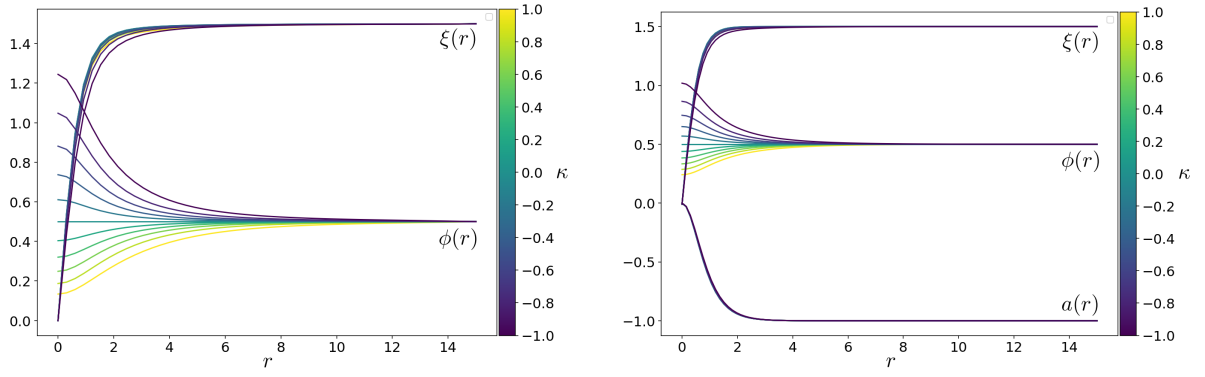

(a) (b)

Figure 4.5: Cosmic string solutions with (a) global symmetry (eq. (4.34)) and (b) local symmetry (eq. (4.58)) with a gauge field, with parameters $v = 0.5$, $v' = 1.5$, $\lambda = 0.5$, $\lambda' = 1$, $n = h = 0$, $n' = h' = 1$.

Figure 4.6 shows a case with winding numbers $n = n' = 1$. We can also take distinct values for the self-couplings as $\lambda' = 0.5$ and $\lambda = 1$. In addition, the couplings of the Higgs fields with the gauge field can also be taken differently as $h = 0.5 = h'$. This last condition induces a different asymptotic behaviour for the gauge field as we can see in the plot, as it attains the quotient $-n/h$.

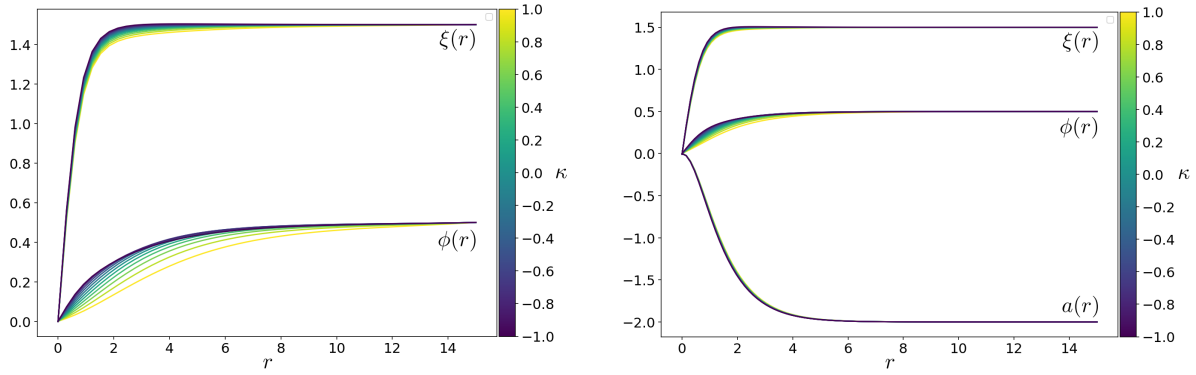

(a) (b)

Figure 4.6: Cosmic string solutions with (a) global symmetry (eq. (4.34)) and (b) local symmetry (eq. (4.58)) a with gauge field, with parameters $v = 0.5$, $v' = 1.5$, $\lambda = 0.5$, $\lambda' = 1$, $n = 1 = n'$, $h = 0.5 = h'$.

For the case of winding numbers $n = 1$ and $n' = 2$ we have Fig. 4.7. But now by taking $h' = 0.5$, the asymptotic condition necessarily demands $h' = 1$ as eq. (4.59) states. We also note in this plot the same behaviour in which the standard Higgs field grows faster than the new one in the origin and the "overshooting".

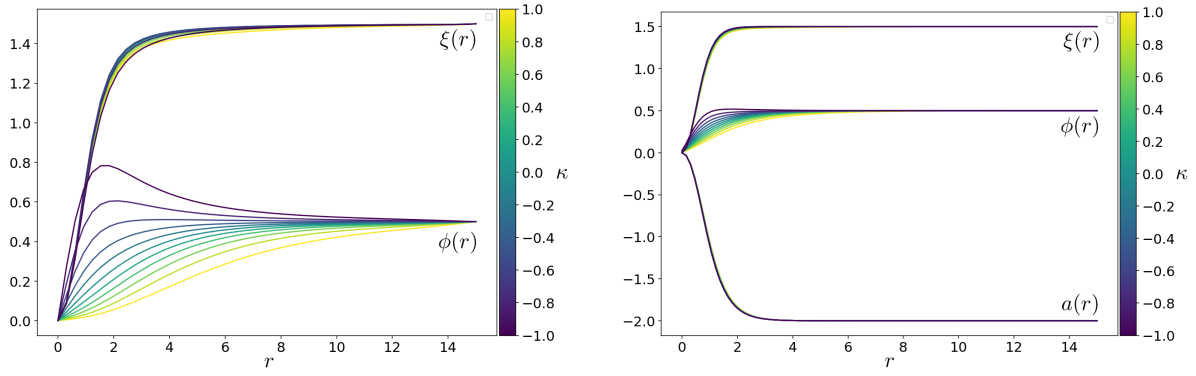

(a) (b)

Figure 4.7: Cosmic string solutions with (a) global symmetry (eq. (4.34)) and (b) local symmetry (eq. (4.58)) with a gauge field, with parameters $v = 0.5$, $v' = 1.5$, $\lambda = 0.5$, $\lambda' = 1$, $n = 1$, $n' = 2$, $h = 0.5$, $h' = 1$.

As we mentioned above, the $SO(10)$ GUT subgroup $SU(3)_c \otimes SU(2)_L \otimes U(1)_{Y'} \otimes U(1)_Y$ is obtained by fixing the parameters in eq. (4.20). Recalling that we absorbed α and β inside the couplings h and h', we get

$$h \to h\frac{\alpha}{2} = \sqrt{\frac{2}{3}}g'\frac{1}{2} = \sqrt{\frac{1}{6}}g', \tag{4.61}$$

$$h' \to 2h\beta = -2\sqrt{\frac{2}{3}}g'\frac{5}{4} = -5\sqrt{\frac{1}{6}}g', \tag{4.62}$$

for the same equations of motion and using this fixed parameters we find an additional constraint in the winding numbers

$$n' = -5n, \tag{4.63}$$

due to the asymptotic condition in eq. (4.59). Figure 4.8 shows this case for the winding numbers (a) $n = 1$, $n' = -5$ and (b) $n = -2$, $n' = 10$. In both plots we see the "overshooting" behaviour in $\phi(r)$ is enhanced by an increasing value of the winding number $|n'|$. Additionally we identify $\xi(r)$ being kept close to zero at small r, also by an increasing value of $|n'|$.

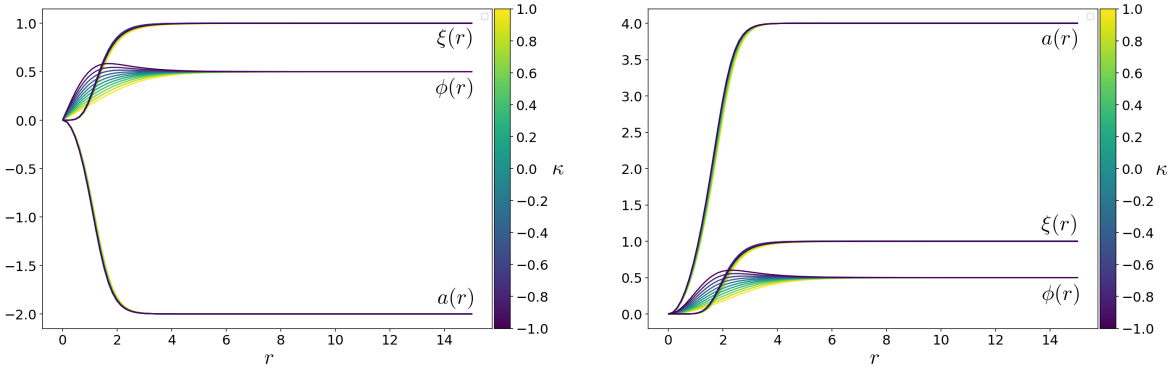

(a) (b)

Figure 4.8: Cosmic string solutions with local symmetry (eq. (4.58)) with a gauge field, winding numbers (a) $n = 1$, $n' = -5$ and (b) $n = -2$, $n' = 10$, the parameters are $v = 0.5$, $v' = 1$, $\lambda = 1 = \lambda'$, $h = 0.5$, $h' = -2.5$.

4.3 Fixed points

Cosmic string solutions had been found inside a region $(\kappa_{\min}, \kappa_{\max})$, using Python. Solutions exist outside this region as Appendix B shows, but Python is unable to obtain them. This can be justified by analyzing the Python algorithm and concluding that it might be because of a bad initial guess function. A different behaviour of solutions, inside and outside this region can be shown by performing an analysis of the stability matrix $\mathcal{M}$ at the fixed point of interest $\phi \to v$ and $\xi \to v'$. The signs of the eigenvalues of this matrix determine the conditions of stability for a fixed point of a system of differential equations. We write our model as a first order system of

differential equations

$$\begin{aligned}
\frac{d\phi}{dr} &= \phi_d, \\
\frac{d\xi}{dr} &= \xi_d, \\
\frac{d\phi_d}{dr} &= -\frac{1}{r}\phi_d + \frac{n^2}{r^2}\phi + \mu^2\phi + 2\lambda\phi^3 - \kappa\phi\xi^2, \\
\frac{d\xi_d}{dr} &= -\frac{1}{r}\xi_d + \frac{n'^2}{r^2}\xi + \mu'^2\xi + 2\lambda'\xi^3 - \kappa\xi\phi^2.
\end{aligned} \tag{4.64}$$

The Hessian, or stability matrix is

$$\begin{aligned}
\mathcal{M} &= \begin{pmatrix}
\frac{\partial}{\partial\phi_d}\frac{d\phi}{dr} & \frac{\partial}{\partial\phi}\frac{d\phi}{dr} & \frac{\partial}{\partial\xi_d}\frac{d\phi}{dr} & \frac{\partial}{\partial\xi}\frac{d\phi}{dr} \\
\frac{\partial}{\partial\phi_d}\frac{d\phi_d}{dr} & \frac{\partial}{\partial\phi}\frac{d\phi_d}{dr} & \frac{\partial}{\partial\xi_d}\frac{d\phi_d}{dr} & \frac{\partial}{\partial\xi}\frac{d\phi_d}{dr} \\
\frac{\partial}{\partial\phi_d}\frac{d\xi}{dr} & \frac{\partial}{\partial\phi}\frac{d\xi}{dr} & \frac{\partial}{\partial\xi_d}\frac{d\xi}{dr} & \frac{\partial}{\partial\xi}\frac{d\xi}{dr} \\
\frac{\partial}{\partial\phi_d}\frac{d\xi_d}{dr} & \frac{\partial}{\partial\phi}\frac{d\xi_d}{dr} & \frac{\partial}{\partial\xi_d}\frac{d\xi_d}{dr} & \frac{\partial}{\partial\xi}\frac{d\xi_d}{dr}
\end{pmatrix} \\
&= \begin{pmatrix}
1 & 0 & 0 & 0 \\
-\frac{1}{r} & \frac{n^2}{r^2} + \mu^2 + 6\lambda\phi^2 - \kappa\xi^2 & 0 & -2\kappa\phi\xi \\
0 & 0 & 1 & 0 \\
-\frac{1}{r} & -2\kappa\phi\xi & 0 & \frac{n'^2}{r^2} + \mu'^2 + 6\lambda'\xi^2 - \kappa\phi^2
\end{pmatrix}.
\end{aligned} \tag{4.65}$$

We look for a restriction in the free parameters for a cosmic string solution which should have a fixed point in the large-r limit. The matrix takes the asymptotic form

$$\lim_{r\to\infty}\mathcal{M} = \begin{pmatrix}
1 & 0 & 0 & 0 \\
0 & \mu^2 + 6\lambda v^2 - \kappa v'^2 & 0 & -2\kappa v v' \\
0 & 0 & 1 & 0 \\
0 & -2\kappa v v' & 0 & \mu'^2 + 6\lambda' v'^2 - \kappa v^2
\end{pmatrix} \tag{4.66}$$

and it has the eigenvalues

$$\begin{aligned}
\lambda_1 &= 1, \\
\lambda_2 &= 1, \\
\lambda_3 &= 2\left(\lambda v^2 + \lambda' v'^2 + \sqrt{(\kappa^2 - 2\lambda\lambda')v^2 v'^2 + \lambda^2 v^4 + \lambda'^2 v'^4}\right), \\
\lambda_4 &= 2\left(\lambda v^2 + \lambda' v'^2 - \sqrt{(\kappa^2 - 2\lambda\lambda')v^2 v'^2 + \lambda^2 v^4 + \lambda'^2 v'^4}\right).
\end{aligned} \tag{4.67}$$

For the case we treated before in the Figs. 4.2-4.4 where the parameters are chosen as $v = 0.5$, $v' = 1$, $\lambda = 1$ and $\lambda' = 1$, the eigenvalues evaluated at the fixed point are

$$\lambda_1 = 1, \quad \lambda_2 = 1, \quad \lambda_3 = \frac{5 + \sqrt{9 + 4\kappa^2}}{2}, \quad \lambda_4 = \frac{5 - \sqrt{9 + 4\kappa^2}}{2}, \tag{4.68}$$

and we can see that λ_4 takes both signs. Indeed, this eigenvalue is positive for $\kappa \in (-2, 2)$. This is an argument to restrict the values of the free parameter κ due to stability. Cosmic strings in Python are found inside this region.

This analysis can be extended if we see that the differential equations define a phase space. The set of all solutions and its behaviour can be seen here. Unfortunately even in the global

symmetry case with $\kappa = 0$, the phase space has 3 dimensions: r, ϕ and $\frac{d\phi}{dr}$ or r, ξ and $\frac{d\xi}{dr}$. At least in 3 dimensions we can take the projections for different r like Fig. 4.9 as a ϕ vs $\frac{d\phi}{dr}$ or a ξ vs $\frac{d\xi}{dr}$ plot with fixed r.

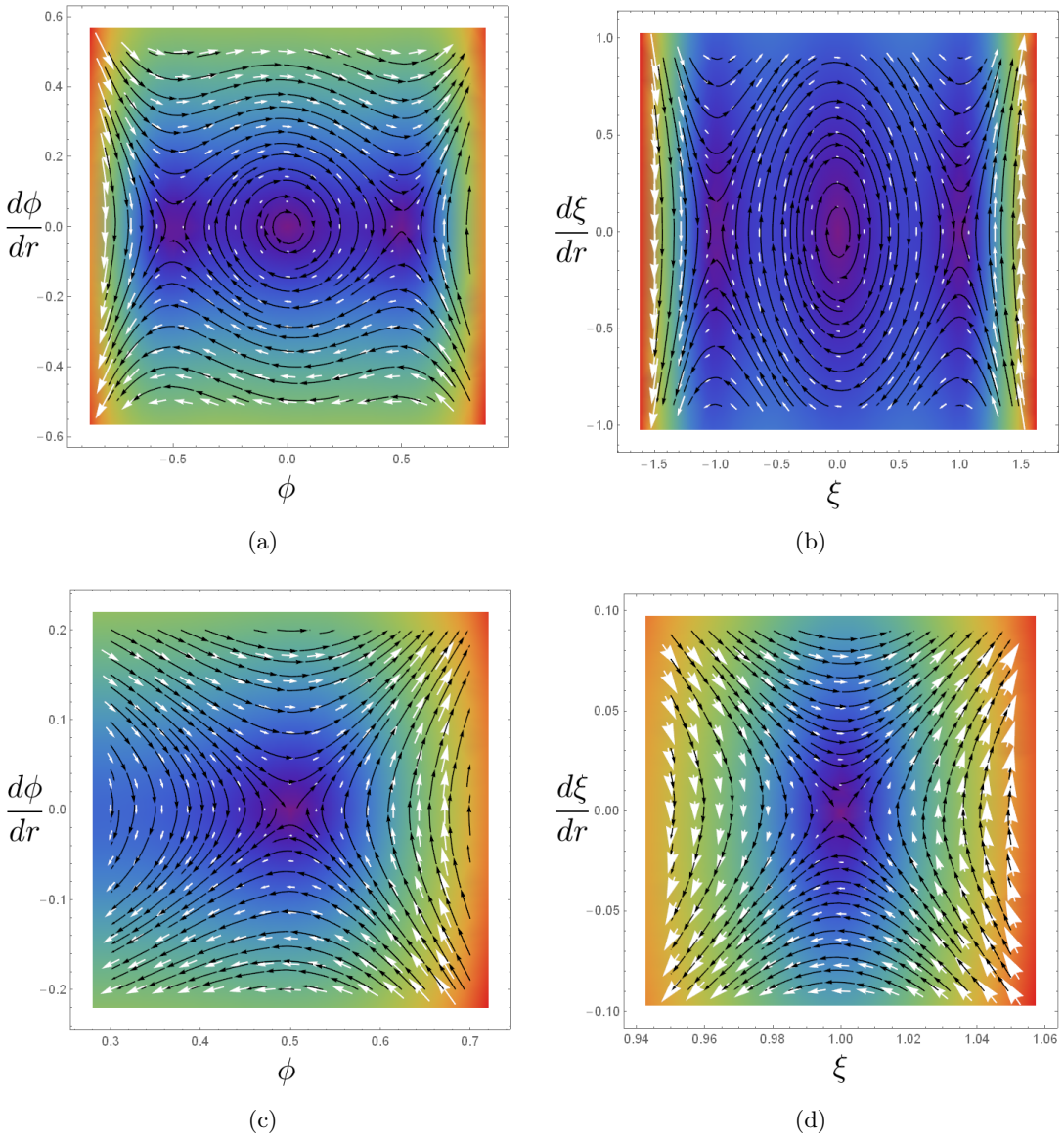

Figure 4.9: Phase space for the differential equations with $\kappa = 0$ showing three fixed points for the fields ϕ and ξ, respectively in (a) and (b). A closer look is shown in (c) and (d), respectively. The parameters are $v = 0.5$, $v = 1$, $\lambda = 1 = \lambda'$ and $r = 15$.

From these projections in Fig. 4.9 we can see there are three critical points in each plot, including a fixed point in $(0, 0)$ which is stationary. Around it we see oscillatory solutions and as we vary r they are damped towards zero. Outside these solutions we have two fixed points where the fields attain their VEV $\phi \to \pm v$ and $\xi \to \pm v'$. We see a region of solutions that fall into these fixed points and others which are repelled from them, those are divergent solutions.

When we consider $\kappa \neq 0$, the phase space has 5 dimensions. As we discussed before, there is an interval $(\kappa_{\min}, \kappa_{\max})$ where the eigenvalue λ_4 is positive and outside, it is negative. For the parameters chosen in this section we found the region $\kappa \in (-2, 2)$. Following the classification of stability analysis from the Hessian matrix, this would mean the fixed points $\phi \to \pm v$ and $\xi \to \pm v'$ are nodal sources, while for κ outside this region they are saddle points.

Now if we consider the full system of equations with the gauge symmetry, we obtain a first order system of differential equations given by

$$\begin{aligned}
\frac{d\phi}{dr} &= \phi_d, \\
\frac{d\xi}{dr} &= \xi_d, \\
\frac{da}{dr} &= a_d, \\
\frac{d\phi_d}{dr} &= -\frac{1}{r}\phi_d + \frac{n^2}{r^2}\phi + \mu^2\phi + 2\lambda\phi^3 - \kappa\phi\xi^2 + h\frac{a}{r^2}\phi(2n + ha), \\
\frac{d\xi_d}{dr} &= -\frac{1}{r}\xi_d + \frac{n'^2}{r^2}\xi + \mu'^2\xi + 2\lambda'\xi^3 - \kappa\xi\phi^2 + h'\frac{a}{r^2}\xi(2n' + h'a), \\
\frac{da_d}{dr} &= \frac{1}{r}a_d + 2h\phi^2(n + ha) + 2h'\xi^2(n' + h'a).
\end{aligned} \tag{4.69}$$

Now the Hessian is the matrix

$$\mathcal{M} = \begin{pmatrix}
\frac{\partial}{\partial\phi_d}\frac{d\phi}{dr} & \frac{\partial}{\partial\phi}\frac{d\phi}{dr} & \frac{\partial}{\partial\xi_d}\frac{d\phi}{dr} & \frac{\partial}{\partial\xi}\frac{d\phi}{dr} & \frac{\partial}{\partial a_d}\frac{d\phi}{dr} & \frac{\partial}{\partial a}\frac{d\phi}{dr} \\
\frac{\partial}{\partial\phi_d}\frac{d\phi_d}{dr} & \frac{\partial}{\partial\phi}\frac{d\phi_d}{dr} & \frac{\partial}{\partial\xi_d}\frac{d\phi_d}{dr} & \frac{\partial}{\partial\xi}\frac{d\phi_d}{dr} & \frac{\partial}{\partial a_d}\frac{d\phi_d}{dr} & \frac{\partial}{\partial a}\frac{d\phi_d}{dr} \\
\frac{\partial}{\partial\phi_d}\frac{d\xi}{dr} & \frac{\partial}{\partial\phi}\frac{d\xi}{dr} & \frac{\partial}{\partial\xi_d}\frac{d\xi}{dr} & \frac{\partial}{\partial\xi}\frac{d\xi}{dr} & \frac{\partial}{\partial a_d}\frac{d\xi}{dr} & \frac{\partial}{\partial a}\frac{d\xi}{dr} \\
\frac{\partial}{\partial\phi_d}\frac{d\xi_d}{dr} & \frac{\partial}{\partial\phi}\frac{d\xi_d}{dr} & \frac{\partial}{\partial\xi_d}\frac{d\xi_d}{dr} & \frac{\partial}{\partial\xi}\frac{d\xi_d}{dr} & \frac{\partial}{a_d}\frac{d\xi_d}{dr} & \frac{\partial}{\partial a}\frac{d\xi_d}{dr}
\end{pmatrix}, \tag{4.70}$$

and in the large-r limit

$$\lim_{r\to\infty}\mathcal{M} = \begin{pmatrix}
1 & 0 & 0 & 0 & 0 & 0 \\
0 & \mu^2 + 6\lambda v^2 - \kappa v'^2 & 0 & -2\kappa v v' & 0 & 0 \\
0 & 0 & 1 & 0 & 0 & 0 \\
0 & -2\kappa v v' & 0 & \mu'^2 + 6\lambda' v'^2 - \kappa v^2 & 0 & 0 \\
0 & 0 & 0 & 0 & 0 & 2(h^2v^2 + h'^2v'^2)
\end{pmatrix}. \tag{4.71}$$

$$\begin{aligned}
\lambda_1 &= 1, \\
\lambda_2 &= 1, \\
\lambda_3 &= 1, \\
\lambda_4 &= 2(h^2v^2 + h'^2v'^2), \\
\lambda_5 &= 2\left(\lambda v^2 + \lambda' v'^2 + \sqrt{(\kappa^2 - \lambda\lambda')v^2v'^2 + \lambda^2v^4 + \lambda'^2v'^4}\right), \\
\lambda_6 &= 2\left(\lambda v^2 + \lambda' v'^2 - \sqrt{(\kappa^2 - \lambda\lambda')v^2v'^2 + \lambda^2v^4 + \lambda'^2v'^4}\right).
\end{aligned} \tag{4.72}$$

These are the same eigenvalues as in the global symmetry plus two more which are positive. Thus, in general we find that all eigenvalues are positive if $\kappa^2 < 4\lambda\lambda'$ or equivalently, if $\kappa \in (-2\sqrt{\lambda\lambda'}, 2\sqrt{\lambda\lambda'})$.

Chapter 5

Conclusions

In this thesis we have reviewed the SM of particle physics with the goal of proposing an extension and looking for cosmic string solutions. We gave a short historical perspective which motivated the construction of the SM, emphasising symmetries and conservation laws such as baryon number or lepton number. In this review we paid special attention to the Higgs mechanism, where a SSB gives mass to quarks, leptons and the bosons $W^{\pm}$ and Z^0. We have discussed the three generations of quarks and leptons, pointing out that the SM treats neutrinos as massless left-handed particles. Afterwards we reviewed topological defects, particularly vortices which are present in condensed matter systems like superconductors and superfluids. Taking these systems as an example, gave us a picture of the cosmic strings we are looking for, since they are also based on one-dimensional topological defects. These systems are analogous to cosmic strings and can be studied in controlled experiments, so their mathematical description gives physical clarity through an available realization in nature. At last we connected these systems with particle physics by referring to cosmic strings as vortices arising in field theory for topological reasons.

We then proposed our extension of the SM taking into account the $B-L$ conservation. We previously mentioned that baryon and lepton number violation were allowed by the SM, but the difference is conserved. This is why we gauge this symmetry in our proposal, using explicitly the symmetry group $U(1)_{Y'}$ with $Y' = \alpha Y + \beta(B-L)$. To prevent the model from having gauge anomalies, we have to include a right-handed neutrino to each fermion generation. With right-handed neutrinos we can give mass to neutrinos using a Dirac mass term and an additional Majorana mass term for the right-handed neutrinos. We use the Higgs mechanism and add a new Higgs field which gives mass to right-handed neutrinos without breaking the $B-L$ gauge symmetry. We end up adding a gauge field, a new Higgs field and a right-handed neutrino to each fermion generation. The model is well posed since $B-L$ is a gauge symmetry, there are no gauge anomalies, neutrinos can have mass and none of the new terms in the Lagrangian violates $B-L$ conservation. Furthermore we can justify the lack of evidence of these particles using properties for the Higgs VEVs, interactions and masses. As an hypothetical model, it needs to be confronted with experimental data to relate it to a realistic scenario. Fortunately, the $SO(10)$ GUT subgroup $SU(3)_c \otimes SU(2)_L \otimes U(1)_{Y'} \otimes U(1)_Y$ is well posed under the constraints established for its new free parameters using experimental data.

With this model we then look for cosmic string solutions but we restrict ourselves to a sector of this extension. This sector involves the standard and new Higgs fields and the $U(1)_{Y'}$ gauge field. Simplicity is one of the main guidelines but we can also invoke a constant fermion background and a low energy regime. Semi-local cosmic string in this new Higgs and electroweak sectors are a valid starting point for calculations. Certainly a full analysis would involve the $W^{\pm}$ and Z bosons, quarks, leptons and gluons.

The cosmic string involves the Higgs fields Φ, χ and the gauge field $\mathcal{A}_{\mu}$. This behaviour is shown in the plotted solutions in Section 4.2 and it arises from the coupling terms in the equations of motion. We find our solutions to be strongly dependent on the winding numbers but not on any other free parameters. As we can see in the plots, the profiles of the fields change their qualitative behaviour depending on the values of the winding numbers n and n', While differences in κ, λ, λ' or the VEVs v and v' lead to a continuous change of the curves. A property we should point out is that the penetration depth of the cosmic string is modified by these parameters. But in general everything else is qualitatively invariant.

Let us take a look at the case when there is no direct coupling between the standard Higgs field and the gauge field, that is the case $h = 0$ (or $\alpha = 0$) in Figs. 4.2 and 4.5. Physically, taking this coupling to zero means that we are taking just $B - L$ as the gauge symmetry, since we are working with $U(1)_{Y'}$. We can also give it another perspective as a semi-local cosmic string, where the hypercharge is not a gauge symmetry but a global one. Here, the winding number of this Higgs field can be taken as non-trivial zero according to eq. (4.59). Furthermore, when $\kappa = 0$ the Higgs field is constant and it takes its usual VEV everywhere. This is expected since then the Higgs field decouples to the new Higgs field. But when $\kappa \neq 0$, the standard Higgs field is indirectly coupled to the gauge field through the new Higgs field. This changes the constant behaviour and it can take larger or smaller values at the origin and then present an asymptotic behaviour towards its VEV. On the other hand, the new Higgs field depicts the characteristic behaviour of a cosmic string solution, growing fast from zero to its VEV. It is the $\kappa = 0$ case where the system reduces to the Abelian Higgs model and the penetration depth is given by $L = 1/h'v'$. For $\kappa \neq 0$ we can see the penetration depth depending on it. At last, the gauge field also depicts the same cosmic string profile going from zero towards its asymptotic condition. Variation of the parameters v, v', λ, λ' and κ changes the numerical values of the fields but not this qualitative behaviour. The same arguments apply for the opposite case when $h' = 0$ (or $\beta = 0$). We have here a semi-local cosmic string in the gauged symmetry group $U(1)_Y$ and a penetration depth $L = 1/hv$ when $\kappa = 0$.

The second case of interest is the one where the winding numbers are $n = 1 = n'$ which can be seen in Figs. 4.3 and 4.6. Here, both Higgs fields wind around the cosmic string once. The solutions perform the regular behaviour of a cosmic string profile. Variation of the free parameters between these figures does not change the characteristic behaviour of the profiles. Particularly, taking $\kappa = 0$ establishes a curve in the plots, while taking it as non-zero changes the behaviour near the cosmic string core. It turns out that the profiles acquire their asymptotic conditions closer to the core for negative κ and further away for positive κ. These figures are ideal for appreciating the smooth change in the plots depending on the parameters. As we mentioned before, the penetration depth depends on the free parameters and variation of κ is well represented as a continuous change in it. This can be seen in the figures, reducing the coupling κ from positive to negative values results in a smaller penetration depth.

At last, the third case of interest is the one depicted in Figs. 4.4 and 4.7. Here the winding numbers are $n = 1$ and $n' = 2$, implying that the standard Higgs field takes one loop around the cosmic string while the new field takes two loops. This case is different from the others above for two reasons. First there is a region where the standard Higgs field grows faster than the new one. Even if the standard Higgs VEV is smaller, we can see this behaviour near the core for certain negative values of κ. The second reason for which this case is different is the "overshooting" effect, where the standard Higgs field can take larger values than its asymptotic VEV in the core. Further analysis of this feature is needed and there is a possibility that these solutions might be excluded for being dynamically unstable.

The results for the other winding numbers can be inferred from the cases above. Case 1 applies to $n = 0$, $n' \neq 0$, with the observation that the sign of n' will change the sign of the asymptotic condition of the gauge field. For $n = n'$ case 2 is applied and we can expect regular cosmic string profiles, the gauge field can change its asymptotic value or not, depending on the values of the couplings h and h'. For $|n| < |n'|$ we can apply case 3. Numerically we can expect the same type of behaviour, but a stability analysis for this new conditions should be done.

Figure 4.8 shows the cosmic string solutions for the $SO(10)$ GUT subgroup which we considered as a more valid physical scenario. This corresponds to the case 3 where $|n| < |n'|$ and we can see that the "overshooting" effect is enhanced by the large value of $|n'|$. This large value is a constraint set by the asymptotic condition for $a(r)$ in eq. (4.59) leading to $n' = -5n$. This condition can be relaxed to eq. (4.60) providing freedom for the winding numbers, so that we can choose small values if stability conditions for this realistic model require them. This scenario can be interpreted as the limiting case where the mixing angle is $\Theta = 0$ and the gauge field $\mathcal{A}_\mu$ corresponds to the Z' boson. Furthermore, the validity of these solutions relies on the argument of the constant fermion background to justify the absence of fermions in the Lagrangian. We also have the argument of a low energy effective theory which we used to justify the absence of the $W^\pm$ and Z^0 bosons. An additional argument in this mixing angle is extremising the energy, as it is usually done (see for example Refs. [75, 76]) where we can take $W^1_\mu = W^2_\mu = A_\mu = 0$, but this would require another differential equation for the Z^0_μ field with an ansatz in cylindrical coordinates as the one for $\mathcal{A}_\mu$. Thus, this would be the next logical step to work out a full analysis.

The first physical consequence in this proposal is the change of particles masses when they go across or nearby the string. This can be seen in the Yukawa terms in the SM Lagrangian and the profile of the Higgs field throughout the plots. The neutrino masses have the same behaviour due to the new terms we added in the Lagrangian. There is just a single case in which the cosmic string is not present in the standard Higgs field as we can see in Fig. 4.2: for $\kappa = 0$ and $n = 0$ this field takes its VEV everywhere. Thus in this scenario, just neutrinos masses will be affected when passing near the cosmic strings.

As we mentioned before, for future work a full analysis is needed. This would involve the W, B bosons and fermion fields. In order to achieve this, we should consider more terms in the Lagrangian, resulting in a larger system of coupled non-linear differential equations. In this work we got a system of three equations, considering the W and B fields would give us a system of 7 equations since they are vector fields. These $SU(2)_L$ gauge fields are used in the Lagrangian given in eq. (4.6) in an analogous way as the $U(1)_{Y'}$ gauge field. But we should notice that the

Lagrangian contains the field strength tensor and that they are only coupled to the standard Higgs field through the covariant derivative. If we want to solve this problem, we should follow the same steps by getting the equations of motion and imposing boundary conditions under a cylindrically symmetric ansatz. Because of the Lagrangian structure, the equations of motion for the $SU(2)_L$ fields will take a form similar to the $U(1)_{Y'}$ field. We would expect these fields to be related to the cosmic string, but only if the standard Higgs field winding number is non-zero $n \neq 0$. If $n = 0$ then we would expect the radial part of the W and B fields to have a constant behaviour with $\kappa = 0$, while for $\kappa \neq 0$ there would be an indirect coupling to the cosmic string through the Higgs fields. For all the other cases we expect similar cosmic string profiles in the solutions. We can get this equations of motion for the fields Φ, ξ, $\mathcal{A}_\mu$, B_μ and W^a_μ or equivalently in the physical fields Φ, ξ, Z'_μ, Z_μ, $W^\pm_\mu$ and A_μ if we use the mixing angles θ_W and Θ.

Adding a first generation of fermions implies adding left- and right-handed electrons, neutrinos, up and down quarks. By following the same steps, we would start obtaining the equations of motion in a cylindrically symmetric ansatz, we would find that there are 8 new fields in total to add. If we take into account also the W and B fields, then we are in a new and extended electroweak sector. Our result would be a system of 15 non-linear second order differential equations. Unfortunately, an analysis like the one above can't be performed easily because of the complexity and diversity of terms in the new Lagrangian. We can't say how would be the behaviour of the fermion fields or if they would change the profiles of the Higgs and gauge fields solved and analyzed before. It is required to do the full calculations and numerical solutions in order to go beyond. Furthermore adding the two remaining generations would lead to a system of 31 coupled and non-linear second order differential equations. A full quantum field analysis is beyond the scope of this thesis, with all these fields at hand it would be important to do it in the future.

Throughout this analysis we have found three types of cosmic strings described in the three cases above. However we could imagine a fourth type, the co-axial cosmic string. We have not found this type of solution numerically and other methods should be proposed to look for them. If we look for a co-axial solution, it would look like a line in the phase space in Fig. 4.9, that travels around the ϕ (ξ) axis taking both negative and positive values before reaching the fixed point $\phi \to v$ ($\xi \to v'$). The phase space does not need to give some initial values, we obtain all the solutions admitted by the equations of motion. There is no co-axial solution in this plot. Even though, one can argue that this plot has not enough resolution. If there exist a co-axial string solution, it is between the damped oscillations and the axial cosmic string, in a very small range.

Some other physical properties and effects can be studied in the future, of the cosmic strings reported here and in the possible extension of the full electroweak sector we considered before. For example, we can look for superconducting properties in the core, since the photon field is included in the full gauge symmetry, and the effects on the scattering of particles. Also a dynamical analysis can be done, including mass and string tension. This would lead us to perform a dynamical stability analysis and to production of gravitational waves. The complexity of all these properties is clearly beyond the scope of this thesis but they are certainly important for observational purposes, since our analysis does not provide predictions for these kind of effects.

Appendix A

Derivatives with respect to a field

This appendix clarifies the variational derivative with respect to the Higgs field. This means that we have to analyze how the variational derivative of a complex scalar or a doublet acts. We do this in two different forms, using real scalar fields and complex scalar fields, finding the same and consistent result. Finally we are going to justify the result

$$\frac{\delta}{\delta\Phi^\dagger}(\Phi^\dagger\Phi) = \Phi. \tag{A.1}$$

A.1 Derivative with respect to a complex scalar field

First, let us consider a one-component scalar field $\phi \in \mathbb{C}$. We can write it as a real and imaginary part,

$$\phi = \phi_1 + i\phi_2, \quad \phi^* = \phi_1 - i\phi_2, \tag{A.2}$$

where ϕ_1, $\phi_2 \in \mathbb{R}$ are real scalar fields. Using eq. (A.2) the real components are

$$\phi_1 = \frac{1}{2}(\phi + \phi^*), \quad \phi_2 = -\frac{i}{2}(\phi - \phi^*). \tag{A.3}$$

Now we want to define the derivative with respect to a complex scalar field, so we use the derivatives of the real fields, that we already know how to compute. As it is a derivative, the Leibniz rule is a condition we must impose

$$\frac{\delta}{\delta\phi^*} = \frac{\delta\phi_1}{\delta\phi^*}\frac{\delta}{\delta\phi_1} + \frac{\delta\phi_2}{\delta\phi^*}\frac{\delta}{\delta\phi_2}, \tag{A.4}$$

Equation (A.3) specifies how to compute the variational derivatives

$$\frac{\delta\phi_1}{\delta\phi^*} = \frac{1}{2}, \quad \frac{\delta\phi_2}{\delta\phi^*} = \frac{i}{2}, \tag{A.5}$$

thus

$$\frac{\delta}{\delta\phi^*} = \frac{1}{2}\frac{\delta}{\delta\phi_1} + \frac{i}{2}\frac{\delta}{\delta\phi_2}. \tag{A.6}$$

With this definition, a consistency check confirms the treatment of ϕ and ϕ^* as independent fields

$$\frac{\delta\phi^*}{\delta\phi^*} = \frac{1}{2}\frac{\delta\phi^*}{\delta\phi_1} + \frac{i}{2}\frac{\delta\phi^*}{\delta\phi_2} = \frac{1}{2}\frac{\delta}{\delta\phi_1}(\phi_1 - i\phi_2) + \frac{i}{2}\frac{\delta}{\delta\phi_2}(\phi_1 - i\phi_2) = \frac{1}{2} - \frac{i^2}{2} = 1, \tag{A.7}$$

$$\frac{\delta\phi}{\delta\phi^*} = \frac{1}{2}\frac{\delta\phi}{\delta\phi_1} + \frac{i}{2}\frac{\delta\phi}{\delta\phi_2} = \frac{1}{2}\frac{\delta}{\delta\phi_1}(\phi_1 + i\phi_2) + \frac{i}{2}\frac{\delta}{\delta\phi_2}(\phi_1 + i\phi_2) = \frac{1}{2} + \frac{i^2}{2} = 0. \tag{A.8}$$

This consideration confirms that ϕ and ϕ^* can be treated as independent with respect to the variational derivative. Now we want to compute the derivative of the product

$$\phi^*\phi = (\phi_1 - i\phi_2)(\phi_1 + i\phi_2) = \phi_1^2 + \phi_2^2, \tag{A.9}$$

so

$$\frac{\delta}{\delta\phi^*}(\phi^*\phi) = \left(\frac{1}{2}\frac{\delta}{\delta\phi_1} + \frac{i}{2}\frac{\delta}{\delta\phi_2}\right)(\phi_1^2 + \phi_2^2) = \frac{1}{2}\frac{\delta}{\delta\phi_1}(\phi_1^2 + \phi_2^2) + \frac{i}{2}\frac{\delta}{\delta\phi_2}(\phi_1^2 + \phi_2^2) = \frac{1}{2}2\phi_1 + \frac{i}{2}2\phi_2 = \phi, \tag{A.10}$$

therefore

$$\frac{\delta}{\delta\phi^*}(\phi^*\phi) = \phi. \tag{A.11}$$

Analogously, with

$$\frac{\delta}{\delta\phi}(\phi^*\phi) = \left(\frac{1}{2}\frac{\delta}{\delta\phi_1} - \frac{i}{2}\frac{\delta}{\delta\phi_2}\right)(\phi_1^2 + \phi_2^2) = \frac{1}{2}\frac{\delta}{\delta\phi_1}(\phi_1^2 + \phi_2^2) - \frac{i}{2}\frac{\delta}{\delta\phi_2}(\phi_1^2 + \phi_2^2) = \frac{1}{2}2\phi_1 - \frac{i}{2}2\phi_2 = \phi^*, \tag{A.12}$$

we find

$$\frac{\delta}{\delta\phi}(\phi^*\phi) = \phi^*. \tag{A.13}$$

A.2 Derivative with respect to a scalar doublet

In this section we obtain the variational derivative of a complex scalar doublet field. We will use the result we obtained in Section A.1 and the two methods we mentioned, starting from real scalar fields to construct the complex doublet.

A.2.1 Using real scalar fields

Now let us consider a complex scalar doublet $\Phi \in \mathbb{C}^2$, we can write it as

$$\Phi = \begin{pmatrix}\phi_1 + i\phi_2 \\ \phi_3 + i\phi_4\end{pmatrix}, \quad \Phi^\dagger = (\phi_1 - i\phi_2, \quad \phi_3 - i\phi_4) \tag{A.14}$$

with ϕ_1, ϕ_2, ϕ_3, $\phi_4 \in \mathbb{R}$ real scalar fields. Following a straightforward generalization of eq. (A.6) we propose a derivative like

$$\frac{\delta}{\delta\Phi^\dagger} = \frac{1}{2}\begin{pmatrix}1\\0\end{pmatrix}\frac{\delta}{\delta\phi_1} + \frac{i}{2}\begin{pmatrix}1\\0\end{pmatrix}\frac{\delta}{\delta\phi_2} + \frac{1}{2}\begin{pmatrix}0\\1\end{pmatrix}\frac{\delta}{\delta\phi_3} + \frac{i}{2}\begin{pmatrix}0\\1\end{pmatrix}\frac{\delta}{\delta\phi_4}. \tag{A.15}$$

As a consistency check we consider

$$\begin{aligned}\frac{\delta\Phi^\dagger}{\delta\Phi^\dagger} &= \left(\frac{1}{2}\begin{pmatrix}1\\0\end{pmatrix}\frac{\delta}{\delta\phi_1}+\frac{i}{2}\begin{pmatrix}1\\0\end{pmatrix}\frac{\delta}{\delta\phi_2}+\frac{1}{2}\begin{pmatrix}0\\1\end{pmatrix}\frac{\delta}{\delta\phi_3}+\frac{i}{2}\begin{pmatrix}0\\1\end{pmatrix}\frac{\delta}{\delta\phi_4}\right)(\phi_1-i\phi_2,\quad \phi_3-i\phi_4)\\ &= \left(\frac{1}{2}\begin{pmatrix}1\\0\end{pmatrix}(1,0)+\frac{i}{2}\begin{pmatrix}1\\0\end{pmatrix}(-i,0)+\frac{1}{2}\begin{pmatrix}0\\1\end{pmatrix}(0,1)+\frac{i}{2}\begin{pmatrix}0\\1\end{pmatrix}(0,-i)\right)\\ &= \frac{1}{2}\begin{pmatrix}1&0\\0&0\end{pmatrix}+\frac{1}{2}\begin{pmatrix}1&0\\0&0\end{pmatrix}+\frac{1}{2}\begin{pmatrix}0&0\\0&1\end{pmatrix}+\frac{1}{2}\begin{pmatrix}0&0\\0&1\end{pmatrix}\\ &= \begin{pmatrix}1&0\\0&1\end{pmatrix}.\end{aligned} \tag{A.16}$$

We want to compute the derivative of

$$\Phi^\dagger\Phi = (\phi_1-i\phi_2,\quad \phi_3-i\phi_4)\begin{pmatrix}\phi_1+i\phi_2\\ \phi_3+i\phi_4\end{pmatrix} = \phi_1^2+\phi_2^2+\phi_3^2+\phi_4^2, \tag{A.17}$$

so

$$\begin{aligned}\frac{\delta}{\delta\Phi^\dagger}(\Phi^\dagger\Phi) &= \left(\frac{1}{2}\begin{pmatrix}1\\0\end{pmatrix}\frac{\delta}{\delta\phi_1}+\frac{i}{2}\begin{pmatrix}1\\0\end{pmatrix}\frac{\delta}{\delta\phi_2}+\frac{1}{2}\begin{pmatrix}0\\1\end{pmatrix}\frac{\delta}{\delta\phi_3}+\frac{i}{2}\begin{pmatrix}0\\1\end{pmatrix}\frac{\delta}{\delta\phi_4}\right)(\phi_1^2+\phi_2^2+\phi_3^2+\phi_4^2)\\ &= \frac{1}{2}\begin{pmatrix}1\\0\end{pmatrix}2\phi_1+\frac{i}{2}\begin{pmatrix}1\\0\end{pmatrix}2\phi_2+\frac{1}{2}\begin{pmatrix}0\\1\end{pmatrix}2\phi_3+\frac{i}{2}\begin{pmatrix}0\\1\end{pmatrix}2\phi_4\\ &= \begin{pmatrix}\phi_1+i\phi_2\\ \phi_3+i\phi_4\end{pmatrix}\\ &= \Phi,\end{aligned} \tag{A.18}$$

and therefore

$$\frac{\delta}{\delta\Phi^\dagger}(\Phi^\dagger\Phi) = \Phi. \tag{A.19}$$

Analogously we find

$$\frac{\delta}{\delta\Phi}(\Phi^\dagger\Phi) = \Phi^\dagger. \tag{A.20}$$

A.2.2 Using complex scalar fields

Now let us consider two scalar fields and write the doublet as

$$\Phi = \begin{pmatrix}\phi_+\\ \phi_0\end{pmatrix},\quad \Phi^\dagger = (\phi_+^*,\phi_0^*). \tag{A.21}$$

where ϕ_+, $\phi_0 \in \mathbb{C}$ are complex scalar fields. We have seen in Section A.1 that we can treat the components of a complex scalar field as independent, so we choose the conjugate ones and write the Leibniz rule as

$$\frac{\delta}{\delta\Phi^\dagger} = \frac{\delta\phi_+^*}{\delta\Phi^\dagger}\frac{\delta}{\delta\phi_+^*}+\frac{\delta\phi_0^*}{\delta\Phi^\dagger}\frac{\delta}{\delta\phi_0^*}, \tag{A.22}$$

and we can take the variational derivatives as

$$\frac{\delta\phi_+^*}{\delta\Phi^\dagger} = \left(\frac{\delta\Phi^\dagger}{\delta\phi_+^*}\right)^{-1} = (1,0)^{-1} = \begin{pmatrix}1\\0\end{pmatrix},\quad \frac{\delta\phi_0^*}{\delta\Phi^\dagger} = \left(\frac{\delta\Phi^\dagger}{\delta\phi_0^*}\right)^{-1} = (0,1)^{-1} = \begin{pmatrix}0\\1\end{pmatrix}, \tag{A.23}$$

thus the derivative is

$$\frac{\delta}{\delta\Phi^\dagger} = \begin{pmatrix}1\\0\end{pmatrix}\frac{\delta}{\delta\phi_+^*} + \begin{pmatrix}0\\1\end{pmatrix}\frac{\delta}{\delta\phi_0^*}. \tag{A.24}$$

Notice the self-consistency with eqs. (A.24), (A.15) and (A.6). Starting from eq. (A.24) and introducing the result of eq. (A.6) for the variational derivative of a complex field, we arrive again at eq. (A.15) with four real scalar fields. Another consistency check is

$$\begin{aligned}
\frac{\delta\Phi^\dagger}{\delta\Phi^\dagger} &= \left(\begin{pmatrix}1\\0\end{pmatrix}\frac{\delta}{\delta\phi_+^*} + \begin{pmatrix}0\\1\end{pmatrix}\frac{\delta}{\delta\phi_0^*}\right)\Phi^\dagger = \left(\begin{pmatrix}1\\0\end{pmatrix}\frac{\delta}{\delta\phi_+^*} + \begin{pmatrix}0\\1\end{pmatrix}\frac{\delta}{\delta\phi_0^*}\right)(\phi_+^*,\phi_0^*)\\
&= \begin{pmatrix}1\\0\end{pmatrix}\frac{\delta}{\delta\phi_+^*}(\phi_+^*,\phi_0^*) + \begin{pmatrix}0\\1\end{pmatrix}\frac{\delta}{\delta\phi_0^*}(\phi_+^*,\phi_0^*)\\
&= \begin{pmatrix}1\\0\end{pmatrix}(1,0) + \begin{pmatrix}0\\1\end{pmatrix}(0,1)\\
&= \begin{pmatrix}1&0\\0&0\end{pmatrix} + \begin{pmatrix}0&0\\0&1\end{pmatrix}\\
&= \begin{pmatrix}1&0\\0&1\end{pmatrix}.
\end{aligned} \tag{A.25}$$

And at last we reproduce the same result for the derivative of the product that we are interested in

$$\begin{aligned}
\frac{\delta}{\delta\Phi^\dagger}(\Phi^\dagger\Phi) &= \left(\begin{pmatrix}1\\0\end{pmatrix}\frac{\delta}{\delta\phi_+^*} + \begin{pmatrix}0\\1\end{pmatrix}\frac{\delta}{\delta\phi_0^*}\right)\Phi^\dagger\Phi = \left(\begin{pmatrix}1\\0\end{pmatrix}\frac{\delta}{\delta\phi_+^*} + \begin{pmatrix}0\\1\end{pmatrix}\frac{\delta}{\delta\phi_0^*}\right)(\phi_+^*\phi_+ + \phi_0^*\phi_0)\\
&= \begin{pmatrix}1\\0\end{pmatrix}\frac{\delta}{\delta\phi_+^*}(\phi_+^*\phi_+ + \phi_0^*\phi_0) + \begin{pmatrix}0\\1\end{pmatrix}\frac{\delta}{\delta\phi_0^*}(\phi_+^*\phi_+ + \phi_0^*\phi_0)\\
&= \begin{pmatrix}1\\0\end{pmatrix}\phi_+ + \begin{pmatrix}0\\1\end{pmatrix}\phi_0\\
&= \begin{pmatrix}\phi_+\\\phi_0\end{pmatrix}\\
&= \Phi.
\end{aligned} \tag{A.26}$$

Therefore we obtain

$$\frac{\delta}{\delta\Phi^\dagger}(\Phi^\dagger\Phi) = \Phi, \tag{A.27}$$

and

$$\frac{\delta}{\delta\Phi}(\Phi^\dagger\Phi) = \Phi^\dagger, \tag{A.28}$$

Appendix B

Algorithms

In this appendix we describe the algorithms used to obtain the solutions and the self-consistency tests we performed. We will describe the algorithms in the following way:

- In Section B.1 we show how the Python function `scipy.integrate.solve_bvp` works. This function solves boundary value problems and is the one we used to obtain the solutions to the equations of motion.
- In Section B.2 we describe the self-consistency test we performed to the reported solutions. We use a discretization of the equations of motion and insert the data we obtained from Python solutions.
- In Section B.3 we apply the Runge-Kutta method as an alternative to obtain solutions for the equations of motion. While this is a less appropriate algorithm than Python because of the type of problem we deal with, we use it for a comparison. The special feature of this method is solving the differential equations as an initial value problem.
- In Section B.4 we apply the relaxation method, as yet another alternative to Python. This algorithm is less appropriate too but the equations of motion are solved as a boundary value problem.

B.1 Python Algorithm

The Python function `scipy.integrate.solve_bvp` implements a collocation algorithm with control of residuals for a damped Newton method. A brief description can be found in Python documentation [103], but here we describe explicitly some relevant technical details we need to discuss. This function can be used to solve a system of differential equations subject to boundary conditions.

The Newton method consists of an iteration procedure to solve linear or non-linear equations. Given a function $f(x)$, we look for a root x^* of this function, $f(x^*) = 0$. We start from an initial

guess x_0 and then a sequence of approximations is done. Given a root approximation x_k, the next element x_{k+1} is given by

$$x_{k+1} = x_k - \frac{f(x_k)}{f'(x_k)}. \tag{B.1}$$

If $|x^* - x_0|$ is small enough and f satisfies some weak conditions, then this procedure attains the root in a quadratic convergence, this means

$$\lim_{k\to\infty} \frac{|x_{k+1} - x^*|}{|x_k - x^*|^2} = c, \tag{B.2}$$

for some positive number c.

To solve a differential equation system using this method, we can discretize the system of equations of the boundary value problem as a system of non-linear algebraic equations. To exemplify we can start from a differential equation given by

$$\frac{dy}{dx}(x) = F(x, y(x)). \tag{B.3}$$

Then we discretize using the collocation algorithm, this is done as follows. We take a collection of $n+1$ points $(x^0, \ldots, x^n)$ and the respective solutions to be approximated are given by $(y^0, \ldots, y^n)$. Upper indices denote the elements of the discretization. We assume the solution to be approximated by a linear combination of continuous functions ψ_ℓ as

$$y^i = y(x^i) = \sum_{\ell=0}^{n} a_\ell \psi_\ell(x^i). \tag{B.4}$$

A set of differential equations can be defined with this decomposition

$$\frac{dy}{dx}(x^i) = F(x^i, y^i), \tag{B.5}$$

by substituting the approximate solution for the derivative

$$\sum_{\ell=0}^{n} a_\ell \frac{d\psi_\ell}{dx}(x^i) = F(x^i, y^i). \tag{B.6}$$

Here x^i are the input while our objective is to find numerical values for all the y^i. Therefore we are working with an algebraic system of equations

$$\vec{f}(\vec{y}) = \vec{0}, \tag{B.7}$$

with the vectors $\vec{f} = (f^0, ..., f^n)^T$, $\vec{y} = (y^0, ..., y^n)^T$, the latter vector represents the solution of the differential equation. We repeat that the upper indices in this convention are the entries of the vectors which are the set of elements of the discretization. The iterations take the form

$$\vec{y}_{k+1} = \vec{y}_k - J(\vec{y}_k)^{-1}\vec{f}(\vec{y}_k) = \vec{y}_k + \vec{Y}, \tag{B.8}$$

where the vector $\vec{Y}$ is known as the Newton direction and the lower indices correspond to the iteration step. The Jacobian matrix is given by

$$J(\vec{f}_k, \vec{y}_k) = \frac{\partial f_k^i}{\partial y_k^j}. \tag{B.9}$$

The Newton method itself needs to be improved because of certain inconveniences, one of them is the need of an initial guess which should be sufficiently close to the solution as the Newton-Kantorovich theorem states [104]. This is why the damped Newton method is used as an improvement. From eq. (B.8) we can see that each iteration gives a unit step in Newton's direction. The improvement consists in reducing the size of the step (as it might move further away from the solution) by taking the iteration as

$$\vec{y}_{k+1} = \vec{y}_k + \epsilon\vec{Y}, \quad 0 < \epsilon \leqslant 1. \tag{B.10}$$

ϵ is the damping factor, it can be chosen by minimizing an objective function $g(y)$, for example

$$g(\vec{y}_{k+1}) = \frac{1}{2}\left|\vec{f}(\vec{y}_{k+1})\right|^2. \tag{B.11}$$

For the case of `solve_bvp` an affine invariant function is used, like

$$g(\vec{y}_{k+1}) = \frac{1}{2}|J(y_k)^{-1}\vec{f}(\vec{y}_{k+1})|^2. \tag{B.12}$$

It is important to mention that this improvement does not necessarily lead to convergence when the normal Newton method fails. But the damped Newton method can indeed detect quickly when it fails. This might justify our finding in Chapter 4 of an interval outside $(\kappa_{\min}, \kappa_{\max})$ where the program is unable to find a solution. The failure of this algorithm might be because solutions outside this interval are different or away from the proposed initial guess functions. The other numerical methods, applied below, show that solutions outside the interval exist, but they do not correspond to cosmic strings.

Let us consider our system of equations in the small-r regime, they read

$$\begin{aligned} \frac{d^2\phi}{dr^2} + \frac{1}{r}\frac{d\phi}{dr} &= \frac{n^2}{r^2}\phi, \\ \frac{d^2\xi}{dr^2} + \frac{1}{r}\frac{d\xi}{dr} &= \frac{n'^2}{r^2}\xi. \end{aligned} \tag{B.13}$$

These equations have a general solution

$$\phi(r) = \phi_0 r^{|n|}, \quad \xi(r) = \xi_0 r^{|n'|}. \tag{B.14}$$

Using these functions as an initial guess, does not work in the case $|n| > 1$ or $|n'| > 1$. This is because the algorithm treats every point in the function as an independent initial guess. So as we mentioned before, a better initial guess function should be one that better approximates the solution in each point. That is why we use asymptotic functions as

$$\phi(r) = v(1 - e^{-r}), \quad \xi(r) = v'(1 - e^{-r}), \tag{B.15}$$

which satisfy the boundary conditions.

B.2 Self-consistency test

Using the data for a given solution in Python we perform a self-consistency test by defining the discretized version of the differential equations as the error estimates

$$E_\phi = \left| \frac{\phi_{i+1} + \phi_{i-1} - 2\phi_i}{\epsilon^2} + \frac{\phi_{i+1} - \phi_{i-1}}{2r_i\epsilon} - \frac{n^2\phi_i}{r_i^2} - \mu^2\phi_i^2 - 2\lambda\phi_i^3 + \kappa\phi_i\xi_i^2 \right|, \tag{B.16}$$

$$E_\xi = \left| \frac{\xi_{i+1} + \xi_{i-1} - 2\xi_i}{\epsilon^2} + \frac{\xi_{i+1} - \xi_{i-1}}{2r_i\epsilon} - \frac{n'^2\phi_i}{r_i^2} - \mu'^2\xi_i^2 - 2\lambda'\xi_i^3 + \kappa\phi_i^2\xi_i \right|, \tag{B.17}$$

which should be approximately zero according to the system in eq. (4.34). We achieve numerical values of the order of 10^{-4} for the global symmetry case. We present an example of these error estimates for the parameters $v = 0.5$, $v' = 1$, $\lambda = 1$, $\lambda' = 1$, $n = 1$, $n' = 2$ in Fig. B.1. This figure contains the plots for the error estimates associated with the fields ϕ and ξ for two distinct values of κ, namely $\kappa = \pm 0.5$. These errors correspond to the solutions in Fig. 4.4.

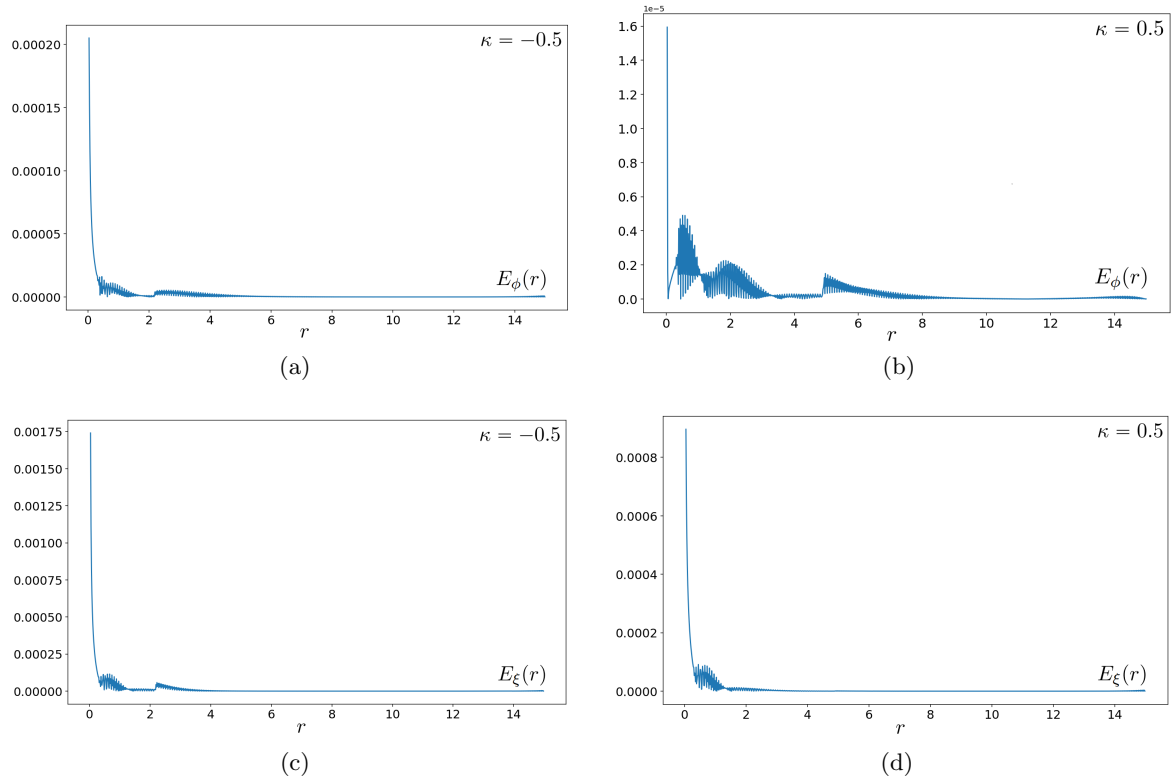

Figure B.1: Error estimate E_ϕ for $\kappa = -0.5$ (a), $\kappa = 0.5$ (b) and error estimate E_ξ for $\kappa = -0.5$ (c), $\kappa = 0.5$ (d).

Analogously, for the local symmetry case we can define the error estimates using the system of eq. (4.58) as

$$E_\phi = \left| \frac{\phi_{i+1} + \phi_{i-1} - 2\phi_i}{\epsilon^2} + \frac{\phi_{i+1} - \phi_{i-1}}{2r_i\epsilon} - \frac{n^2\phi_i}{r_i^2} - \mu^2\phi_i^2 - 2\lambda\phi_i^3 + \kappa\phi_i\xi_i^2 - h\frac{a_i}{r_i^2}\phi_i(2n + ha_i) \right|, \tag{B.18}$$

$$E_\xi = \left| \frac{\xi_{i+1} + \xi_{i-1} - 2\xi_i}{\epsilon^2} + \frac{\xi_{i+1} - \xi_{i-1}}{2r_i\epsilon} - \frac{n'^2\phi_i}{r_i^2} - \mu'^2\xi_i^2 - 2\lambda'\xi_i^3 + \kappa\phi_i^2\xi_i - h'\frac{a_i}{r_i^2}\xi_i(2n' + h'a_i) \right|, \tag{B.19}$$

$$E_a = \left| \frac{a_{i+1} + a_{i-1} - 2a_i}{\epsilon^2} - \frac{a_{i+1} - a_{i-1}}{2r_i\epsilon} - 2h\phi_i^2(n + ha_i) - 2h'\xi_i^2(n' + h'a_i) \right|, \tag{B.20}$$

and we achieve numerical errors of the order of 10^{-3} which decrease rapidly as r increases. An example is shown in Fig. B.2 also for the two selected options for $\kappa = \pm 0.5$. These error estimates are associated to the solutions in Fig. 4.3.

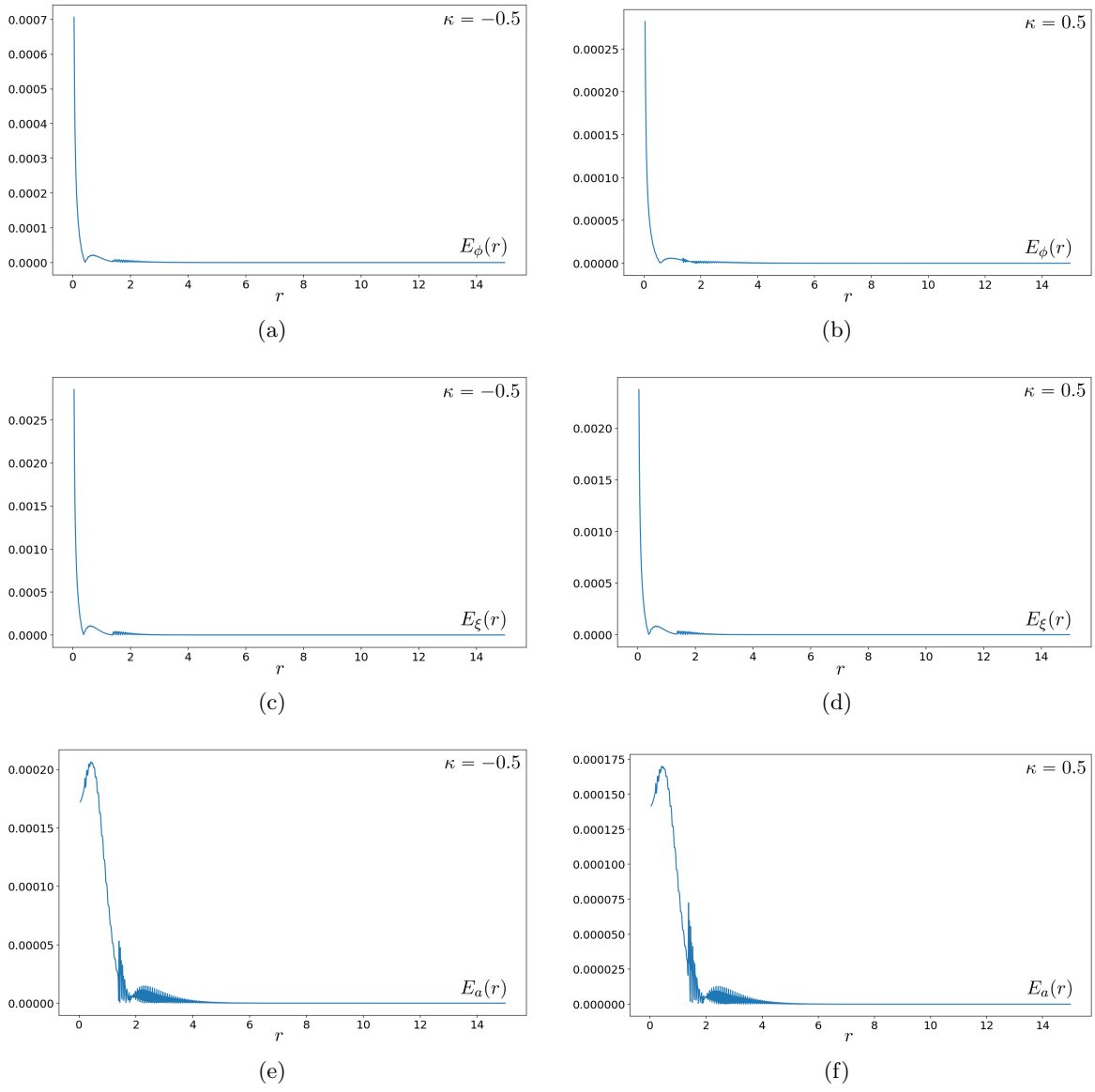

Figure B.2: Error estimate E_ϕ for $\kappa = -0.5$ (a), $\kappa = 0.5$ (b), error estimate E_ξ for $\kappa = -0.5$ (c), $\kappa = 0.5$ (d) and error estimate E_a for $\kappa = -0.5$ (e), $\kappa = 0.5$ (f).

In all these plots we appreciate that the largest errors appear near the origin and then they decrease for larger r as the solutions converge asymptotically. In any case, the numerical error

is quite small and we can justify it with our previous discussion about the numerical inability to impose the boundary values at the origin, due to the removable singularity of the equations of motion. The errors can also be slightly reduced by taking a refined discretization $\epsilon \to \epsilon/2$, but this procedure maintains the same order in the error.

B.3 Runge-Kutta method

Another method to solve our equations of motion is fourth order Runge-Kutta method. This method allows us to solve this problem as an initial value problem. The case $\kappa = 0$ with global symmetry is a good simplification to analyze because then the Higgs fields are uncoupled. We can fix the parameters, for instance, as $v = 0.1$, $v' = 2$, $\lambda = 1$, $\lambda' = 1/4$, $n = 1$, $n' = 1$ and this section condition $\kappa = 0$. The bare masses satisfy $\mu^2 = -2\lambda v^2 + \kappa v'^2$ and $\mu'^2 = -2\lambda' v'^2 + \kappa v^2$ as can be seen from eq. (4.34) for the large-r limit. So introducing the parameters, the bare masses take the value $\mu^2 = -1/50$ and $\mu'^2 = -2$.

The conditions at $r \to \infty$ of the fields taking their VEVs are already taken into account because of the dependence on the bare masses to the other parameters. The equations of motion as differential equations contain fixed points which will be attained for a set of solutions, provided the initial conditions are adequate. Now, if we want to solve this problem numerically we need to specify the initial conditions $\phi(r_0)$ and $\frac{d\phi}{dr}(r_0)$ ($\xi(r_0)$ and $\frac{d\xi}{dr}(r_0)$). Taking $r_0 = 0$ is not viable numerically because of the $1/r$ dependence of the equations. So this is why we start at an arbitrary value $r_0 = 0.01$. Then we fix $\phi(r_0) = 0$ and $\xi(r_0) = 0$. The initial values $\frac{d\phi}{dr}(r_0)$ and $\frac{d\xi}{dr}(r_0)$ are left as free parameters so that we can vary them using a program written in Fortran, applying the fourth order Runge-Kutta method. This fixing does not necessarily reveal all solutions, even in this $\kappa = 0$ case.

In the case of ϕ, three types of solutions were found with this method: damped oscillations, regular cosmic strings that take their VEV asymptotically and divergent solutions. We can see these solutions in Fig. B.3. Around the value $\frac{d\phi}{dr}(r_0) \approx 11.44$ we can find the cosmic string solution with the usual profile reported in literature for $U(1)$ symmetry. There is also the trivial solution and symmetry under $\phi \to -\phi$. In the case of ξ there are the same kind of solutions, as we can see in Fig. B.4. The only difference is the VEV and the range where the solutions change. Around $\frac{d\xi}{dr}(r_0) \approx 3.2989972$ the solution corresponds to a cosmic string that attains the VEV at infinity. Solutions with $\frac{d\xi}{dr}(r_0) < 3.2989972$ are damped oscillations around zero and $\frac{d\xi}{dr}(r_0) > 3.2989972$ are divergent solutions. As the value of $\frac{d\xi}{dr}$ grows, the oscillatory solutions approach the VEV and the amplitude of the first oscillation becomes flat as we can see in Fig. B.5. Still this solution does not attain the VEV at infinity which is present in the analysis, instead it goes to zero.

We see how this analysis gives us the same cosmic string profiles found with Python and reported in the thesis. Moreover, this method allows us to find the damped oscillations and divergent solutions which were present in the analysis of the phase space. Most importantly this is an initial value problem which shows the asymptotic behaviour of the cosmic string solutions.

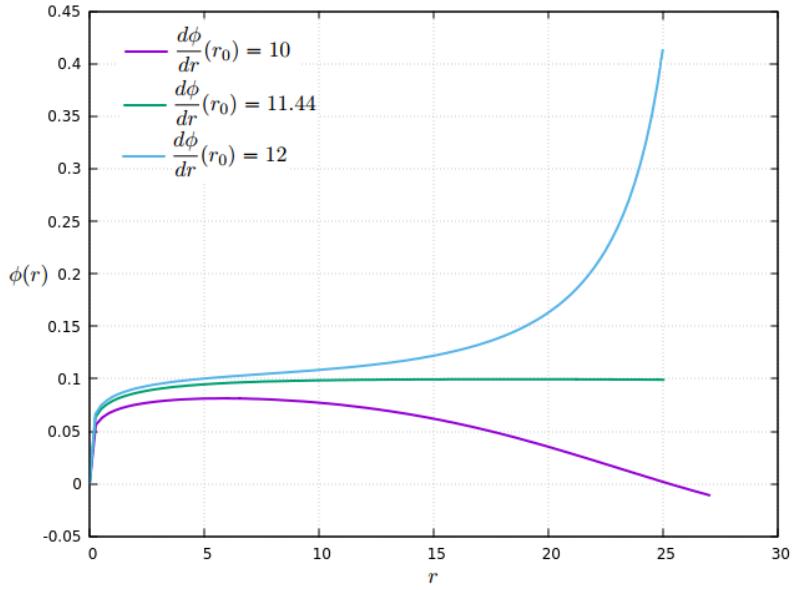

Figure B.3: The three types of solutions for the standard Higgs field radial part $\phi(r)$, for different initial conditions in the derivative, for the parameters $v = 0.1$, $\lambda = 1$ and $n = 0$.

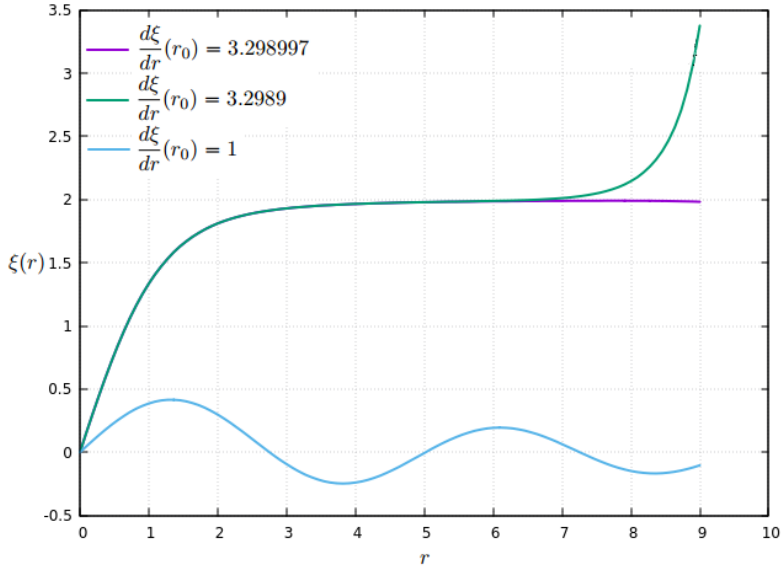

Figure B.4: The three types of solutions for the extra Higgs field radial part $\xi(r)$, for different initial conditions in the derivative, for the parameters $v' = 2$, $\lambda' = 1/4$, and $n' = 1$.

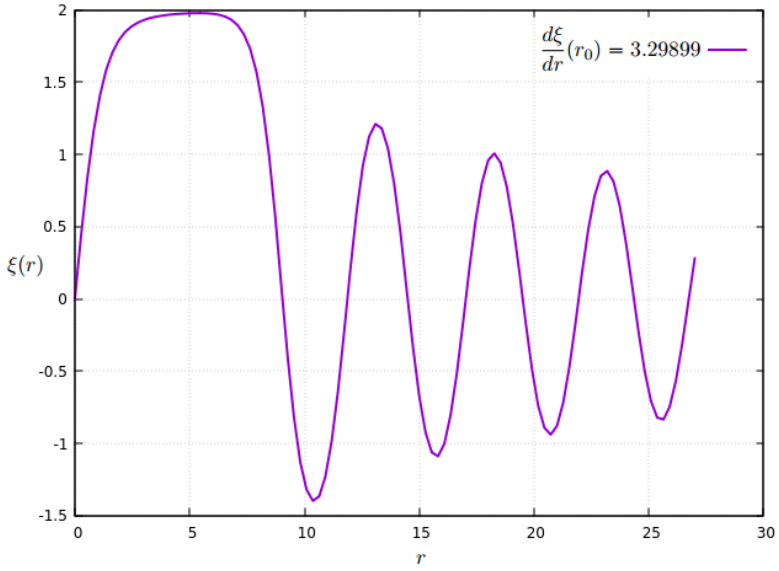

Figure B.5: Damped oscillation solution for the extra Higgs field $\xi(r)$ near the cosmic string solution, for the parameters $v' = 2$, $\lambda' = 1/4$ and $n' = 1$.

B.4 Relaxation method

In order to explore solutions for the values of κ where Python is unable to find, we implement the relaxation method. This approach solves second order, non-linear differential equations subject to boundary conditions. Furthermore, as we implement it directly in a Fortran code, we avoid the numerical problems at $r_0 = 0$ which are related to the structure of Python function. First we discretize a function $f(r)$ and its derivatives in the form

$$f(r) \approx \frac{f(r+\epsilon)+f(r-\epsilon)}{2}, \quad \frac{df}{dr}(r) \approx \frac{f(r+\epsilon)-f(r-\epsilon)}{2\epsilon}, \quad \frac{d^2f}{dr^2}(r) \approx \frac{f(r+\epsilon)+f(r-\epsilon)-2f(r)}{\epsilon^2}, \tag{B.21}$$

for small ϵ, and the mean value of $f(r)$ is used in the non-linear terms. For the case of a global cosmic string, starting from the differential equations we obtain the expressions for the fields at r in terms of the fields at $r \pm \epsilon$. Equivalently, writing a discretization $r = i\epsilon$ for $i \in \{1, \ldots, N\}$, the fields at i depend on the fields at $i \pm 1$ as

$$\phi_i = \frac{(1+i^{-1})\phi_{i+1} + \phi_{i-1} - 4^{-1}\lambda\epsilon^2(\phi_{i+1}+\phi_{i-1})^3 - 8^{-1}\kappa\epsilon^2(\phi_{i+1}+\phi_{i-1})(\xi_{i+1}+\xi_{i-1})^2}{2 - \mu\epsilon^2 + i^{-1} + n^2 i^{-2}}, \tag{B.22}$$

$$\xi_i = \frac{(1+i^{-1})\xi_{i+1} + \xi_{i-1} - 4^{-1}\lambda'\epsilon^2(\xi_{i+1}+\xi_{i-1})^3 - 8^{-1}\kappa\epsilon^2(\xi_{i+1}+\xi_{i-1})(\phi_{i+1}+\phi_{i-1})^2}{2 - \mu'\epsilon^2 + i^{-1} + n'^2 i^{-2}}. \tag{B.23}$$

For the case $v = 0.5$, $v' = 1$, $\lambda = 1$, $\lambda' = 1$, $n = 1$, and $n' = 1$, we can use a small value $\epsilon = 10^{-2}$ and obtain the plots in Figs. B.6 and B.7. Convergence is assured by taking two large values of iterations (like 10^7) and comparing the difference. From this figure we can see that indeed, for κ outside $(-2, 2)$ we have a different behaviour for the solution.

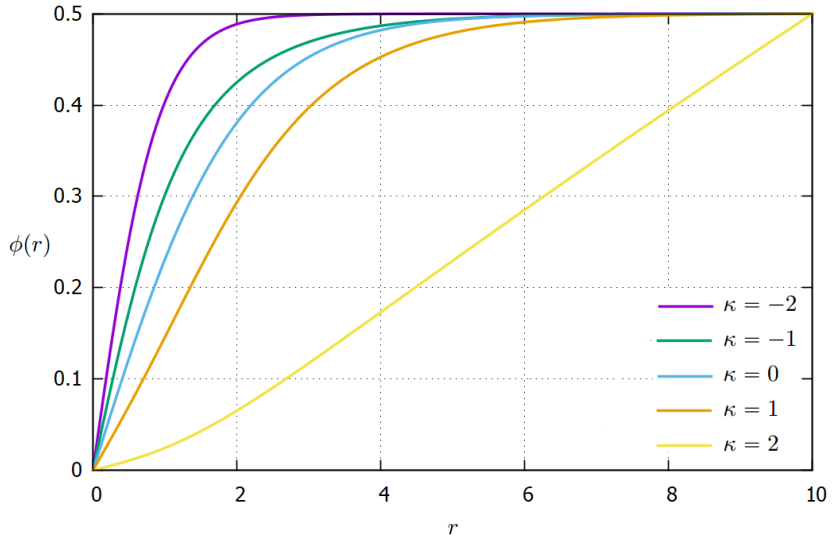

Figure B.6: Cosmic string solutions for the standard Higgs field radial part $\phi(r)$, for different values of κ solved with the relaxation method, using the parameters $v = 0.5$, $v' = 1$, $\lambda = 1$, $\lambda' = 1$, $n = 1$ and $n' = 1$.

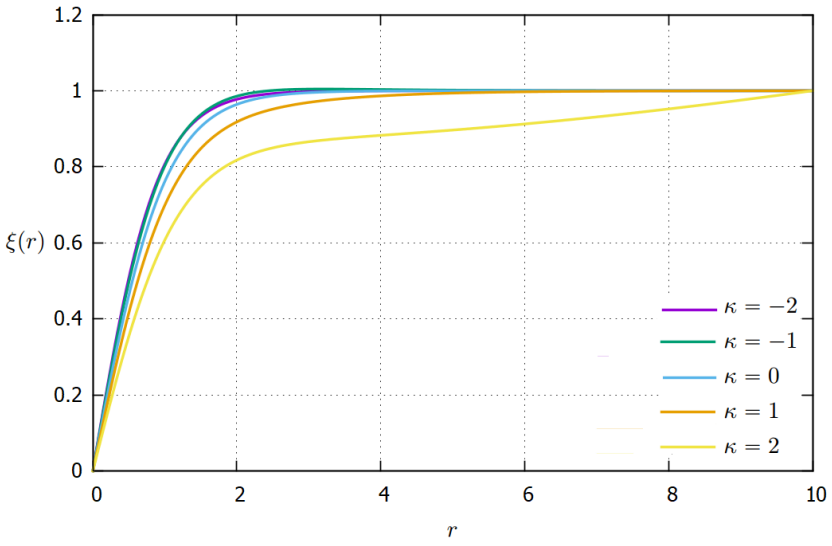

Figure B.7: Cosmic string solutions for the extra Higgs field radial part $\xi(r)$, for different values of κ solved with the relaxation method, using the parameters $v = 0.5$, $v' = 1$, $\lambda = 1$, $\lambda' = 1$, $n = 1$ and $n' = 1$.

In Figures B.6 and B.7 we see the solutions using the relaxation method, they coincide with the solutions using Python. Furthermore, as the value of κ increases to $\kappa = 2$, the solution displays a linear behaviour and as it increases further more at $\kappa > 2$, it changes to an increasing concave up curve in both fields. These might correspond to divergent solutions which satisfy the boundary conditions because of the algorithm. We also point out that, from these plots, we can see that the derivatives at the endpoint $r_f = 10$ are non-zero, thus this solutions for $\kappa \geqslant 2$ are excluded.

Bibliography

[1] Griffiths, D., *Introduction to Elementary Particles*. Second, Revised Edition. WILEY-VCH Verlag GmbH & Co. (2009).

[2] Schwartz, M. D., *Quantum Field Theory and the Standard Model*. Cambridge University Press (2014).

[3] Weyl, H., *Eine neue Erweiterung der Relativitätstheorie. (A new extension of the theory of relativity)*. Annalen der Physik 59, 101 (1919).

[4] Yang, C. N. & Mills R. L., *Conservation of Isotopic Spin and Isotopic Gauge Invariance*. Phys. Rev. 96, 191 (1954).

[5] Thomson, J., *On the Structure of the Atom: an Investigation of the Stability and Periods of Oscillation of a number of Corpuscles arranged at equal intervals around the Circumference of a Circle; with Application of the Results to the Theory of Atomic Structure*. Philos. Mag. 7, 237 (1904).

[6] Chadwick, J., *Possible Existence of a Neutron*. Nature 129, 312 (1932).

[7] Lattes, C.; Occhialini, G.; Muirhead, H. & Powell, C., *Processes Involving Charged Mesons*. Nature 159, 694 (1947).
Lattes, C.; Occhialini, G. & Powell, C., *Observations on the Tracks of Slow Mesons in Photographic Emulsions*. Nature 160, 453 (1947).

[8] Rochester, G. D. & Butler, C. C., *Evidence for the Existence of New Unstable Elementary Particles*. Nature 160, 855 (1947).

[9] Brown, R.; Camerini, U.; Fowler, P. H.; Muirhead, H.; Powell, C. F. & Ritson, D. M., *Observations with Electron-Sensitive Plates Exposed to Cosmic Radiation*. Nature 163, 47 (1949).

[10] Pais, A., *On the Baryon-meson-photon System*. Prog. Theor. Phys. 10, 457 (1953).

[11] Heisenberg, W., *Über den Bau der Atomkerne. (On the construction of the atomic nuclei)*. Z. Phys. 77, 1 (1932).

[12] Hopper, V.D. & Biswas, S., *Evidence Concerning the Existence of the New Unstable Elementary Neutral Particle*. Phys. Rev. 80, 1099 (1950).

[13] Gell-Mann, M. & Ne'eman, Y., *The Eightfold Way*. W. A. Benjamin. (1964).

[14] Barnes, V. E., *Observation of a Hyperon with Strangeness Minus Three*. Phys. Rev. Lett. 12, 204 (1964).

[15] Tanabashi, M. et al. (Particle Data Group), *Review of particle physics*. Phys. Rev. D 98 (2018).

[16] Higgs, P. W., *Broken symmetries and the masses of gauge bosons*. Phys. Rev. Lett. 13, 508 (1964).

[17] Anderson, P. W., *Plasmons, Gauge Invariance, and Mass*. Phys. Rev. 130, 439 (1963).

[18] Englert, F. & Brout, R., *Broken symmetry and the mass of gauge vector mesons*. Phys. Rev. Lett. 13, 321 (1964).

[19] Guralnik, G. S.; Hagen, C. R. & Kibble, T., *Global conservation laws and massless particles*. Phys. Rev. Lett. 13, 585 (1964).

[20] Fermi, E., *Versuch einer Theorie der β-Strahlen. (An attempt of a theory of beta radiation)*. Z. Phys. 88, 161 (1934).

[21] Glashow, S. L., *Partial-symmetries of weak interactions*. Nucl. Phys. 22, 579 (1961).

[22] Bludman, S. A., *On the Universal Fermi Interaction*. Nuovo Cimento 9, 433 (1958).

[23] Weinberg, S., *A Model of Leptons*. Phys. Rev. Lett. 19, 1264 (1967).

[24] Hasert, F. J. et al., *Observation of Neutrino Like Interactions Without Muon Or Electron in the Gargamelle Neutrino Experiment*. Phys. Lett. B 46, 138 (1973).

[25] Arnison, G. et al., *Experimental observation of isolated large transverse energy electrons with associated missing energy at $s = 540$ GeV*. Phys. Lett. B 122, 103 (1983).
Arnison, G. et al., *Experimental observation of lepton pairs of invariant mass around 95 GeV/c^2 at the CERN SPS collider*. Phys. Lett. B 126, 398 (1983).

[26] Aad, G. et al. (ATLAS collaboration), *Observation of a New Particle in the Search for the Standard Model Higgs Boson with the ATLAS Detector at the LHC*. Phys. Lett. B 716, 1 (2012).

[27] Cho, A., *Higgs Boson Makes Its Debut After Decades-Long Search*. Science 337, 141 (2012).

[28] Reines, F & Cowan, C. L., *Detection of the Free Neutrino*. Phys. Rev. 92, 830 (1953).
Cowan, C. L.; Reines, F.; Harrison, F. B.; Kruse, H. W. & McGuire A. D., *Detection of the Free Neutrino: a Confirmation*. Science 124, 103 (1956).

[29] Perl, M. L.; Abrams, G. S.; Boyarski, A. M.; Breidenbach, M.; Briggs, D. D.; Bulos, F. & Wiss, J. E., *Evidence for Anomalous Lepton Production in e^+-e^- Annihilation*. Phys. Rev. Lett. 35, 1489 (1975).

[30] Konopinsky, E. J. & Mahmoud, H. M., *The Universal Fermi Interaction*. Phys. Rev. 92, 1045 (1953).

[31] Wu, C. S.; Ambler, E.; Hayward, R. W.; Hoppes, D. D. & Hudson, R. P., *Experimental Test of Parity Conservation in Beta Decay*. Phys. Rev. 105, 1413 (1957).

[32] Garwin, R. L.; Lederman, L. M. & Weinrich, R. M., *Observations of the Failure of Conservation of Parity and Charge Conjugation in Meson Decays: the Magnetic Moment of the Free Muon*. Phys. Rev. 105, 1415 (1957).

[33] Ioffe, B. L.; Okun, L. B. & Rudik, A. P., *The Problem of Parity Non-conservation in Weak Interactions*. J. Exp. Theor. Phys. 32, 328 (1957).
Lee, T. D.; Oehme, R. & Yang, C. N., *Remarks on Possible Noninvariance under Time Reversal and Charge Conjugation*. Phys. Rev. 106, 340 (1957).

[34] Backenstoss G.; Hyams B. D.; Knop G.; Marin P. C. & Stierlin U., *Helicity of μ-Mesons from π-Meson Decay*. Phys. Rev. Lett. 6, 415 (1961).

[35] Cabibbo, N., *Unitary Symmetry and Leptonic Decays*. Phys. Rev. Lett. 10, 531 (1963).

[36] Glashow, S. L.; Iliopoulos, J. & Maiani L., *Weak Interactions with Lepton-Hadron Symmetry*. Phys. Rev. D 2, 1285 (1970).

[37] Kobayashi, M. & Maskawa, K., *CP-Violation in the Renormalizable Theory of Weak Interaction*. Prog. Theor. Phys. 49, 652 (1973).

[38] Fukuda, Y. et al. (Super-Kamiokande Collaboration), *Evidence for oscillation of atmospheric neutrinos*. Phys. Rev. Lett. 81, 1562 (1998).

[39] Ahmad Q. R. et al. (SNO Collaboration), *Measurement of the rate of $\nu_e + d \rightarrow p + p + e^-$ interactions produced by ^8B solar neutrinos at the Sudbury Neutrino Observatory*. Phys. Rev. Lett. 87, 071301 (2001).
Ahmad Q. R. et al. (SNO Collaboration), *Direct Evidence for Neutrino Flavor Transformation from Neutral-Current Interactions in the Sudbury Neutrino Observatory*. Phys. Rev. Lett. 89, 011301 (2002).

[40] Pontecorvo, B., *Inverse beta processes and non-conservation of lepton charge*. Sov. Phys. JETP 7, 172 (1958).

[41] Maki, Z.; Nakagawa, M. & Sakata, S., *Remarks on the Unified Model of Elementary Particles*. Prog. Theor. Phys. 28 (1962).

[42] Landau, L. D., *On the Theory of Phase Transitions*. Zh. Eksp. Teor. Fiz. 7, 19 (1937).

[43] Onsager, L., *Crystal statistics. I. A two-dimensional model with an order-disorder transition*. Phys. Rev. Series II 65, 117 (1944).

[44] Kamerlingh Onnes, H., *Further experiments with liquid helium. C. On the change of electric resistance of pure metals at very low temperatures etc. IV. The resistance of pure mercury at helium temperatures*. Proceedings of the Section of Sciences 13 (1911).

[45] Meissner, W. & Ochsenfeld, R., *Ein neuer Effekt bei Eintritt der Supraleitfähigkeit*. Naturwissenschaften. 21, 787 (1933).

[46] Bardeen, J.; Cooper, L. & Schrieffer, J. R., *Theory of Superconductivity*. Phys. Rev. 108, 1175 (1957).

[47] Wells, F. S.; Pan, A. V.; Wang, X. R.; Fedoseev, S. A. & Hilgenkamp, H., *Analysis of low-field isotropic vortex glass containing vortex groups in $YBa_2Cu_3O_{7-x}$ thin films visualized by scanning SQUID microscopy.* Sci. Rep. 5, 8677 (2015).

[48] Kopnin, N., *Vortices in type II superconductors: Structure and Dynamics. Part I Isotropic superconductors.* (1996).

[49] Ginzbrug, V. L. & Landau, L. D., *On the theory of superconductivity.* F. Theor. Phys. 20, 1064 (1950).

[50] Zavaritskii, N. V., *Investigation of Superconducting Properties of Films of Thallium and Tin Deposited at Low Temperatures.* Dockl. Acad. Nauk 86, 501 (1952).

[51] Abrikosov, A. A., *The magnetic properties of superconducting alloys.* J. Phys. Chem. Sol. 2, 199 (1957).

[52] Salomaa, M. M. & Volovik G. E., *Quantized vortices in superfluid ^3He.* Rev. Mod. Phys. 59, 533 (1987).

[53] Fonda, E. et al., *Visualization of Kelvin waves on quantum vortices.* arXiv:1210.5194 [physics.flu-dyn] (2012).

[54] Osheroff, D. D.; Richardson, R. C. & Lee, D. M., *Evidence for a New Phase of Solid ^3He.* Phys. Rev. Lett. 28, 885 (1972).

[55] Leggett, A. J., *Interpretation of Recent Results on He3 below 3 mK: A New Liquid Phase?.* Phys. Rev. Lett. 29, 1227 (1972).

[56] Guénault, T., *Basic Superfluids.* Taylor & Francis Master's Series in Physics and Astronomy (2003).

[57] 't Hooft, G., *Symmetry Breaking through Bell-Jackiw Anomalies.* Phys. Rev. Lett. 37, 8 (1976).

[58] Manton, N. S., *Topology in the Weinberg-Salam theory.* Phys. Rev. D 28, 2019 (1983).

[59] Manton, N. S. & Klinkhamer F. R., *A saddle-point solution in the Weinberg-Salam theory.* Phys. Rev. D 30, 2212 (1984).

[60] Papaefstathiou, A.; Plätzer, S. & Sakurai, K., *On the phenomenology of sphaleron-induced processes at the LHC and beyond.* arXiv:1910.04761 [hep-ph] (2019).

[61] Skadhauge, S., *Sphalerons and Electroweak Baryogenesis.* PhD Thesis, University of Copenhagen (1996).

[62] Brandenberger R., *Inflation, Topological Defects and Baryogenesis: Selected Topics at the Interface between Particles & Fields and Cosmology.* arXiv:9702217 [hep-ph] (1997).

[63] Kibble, T. W. B., *Topology of cosmic domains and strings.* J. Phys. A: Math. Gen. 9, 1387 (1976).

[64] Silk, J. & Vilenkin, A., *Cosmic Strings and Galaxy Formation.* Phys. Rev. Lett. 53, 1700 (1984).

[65] Ostriker, J.P.; Thompson, C. & Witten, E., *Cosmological effects of superconducting strings*. Phys. Lett. B 180, 231 (1986).

[66] Zurek, W. H., *Cosmological experiments in superfluid helium?*. Nature 317, 505 (1985).

[67] Chuang, I.; Durrer, R.; Turok, N. & Yurke, B., *Cosmology in the Laboratory: Defect Dynamics in Liquid Crystals*. Science 251, 1336 (1991).

[68] Chuang, I.; Turok, N. & Yurke, B., *Late-time coarsening dynamics in a nematic liquid crystal*. Phys. Rev. Lett. 66, 2472 (1991).

[69] Hindmarsh, M. B. & Kibble, T. W. B., *Cosmic Strings*. Rep. Prog. Phys. 58, 477 (1995).

[70] Shafi, Q. & Hindmarsh, M. B., *Spontaneously broken global symmetries and cosmology*. Phys. Rev. D 29, 1870(R) (1984).

[71] Nielsen, H. B. & Olesen, P., *Vortex-line models for dual strings*. Nucl. Phys. B 61, 45 (1973).

[72] Jacobs, L. & Rebbi, C., *Interaction energy of superconducting vortices*. Phys. Rev. B 19, 4486 (1979).

[73] Hindmarsh, M. B., *Existence and Stability of Semilocal Strings*. Phys. Rev. Lett. 68, 1263 (1992).

[74] Bogomolny, E. B. & Vainshtein, A. I., *Stability of Strings in Gauge Abelian Theory*. Sov. J. Nucl. Phys. 23, 588 (1976).

[75] Vachaspati, T., *Vortex Solutions in the Weinberg-Salam Model*. Phys. Rev. Lett. 68, 1977 (1992).

[76] James, M.; Perivolaropoulos, L. & Vachaspati, T., *Detailed stability analysis of electroweak strings*. Nucl. Phys. B 395, 534 (1994).

[77] Georgi, H. & Glashow, S. L., *Unity of All Elementary-Particle Forces*. Phys. Rev. Lett. 32, 438 (1974).

[78] Pati, J. C. & Salam, A., *Lepton number as the fourth "color"*. Phys. Rev. D 10, 275 (1974).

[79] Wilczek, F. & Zee, A., *Operator Analysis of Nucleon Decay*. Phys. Rev. Lett. 43, 1571 (1979).

[80] Weinberg, S., *Cosmological Production of Baryons*. Phys. Rev. Lett. 42, 850 (1979).

[81] Fritzsch, H. & Minkowski, P., *Unified interactions of leptons and hadrons*. Ann. Phys. 93, 193 (1975).

[82] Ma, C.-P., $SO(10)$ *cosmic strings and baryon number violation*. Phys. Rev. D 48, 530 (1993).

[83] Bhattarcharjee, P.; Turok, N. & Kibble, T. W. B., *Baryon number from collapsing cosmic strings*. Phys. Lett. B 119, 95 (1982).

[84] Kawasaki, M. & Maeda K., *Baryon number generation from cosmic string loops*. Phys. Lett. B 208, 84 (1988).

[85] Davis, A. & Earnshaw M. A., *Baryogenesis from collapsing cosmic string loops*. Nucl. Phys. B 394, 21 (1993).

[86] Peccei, R. D. & Quinn, H., *CP Conservation in the Presence of Pseudoparticles*. Phys. Rev. Lett. 38, 1440 (1977).

[87] Peccei, R. D. & Quinn, H., *Constraints imposed by CP conservation in the presence of pseudoparticles*. Phys. Rev. D 16, 1791 (1977).

[88] Vilenkin, A. & Everet, A. E., *Cosmic Strings and Domain Walls in Models with Goldstone and Pseudo-Goldstone Bosons*. Phys. Rev. Lett. 48, 1867 (1982).

[89] Vilenkin, A., *Gravitational radiation from cosmic strings*. Phys. Lett. B 107, 47 (1981).

[90] Vilenkin, A., *Gravitational field of vacuum domain walls and strings*. Phys. Rev. D 23, 852 (1981).

[91] Schild, R.; Masnyak, I. S.; Hnatyk, B. I. & Zhdanov, V. I., *Anomalous fluctuations in observations of Q0957+561 A,B: Smoking gun of a cosmic string?*. Astron. Astrophys. 422, 477 (2004).

[92] Arzoumanian, Z. et al., *The NANOGrav Nine-year Data Set: Limits on the Isotropic Stochastic Gravitational Wave Background*. Astrophys. J. 821 (2016).

[93] Charnock, T.; Avgoustidis, A.; Copeland, E. J. & Moss, A., *CMB constraints on cosmic strings and superstrings*. Phys. Rev. D 93, 123503 (2016).

[94] Kaiser, N. & Stebbins, A., *Microwave anisotropy due to cosmic strings*. Nature 310, 391 (1984).

[95] Vachaspati, T. & Vilenkin, A., *Gravitational radiation from cosmic strings*. Phys. Rev. D 31, 3052 (1985).

[96] Abbott, B. P. et al. (LIGO and Virgo Collaborations), *Constraints on cosmic strings using data from the first Advanced LIGO observing run*. Phys. Rev. D 97, 102002 (2018).

[97] Fayet, P., *The fifth force charge as a linear combination of baryonic, leptonic (or $B - L$) and electric charges*. Phys. Lett. B 227, 127 (1989).
Fayet, P., *The light U boson as the mediator of a new force, coupled to a combination of Q, B, L and dark matter*. Eur. Phys. J. C 77, 53 (2017).

[98] Witten, E., *Superconducting strings*. Nucl. Phys. B 249, 557 (1985).

[99] Davis, R. L. & Shellard, E. P. S., *The physics of vortex superconductivity*. Phys. Lett. B 207, 404 (1988).

[100] Chikashige, Y.; Mohapatra, R. N. & Peccei, R. D., *Are there real Goldstone bosons associated with broken lepton number?* Phys. Lett. B 98, 265 (1981).

[101] Buchmüller, W; Greub, C. & Minkowski, P., *Neutrino masses, neutral vector bosons and the scale of $B - L$ breaking*. Phys. Lett. B 267, 395 (1991).

[102] Fritsch, H. & Minkowski, P., *Vectorlike weak currents, massive neutrinos, and neutrino beam oscillations*. Phys. Lett. B 62, 72 (1976).

[103] The Scipy Community 2022, accessed January 2022, https://docs.scipy.org/doc/scipy/reference/generated/scipy.integrate.solve_bvp.html.

[104] Ascher, U.; Mattheij, R. & Russell, R., *Numerical Solution of Boundary Value Problems for Ordinary Differential Equations*. Classics in Applied Mathematics, SIAM (1995).

[105] Boyce, W. E. & DiPrima R. C., *Elementary differential equations and boundary value problems*. John Wiley and Sons, 7th ed (2001).